

RECEIVED
DEC 29 1994
OSTI

**The Railplug:
Development of a New Ignitor for Internal
Combustion Engines**

Final Report

R.D. Matthews, S.P. Nichols, and W.F. Weldon
Center for Energy Studies and Center for Electromechanics
The University of Texas at Austin
Austin, Texas 78712

November 29, 1994

Prepared for the U.S. Department of Energy
Under Grant Number DE-FG05-91ER12115

DISCLAIMER

Portions of this document may be illegible in electronic image products. Images are produced from the best available original document.

DOE/ER/12115-T.1

DISCLAIMER

This report was prepared as an account of work sponsored by an agency of the United States Government. Neither the United States Government nor any agency thereof, nor any of their employees, makes any warranty, express or implied, or assumes any legal liability or responsibility for the accuracy, completeness, or usefulness of any information, apparatus, product, or process disclosed, or represents that its use would not infringe privately owned rights. Reference herein to any specific commercial product, process, or service by trade name, trademark, manufacturer, or otherwise does not necessarily constitute or imply its endorsement, recommendation, or favoring by the United States Government or any agency thereof. The views and opinions of authors expressed herein do not necessarily state or reflect those of the United States Government or any agency thereof.

The Railplug: Development of a New Ignitor for Internal Combustion Engines

Final Report

R.D Matthews, S.P. Nichols, and W.F. Weldon
Center for Energy Studies and Center for Electromechanics
The University of Texas at Austin
Austin, Texas 78712

November 29, 1994

Prepared for the U.S. Department of Energy
Under Grant Number DE-FG05-91ER12115

MASTER

DISTRIBUTION OF THIS DOCUMENT IS UNLIMITED

yo

TABLE OF CONTENTS

1.0 INTRODUCTION	1
1.1 Alternative Ignitors	1
1.2 Railgun Theory	2
1.3 Railplugs	5
2.0 PROJECT OVERVIEW	6
3.0 FUNDAMENTAL RAILPLUG EXPERIMENTS	15
3.1 Initial Fundamental Studies	15
3.2 Continued Fundamental Studies	17
3.3 Final Fundamental Studies	17
4.0 RAILPLUG MODELING TASKS	24
4.1 Railplug Plasma Jet Modeling	24
4.2 Multidimensional Engine Modeling	27
5.0 PROOF OF PRINCIPLE: EXTENSION OF THE DILUTION TOLERANCE OF SPARK IGNITION ENGINES	32
5.1 Initial Results in a Research-Type Engine	32
5.2 Further Lean Limit Studies	34
5.2.1 Experimental System	34
5.2.2 Engine Results	35
5.3 Application to a Production SI Engine	38
6.0 PROOF OF PRINCIPLE: DIESEL COLD START	41
6.1 Experimental System	41
6.2 Engine Results	43
7.0 DURABILITY	46
7.1 Initial Studies	48
7.2 Erosion Studies	50
7.2.1 Experimental Setup	50
7.2.2 Results of the Erosion Studies	51
7.3 Engine Studies	53
7.3.1 Experimental Setup	55
7.3.2 Engine Results	56
7.4 Continuing Work	62
8.0 SUMMARY AND CONCLUSIONS	63
ACKNOWLEDGEMENTS	65
BIBLIOGRAPHY	65
APPENDICES	
App. A. List of Theses and Dissertations Supported in Whole or in Part by the Railplug Project	69
App. B. Copies of Publications Resulting from the Railplug Project	70

1.0 INTRODUCTION AND BACKGROUND

A three year investigation of a new type of ignitor for internal combustion engines has been performed using funds from the Advanced Energy Projects Program of The Basic Energy Sciences Division of the U.S. Department of Energy and with matching funding from Research Applications, Inc. This project was a spin-off of "Star Wars" defense technology, specifically the railgun. The "railplug" is a miniaturized railgun which produces a high velocity plume of plasma that is injected into the combustion chamber of an engine. Unlike other types of alternative ignitors, such as plasma jet ignitors, electromagnetic forces enhance the acceleration of the plasma generated by a railplug. Thus, for a railplug, the combined effects of electromagnetic and thermodynamic forces drive the plasma into the combustion chamber.

Several engine operating conditions or configurations can be identified that traditionally present ignition problems, and might benefit from enhanced ignition systems. One of these is ultra-lean combustion in spark ignition (SI) engines. This concept has the potential for lowering emissions of NO_x while simultaneously improving thermal efficiency. Unfortunately, current lean burn engines cannot be operated sufficiently lean before ignition related problems are encountered to offer any benefits. High EGR engines have similar potential for emissions improvement, but also experience similar ignition problems, particularly at idle. Other potential applications include diesel cold start, alcohol and dual fuel engines, and high altitude relight of gas turbines. The railplug may find application for any of the above. This project focused on three of these potential applications: lean burn SI engines, high EGR SI engines, and diesel cold start.

Other than the background information that is presented in the remainder of this section, this final report consists of:

- overview of the project
- detailed discussions of each of the tasks
- Summary and Conclusions

As noted above, the remainder of this section presents relevant background information. Alternative ignitors are reviewed in the next subsection, followed by a discussion of railgun theory, and then by a discussion of the characteristics of railguns that make a miniaturized version attractive as a new type of alternative ignitor.

1.1 Alternative Ignitors

Driven primarily by the potential of lean burn engines, many advanced ignitors have been proposed and studied. The most actively studied concepts include 1) conventional and surface discharge spark plugs with a higher energy input, 2) prechamber torch ignition systems, 3) various types of plasma jet ignitors, and 4) pulsed jet ignitors. The attributes of many of these advanced ignitors were discussed in a paper by Dale and Oppenheim (1981). A brief review is presented below.

High energy and surface discharge spark plugs are, at present, the ignitors most often used in attempts to develop lean-burn engines. Such spark plugs have been used to operate an engine at an air-fuel ratio (AF) of 23.5:1 ($\phi = 0.62$, where ϕ is the equivalence ratio, which is the fuel-air ratio normalized by its stoichiometric value) but, although this is essentially as lean as any realistic engine has operated on gasoline (natural gas engines have reached 26:1, but ϕ is still ≈ 0.64), it is not sufficiently lean to offer significant advantages. Also, although these plugs have the capability of igniting lean mixtures, they do nothing to solve the other problems of lean burn engines, such as slow combustion. Honda and Mitsubishi have recently announced production engines which will operate with an AF = 23:1. However, the goal is an air-fuel ratio of at least $\phi = 0.57$ (AF = 26:1 for gasoline).

Torch ignitors or torch cells have an essentially conventional spark plug located in a prechamber that is separated from the main chamber by an orifice (e.g., Namekawa et al., 1988), and thus rely solely on thermal expansion to produce a hot jet of reactive species that ignites a lean mixture in the main chamber. One of the problems of this method is that

a fresh mixture must be externally supplied to the prechamber prior to each ignition. The Honda CVCC engine is the most widely recognized example of this concept and uses an auxiliary intake valve to admit an ignitable mixture to the prechamber. High hydrocarbon emissions and high brake specific fuel consumption (bsfc) are encountered as the system approaches $\phi \approx 0.66$ (Wyczalek, 1975).

The plasma jet ignitor is similar to the torch cell in that it has a very small prechamber, or cavity, near the exit of the ignitor. An orifice at the cavity exit is often used to pressurize the ionization and combustion products and cause a hot jet of reactive species to issue into the combustion chamber. Open cavity designs are also common (Asik et al., 1977; Edwards et al., 1983; Kupe et al., 1987). Plasma jet ignitors can effectively ignite a mixture outside the ignitor when there is not a combustible mixture in the cavity (Smy et al., 1985). When fuel is introduced into the cavity, it acts as a feed stock of hydrogen atoms to the plasma, creating a more chemically active plasma with enhanced ignition capabilities (Orrin et al., 1981). The fuel/air mixture within the cavity need not be within normal combustion limits to achieve this effect. An ignition energy of 0.5-10 J is typically used. Asik and coworkers (1977) compared the performance of plasma jet ignitors with conventional spark plugs and with high energy spark plugs in both a single cylinder engine and a 4 cylinder test vehicle. They found that the plasma jet ignitors extended the lean limit and decreased the duration of combustion, but increased NO_x emissions. They concluded that the plasma jet ignitors showed no overwhelming advantages, but noted that their test data were both preliminary and limited in scope. Dale and coworkers (1978) compared the performance of plasma jet ignitors with conventional spark plugs in two different single cylinder engines. They found that the plasma jet ignitor could ignite mixtures as lean as $\phi \approx 0.58$ (AF = 25:1) on gasoline, but the specific fuel consumption and hydrocarbon emissions began increasing rapidly at $\phi \approx 0.66$ (AF 22:1). Edwards and coworkers (1978, 1983) showed little improvement with use of plasma jet ignitors of various designs, and partial burn was shown to be the limiting factor. The plasma jet ignitors were able to extend the Lean Operating Limit (LOL, the equivalence ratio at which the COV of the imep tends to infinity) of a CFR engine to $\phi \approx 0.54$, whereas for conventional spark plugs the LOL is $\phi \approx 0.67$, but the plasma jet ignitors showed little improvement in the Lean Stability Limit (LSL, the equivalence ratio at which the COV of the imep is 10%) and, at $\phi \approx 0.6$, the indicated thermal efficiency began to decrease drastically and the HCs began to increase rapidly. Some research continues in this area (Kupe et al., 1987; Murase et al., 1989; Modien and Dale, 1991) but the limit is still $\phi \approx 0.6$. Furthermore, one of the primary difficulties with plasma jet ignitors has been high electrode erosion rates due to the high electrical energies associated with these plugs. Tozzi and Dabora (1982) found the lifetimes of plugs they tested to be limited to about one hour of operation. A recent paper claims 40 hours of operation (Kupe et al., 1987), which is much better than prior plasma jet ignitors but translates into only 800 miles for an average speed of 20 mph (approximately the average over the 75 FTP driving cycle). The only type of plasma jet ignitor that claims to function by developing an electromagnetic force and for which experimental evaluations have been reported in the technical literature is that developed by Fitzgerald (1976, 1978). However, Fitzgerald's plasma jet ignitor has an essentially continuously increasing plasma surface area and a continuously decreasing magnetic field strength. This results in a continuously decreasing electromagnetic force available to accelerate the plasma. Further, because the electrodes are exposed to each other for only a very short length, the plasma is weakly accelerated from zero velocity for only a very short period of time. Thus, the resulting electromagnetic pressure has been shown to be negligible (Clements et al., 1981). In recognition that the electromagnetic effect of these plasma jet ignitors was negligible, present designs generally do not incorporate any electromagnetic effect and rely solely on thermal expansion of the product mixture through one or more orifices at the end of the ignitor cavity. Thus, thermal expansion dominates the physics of jet formation and penetration of the plasma jet ignitors.

Pulsed jet ignitors or combustion jet ignitors are similar in concept to plasma jet ignitors. However, in this case the design incorporates a small tube through the plug which is used to supply a fuel-air mixture from a separate source. This assures the availability of an easily ignitable mixture in the plug cavity, so that the high energies that result in poor durability are not needed. Also, the fact that a near-stoichiometric mixture is fed into the cavity assures additional thermal expansion due to energy release by combustion in the cavity. Obviously, this requires a separate fuel/air mixing and delivery system. Early applications in bombs were reported by Oppenheim and coworkers (1978) and by Weinberg and coworkers (1978, 1981). Tozzi and Dabora (1982) applied pulsed jet ignitors to a CFR engine and found that they allowed operation down to $\phi \approx 0.60$, at which point the CO and HCs began to increase rapidly. Recent research in a combustion bomb (Oppenheim et al., 1989) has shown an increase in peak pressure and faster combustion compared to ignition by a spark plug.

With the exception of the high energy spark plugs, all of the ignitors discussed above cause a hot, chemically reactive jet to be injected into the combustion chamber via thermal expansion of the products of ionization and/or combustion which are partially confined in the plug cavity by one or more orifices. That is, when the arc jumps across or within the cavity, the gas within the arc is ionized and the remainder of the mixture in the cavity is thermally heated; the orifice causes a pressure increase until a jet issues from the cavity through the orifice. If a combustible mixture is contained within the cavity, there is a much larger increase of pressure resulting in a higher velocity jet. Thus, thermal expansion dominates the physics of jet formation and penetration of these prior alternative ignitors, and they will not perform optimally unless there is a combustible mixture in the cavity.

1.2 Railgun Theory

Figure 1 is an illustration of a simplified railgun, or a railplug depending upon the magnification assumed by the reader. The simplest railgun consists of two parallel conducting electrodes, or "rails", enclosed in a cavity similar to the barrel of a gun. The rails are fixed in place and the barrel is completed by non-conducting walls. When a sufficiently high voltage is applied across the rails to electrically break down the gap between them, an arc jumps across the rails. The "current loop" attained by the electrical current flowing down one rail, across the arc, and back up the other rail produces a magnetic field. An electromagnetic force or Lorentz force is thereby created as a consequence of the interaction of the self induced magnetic field with the ions (electrons and positive ions) in the plasma arc. The Lorentz force accelerates the plasma out of the railgun (or railplug). In Figure 1, the direction of the magnetic field is perpendicular to the plane of the paper. The electron flow is up one rail, across the arc, and down the other rail. As just noted, this current loop results in the Lorentz force:

$$F = qv \times B \quad (1)$$

where F is the force exerted on a charged particle, q is the charge of the particle, v is the velocity of the particle, and B is the strength of the local magnetic field. The above expression is often written in terms of the force per unit volume acting on the charged particles. This expression, obtained by dividing both sides of the above equation by the charge density is:

$$F = J \times B \quad (2)$$

where J is the current flow per unit area.

If a constant current (i) is supplied to parallel rails, the Lorentz force is:

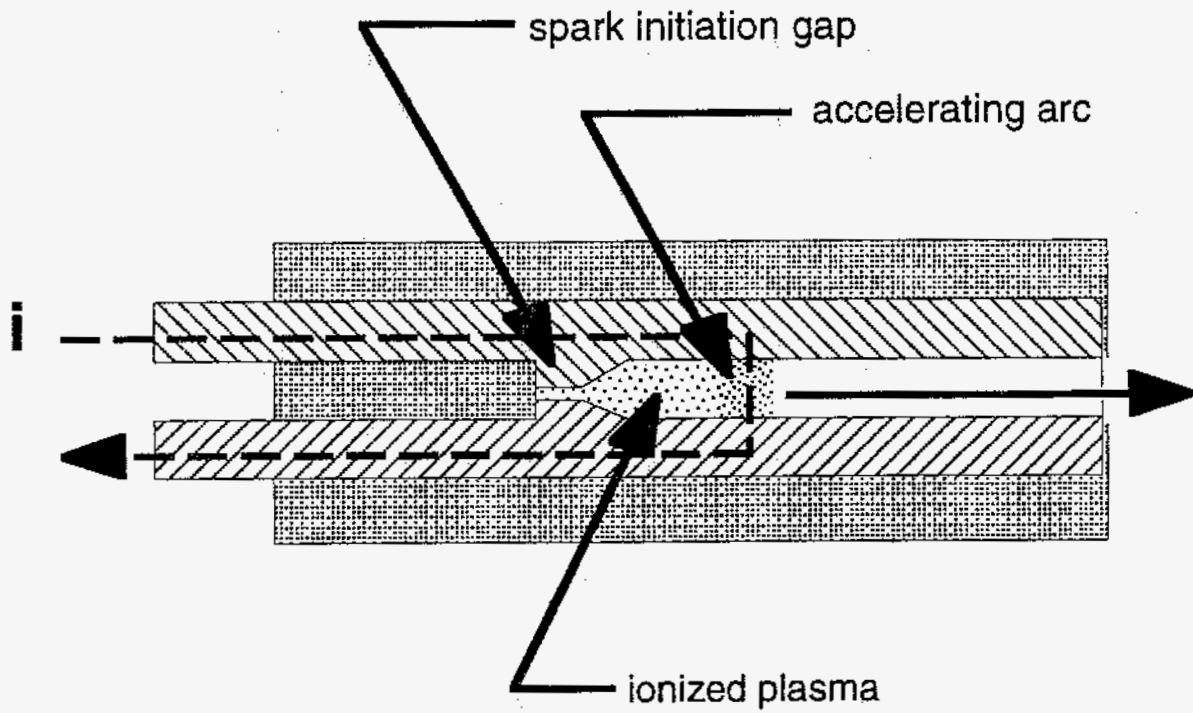


Figure 1. Schematic of a railgun or parallel railplug.

$$F = \frac{1}{2} L' I^2 \quad (3)$$

where L' is the inductance per unit length of the rails. Also, in this case the voltage supplied to the rails (V) is divided into three components:

$$V = iR'x + V_{\text{arm}} + iL'u \quad (4)$$

where R' is the resistance per unit length of the rail pair, x is the distance from the breech, V_{arm} is the voltage drop across the plasma, and u is the plasma velocity. The term $iR'x$ represents the energy dissipated in the rails. The term $iL'u$ is called the "speed voltage", because this term represents the portion of the electrical energy that accelerates the plasma. In turn, the electrical power is:

$$P = i^2R'x + iV_{\text{arm}} + i^2L'u \quad (5)$$

Thus, it is possible to apportion the amount of energy used to heat the plasma from that used to accelerate the plasma via control of the current and L' - high L' yields high acceleration. For cylindrical conductors of radius r that are removed from an external conducting boundary, the inductance per unit length is:

$$L' = 0.4 \times 10^{-6} [\ln(d/r) + (1/4) - (1/R_a)] \quad (6)$$

in $\mu\text{H/m}$, where d is the separation distance between the centroids of current distribution in each rail and R_a is the aspect ratio, which is the rail length divided by the rail separation. For large railguns, the last term is negligible because the aspect ratio is very large. For miniaturized railguns, this term may not be negligible. If the rails are enclosed within a conducting boundary (e.g., a spark plug housing) such that the inside diameter of the boundary is about three times the rail diameter, the result will be about a 10% loss of L' in comparison to the result from Equation 6. As the ratio of the boundary diameter to the rail diameter decreases further, a more substantial loss of L' results.

Large railguns typically use currents of millions of amperes over a few milliseconds (Gigawatts of power) to produce plasma temperatures of 10,000 to 50,000 K and plasma velocities that can exceed the escape velocity from the solar system (tens of kilometers per second). By arranging the rails in coaxial, diverging, converging, or helically wound configurations, a wide variety of plasma jet flow patterns can be achieved. The armature in a full scale railgun is usually a solid, such as aluminum, but hydrogen and metal vapor plasma armatures have also been studied.

1.3 Railplugs

Several characteristics of railguns make their miniaturization attractive as a promising new alternative ignitor. The ability to take full advantage of an electromagnetic force to accelerate the plasma is the most obvious of these. In contrast to other advanced ignitors, thermal expansion augments but does not dominate the jet ejection forces of the railplug. The railplug is designed to maximize the integrated $J \times B$ product to accelerate the plasma. In addition, the self induced magnetic field results in an inherently simple design which will enhance reliability and manufacturing economy. Furthermore, since the arc is not stationary as in the case of a plasma jet ignitor, electrode erosion should be reduced. As noted above, electrode erosion has been one of the most severe limitations preventing the application of plasma jet ignitors. For the railplug, durability should not pose the same difficulty since the energy is deposited over a much larger surface area, since the arc is accelerating down the rails leaving little time available for erosion, since the arc can be initiated with currents equivalent to those of spark plugs (the plasma initiation gap is about

the same as a spark gap) and then the current can be ramped up to higher levels as the arc accelerates down the rails, and since suitable materials can be used near the breech end (i.e., the plasma initiation end) of the railplug where wear rates would be highest. Another strong advantage of the railplug over combustion jet or torch ignitors is that it is not necessary to purge the cavity or to supply fresh mixture - the plasma is created from whatever molecules are present in the cavity at the time of ignition. A final advantage of the railplug is that it generates a relatively large mass of plasma since the arc sweeps down the rails, ionizing essentially all of the gas in its path.

From the present perspective, it is of interest to examine some prior research that appears, at least superficially, to involve examination of railplugs. Bradley and Critchley (1974) studied the electromagnetically induced motion of ignition kernels produced by several different electrode geometries. This included a "parallel" electrode configuration similar to a railplug. However, in their "parallel" electrode configuration, the electrodes were unenclosed and the parallel electrodes were actually angled toward each other to ensure that the spark was initiated at the very end of the rails, which for a railplug is the exit or muzzle end. This left no distance over which to accelerate the arc down the electrodes. Consequently, the induced gas velocities they found were very small (< 25 m/s). In the same year, Harrison and Weinberg (1974) examined what they termed to be a "rail accelerator". However, in this case, the voltage supply was attached to the rails about 40% of the distance down the rail length from where the arc was struck. Thus, the self-induced Lorentz force was acting in the direction opposing the movement of the plasma until the plasma had moved about 40% of the distance down the rails. An external magnetic field was used, which undoubtedly partially compensated for this. At atmospheric pressure, this rail accelerator was able to fire an argon plasma about 5 cm past the exit.

2.0 PROJECT OVERVIEW

This section provides a brief overview of the tasks performed during this project, which included:

- development of railplugs and driver electronics (discussed in this section)
- studies of the effects of railplug geometry and of the driver electronics on railplug performance
- use of models to improve understanding of railplug physics
- proof of principle for extension of the dilution tolerance of SI engines
- proof of principle for diesel cold start
- examination of the factors that influence the durability of railplugs

Each of these is briefly reviewed in this section to provide an understanding of the organization of the project. Here, it should be noted that the various tasks can be generally categorized as either 1) railplug design, 2) power electronics, 3) experimental proofs and principle and related experimental tasks, or 4) durability. Investigators at the Center of Energy Studies (CES) under the direction of Prof. Ron Matthews (PI) and his Project Manager, James Chiu, were in charge of most of the experimental tasks, although a few fundamental experiments, primarily related to durability, were performed by the researchers at the Center for Electromechanics (CEM). The railplug design, power electronics, and durability tasks were performed primarily by investigators at the Center for Electromechanics, under the direction of Prof. Bill Weldon (co-PI) and his Project Manager, Richard Faidley, although some durability studies were performed by the CES researchers. Here, it is important to note that durability studies were not originally included in the proposed work. However, after we began showing that railplugs showed significant promise, our External Advisory Board requested that we examine this issue. This additional task required that we decrease the level of effort on some of the tasks that were originally proposed.

An External Advisory Board was assembled to help guide this project. The members of this board are listed in Table 1. It should be noted that some of the members

Table 1. RAILPLUG EXTERNAL ADVISORY BOARD

Larry Amstutz
Chief, Electrical Machinery Team
Belvoir RD&E Center, Bldg. 326
Fort Belvoir, VA 22060
(703) 664-5081 or 5587

Dr. Richard W. Anderson
Principle Staff Engineer, Engine Research Dept.
Ford Motor Company
Suite 800, VP
23400 Michigan Avenue
Dearborn, MI 48124
(313) 322-4657; FAX 313-323-1875

Dr. Thomas W. Asmus
Powertrain Research Specialist
Chrysler Motors Corporation
Detroit, MI 48288-1118
(313) 252-8568; FAX 313-252-7152

Norris J. Bassett
Manager of Advanced Ignition Development
Mail Station 18-211
Delco-Remy Division
General Motors Corp.
P.O. Box 2439
Anderson, IN 46018
(317) 646-2144; FAX 317-646-7470

Dr. Sam W. Coates
Manager, Computational Engineering
Mercury Marine
P.O. Box 1939
Fond du Lac, WI 54936-1939
(414) 929-5035; FAX 414-929-5060

Dr. Thomas M. Kiehne
Assoc. Director, Institute of Advanced Technologies
The University of Texas
Austin, TX 78712
(512) 471-9060; FAX 512-471-9096

Walter M. Kreucher
Manager, Advanced Environmental Engineering
Ford Motor Company
World Headquarters
The American Road, Room 259
Dearborn, MI 48121-8247
(313) 845-8247

Dr. Scott W. Jorgensen
Sr. Research Engineer, Fuels and Lubricants Dept.
General Motors Research Labs
30500 Mound Road
Warren, MI 48090-9055
(313) 986-1915; FAX 313-986-2094

Don McCaw
Alternative Fuels, 81U
Engine Engineering
John Deere Product Engineering Center
P.O. Box 8000
Waterloo, Iowa 50701
(319) 292-8233

Ron Nitschke
Powertrain Division, General Motors Corporation
895 Joslyn Avenue
Pontiac, MI 48058-1493
(313) 857-2282; FAX 313-857-1251

Dr. Peter J. O'Rourke
Group T-3, MS B216, Los Alamos Natl. Laboratory
Los Alamos, NM 87545
(505) 667-9091; FAX 505-665-4055

James E. Sibley
Sr. Staff Engineer, System Technology Division
Caterpillar, Inc.
Engine Division
P.O. Box 610
Mossville, IL 61552-0610
(309) 578-8329; FAX 309-578-8433

Daniel L. Tribble
Vice President, Product Engineering
Champion Spark Plug Company
P.O. Box 910 (900 Upton Ave.)
Toledo, OH 43661-0001
(419) 535-2190; FAX 419-535-2147

Randy Williams
Supervisor - Combustion Group
Garrett Auxilliary Power Division
Dept. 93-732/1302-2R
2739 E. Washington St., PO Box 5227
Phoenix, AZ 85010
(602) 220-3547; FAX 602-220-3292

Charles D. Wood
Vice President
Engine and Vehicle Research Division
Southwest Research Institute
P.O. Drawer 28510
San Antonio, TX 78284
(512) 522-2618; FAX 512-522-2019

of this board were able to serve for only a portion of the project's duration. Others volunteered to serve but were unable to attend any of the meetings of the board. Several attended all meetings, which were normally held twice each year.

Of course, the first task was to develop miniaturized railguns (railplugs) and suitable driver electronics. These tasks continued over most of the period of this research project. Railplug geometries examined ranged from simple parallel rail configurations (as illustrated in Figure 2) which were useful for fundamental studies but were not suitable for engines, to coaxial railplugs that were fabricated from standard spark plug components and were used for engine studies (as illustrated in Figure 3). Four categories of driver electronics were also developed throughout this project. First, a "low speed" electronics system was used, as illustrated in Figure 4. This first generation of driver electronics was similar to the driver electronics used for plasma jet ignitors and consisted of components that were acceptable for use in single shot combustion bomb experiments and low speed engine experiments. A conventional spark ignition system is used to initiate breakdown at a spark gap at the breech of the cavity. Once breakdown has occurred, additional electrical energy is supplied from storage capacitors, and the arc is accelerated down the rails toward the exit. This is called the "follow-on" circuit. An external spark gap was used to prevent energy flow from the follow-on circuit back through the breakdown circuit, assuring that the follow-on energy would go to the railplug. An inductor was used to isolate the initiation voltage from the capacitor and to control the discharge rate of the capacitors, allowing the current history to be controlled. The amount of energy stored in the capacitors is $1/2 C V^2$, where C is the capacitance and V is the voltage applied to the capacitors. The capacitors initially used were 130 μF , which were later found to have poor durability for repeated firings and also limited the choice of charging capacitance for "electronics matching" studies. Later testing used 50 μF capacitors which were able to withstand repeated firings during engine testing. Also, after our early experiments showed that inductance reduced the acceleration of the plasma, all intentional inductance was removed for the second generation system shown in Figure 5. Furthermore, in the second generation electronics the external spark gap was replaced by a high voltage diode and a blocking capacitor to isolate the breakdown from the follow-on systems. A third firing circuit, shown in Figure 6, was also developed. This "series" or "high voltage" circuit supplies equivalent energy at a high voltage over a shorter period of time. This third circuit was used in some of the tests that were focused on elucidating the effects of the electrical energy parameters on railplug durability. The final electronics circuit design developed was used to run a production four cylinder engine. This system consisted of an optical encoder to determine ignition timing, one capacitor charging unit, one set of capacitors, and four trigger circuits. These four trigger circuits are necessary because this particular engine is a distributorless or direct-fire ignition system. In such systems, one coil fires two spark plugs simultaneously (one of which is on the exhaust stroke). This means that the plug housing on one of the spark plugs is positive while that on the other spark plug is negative. This is not acceptable for railplugs. Thus, an optical encoder is used to tell our electronics system what the instantaneous crank angle is, and then this system sends a signal to the appropriate trigger circuit to send a spark to that cylinder at the appropriate time.

Our experimental tasks consisted of 1) fundamental studies of the effects of various parameters on railplug performance, 2) studies of the ability of railplugs to extend the dilution limit of spark ignition engines, 3) studies of the ability of railplugs to extend the cold start limit of a production indirect injection diesel engine (the type of diesel used for light duty vehicles), and 4) railplug durability studies. In summary:

- 1) We learned much about the effects of railplug geometry on railplug performance (but believe that more can still be learned with respect to geometry effects).
- 2) We learned that the current pulse shape provided by the follow-on circuit must be matched to the specific geometry under study (thus adding another level of complexity to the experiments).

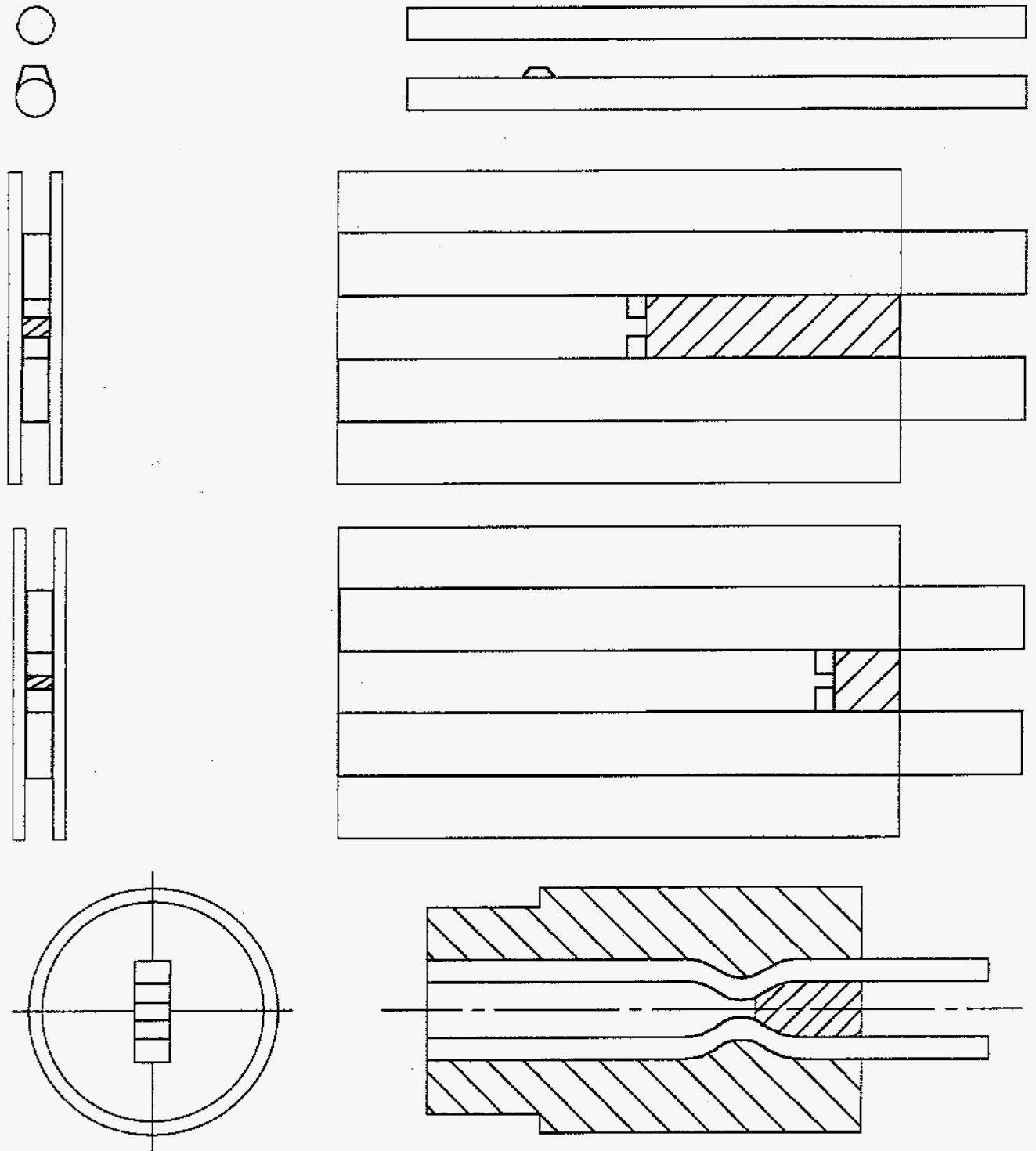


Figure 2. Schematics of parallel railplugs. Top to bottom: unenclosed railplug, short transparent railplug, long transparent railplug, and railplug used in combustion vessel.

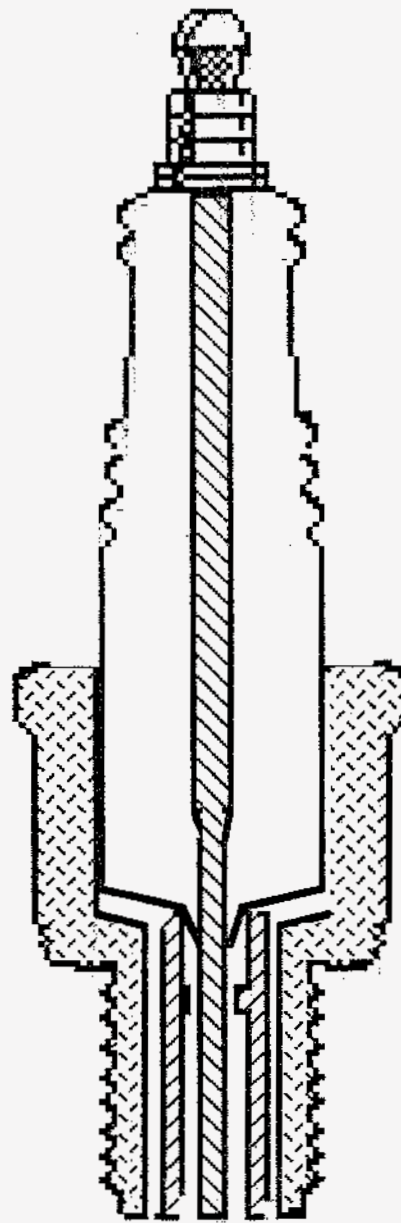


Figure 3. Schematic representation of the Champion 689 coaxial railplug.

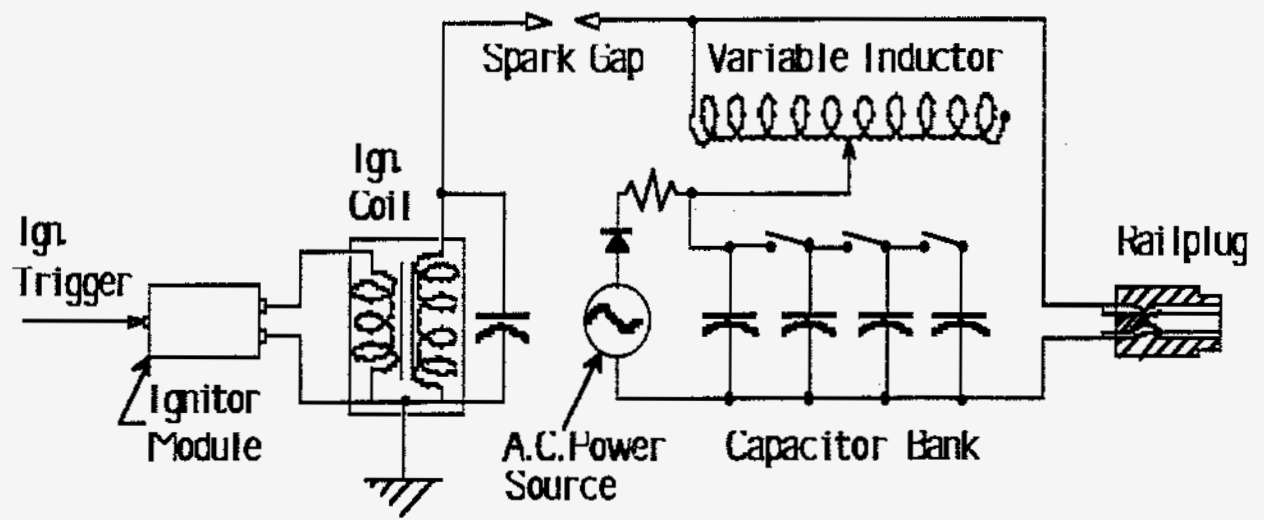


Figure 4. Schematic of first generation railplug electronics.

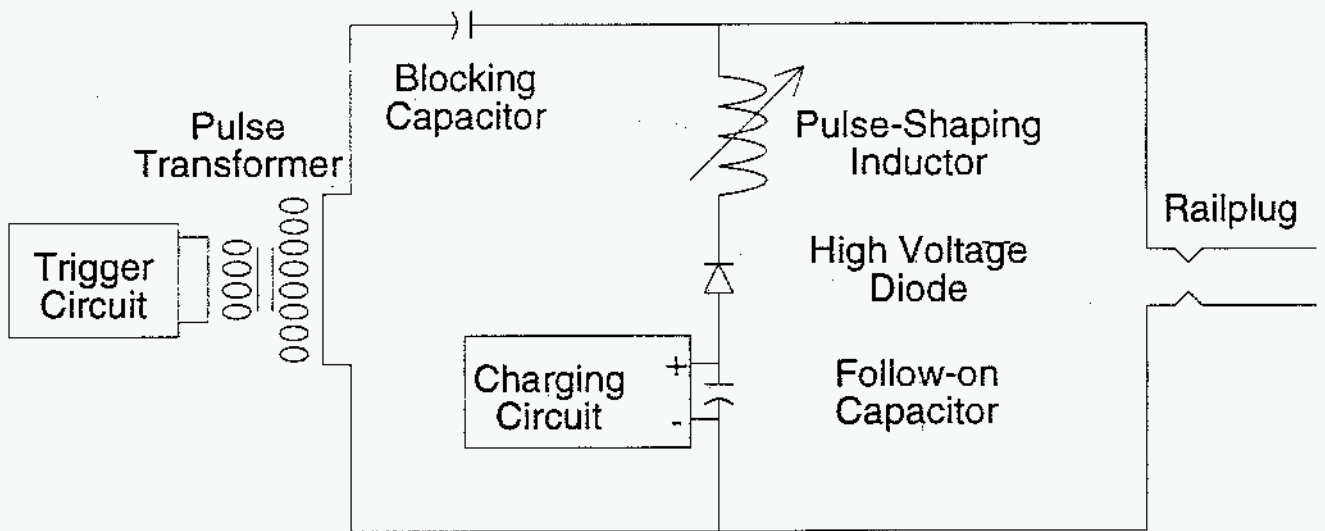


Figure 5. Typical second generation driver electronics for railplugs, including low voltage follow-on circuit.

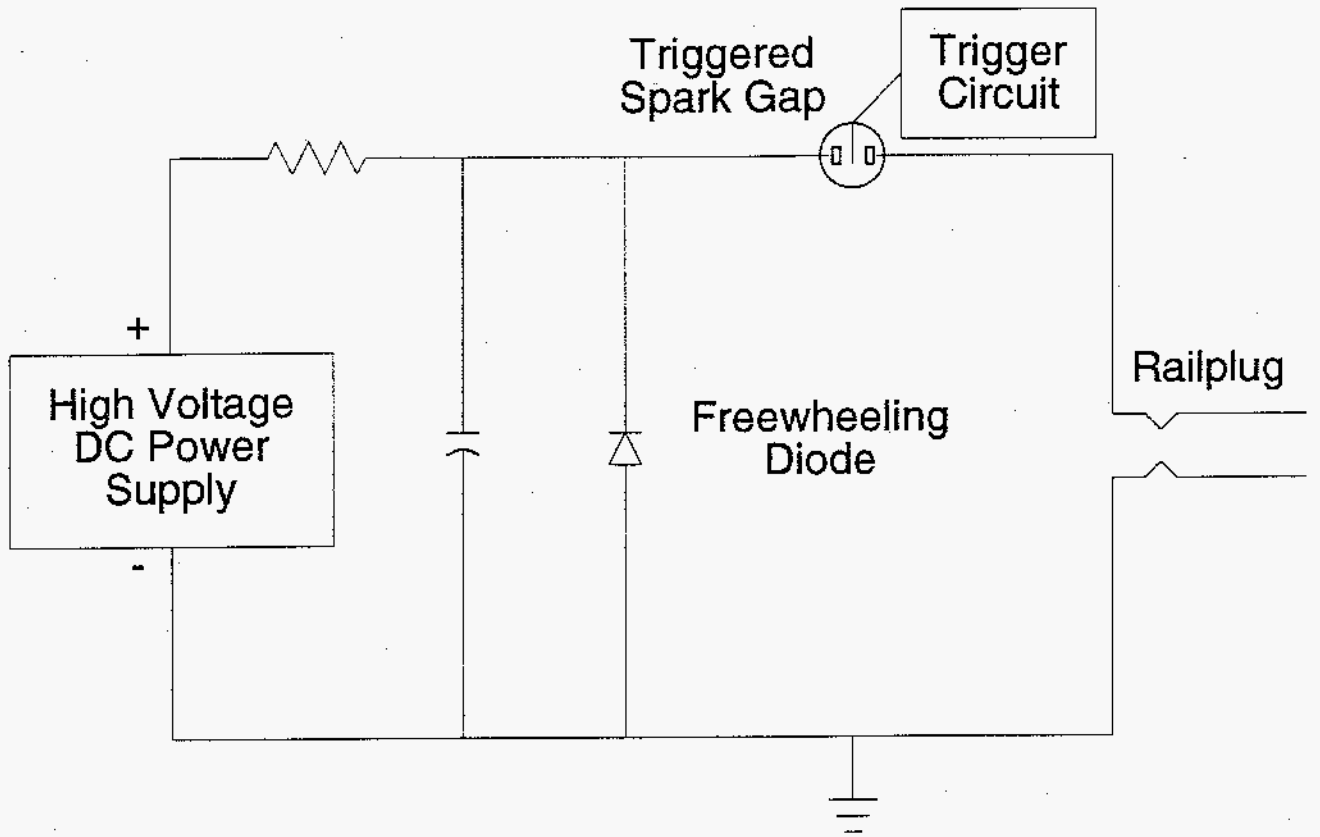


Figure 6. High voltage or series firing circuit for railplugs.

- 3) We learned that extremely high plasma jet velocities can be achieved and that this both creates turbulence at the flame front and induces flow in the unburned gases that, in turn, results in a preferred direction of flame propagation (along the jet axis).
- 4) We learned that parallel rail railplugs perform better than coaxial railplugs. However, parallel railplugs are extremely difficult to fabricate. Thus, we focused our remaining studies on the coaxial design. Most of the railplugs we used thereafter were made for us by Champion Spark Plug Company using standard spark plug production parts. This means that railplugs should cost little more than conventional spark plugs.
- 5) We believe that we convincingly proved that railplugs can extend the dilution limits of SI engines. This belief is supported by feedback from members of our External Advisory Board. Thus, the primary issue for commercialization is durability.
- 6) We proved that we can significantly improve the cold start limit of IDI diesels using railplugs with reasonable energies. While we have not explicitly examined railplug durability in a diesel environment, only about 50,000 successful firings are required to be competitive with glow plugs and we have demonstrated 10 times more firings in a SI engine environment. However, the U.S. auto manufacturers appear to be abandoning the IDI diesel in favor of direct injection (DI) diesels for light duty vehicles. While we believe that our IDI experiments also serve as a proof of principle for DI diesels, others would like to see direct proof and no funds are available for these additional experiments.
- 7) Over the course of the project, we improved the durability of railplugs from ~20,000 firings to ~1,000,000 firings. About 400,000,000 firings are required to be competitive with spark plugs. While we examined several materials (for the center rail, which is the site of failure due to inability to transfer heat away sufficiently fast) and several railplug geometries, we believe that much more can be accomplished in this area. Most importantly, we found that the design of our initiation gap was promoting failure so that additional geometries should be examined. We also know that use of a series power supply for the follow-on circuit aids durability, but never fabricated such a system that was adequate for engine testing. Further, we believe that further progress can be made with respect to center rail materials. Again, it should be noted that this task - durability - was added after the start of the project, so that it was not possible to devote as much manpower to this task as we would have preferred. We are continuing our work in this area, but with a low level of effort due to lack of funds. One option is to explore applications that do not require as much durability. One example is diesel cold start, as discussed under Item 6 above. Another example is cold start of neat alcohol engines. In this case, the railplug would function as a railplug to achieve cold start and then would function as a spark plug during normal operation, thereby minimizing the number of high energy firings required. Although not mentioned in any of our papers, we have shown that railplugs operate very satisfactorily as spark plugs if we only provide the breakdown pulse without the high energy follow-on pulse. We submitted a Letter of Intent for exactly this type of project to NREL, but were not requested to submit a formal proposal. We are now exploring possibilities in this area with researchers at Southwest Research Institute. Another example is drag racing of highly turbocharged engines. Achieving ignition in these engines is very difficult, so that they use very high energies, but find that the spark plugs have vaporized before the end of the 1/4 mile race. We have shown - but have not reported - that railplugs are much more durable than spark plugs when the same high energy is supplied to both. The difficulty with this application is finding a source of funding. One attribute of this application is that it would attract a lot of positive attention, thereby possibly making it easier to attract the funding needed for additional durability research. A different option is to explore SI engine applications for which the achievement of lean-burn may be more important than required plug replacement intervals. The large bore stationary natural gas engine is one example. These engines use lean burn to control NO_x emissions, but suffer high hydrocarbon and

formaldehyde emissions as a result of operating so lean that the partial burn limit is encountered. As noted above, we have shown that railplugs can extend the partial burn limit to leaner mixtures, at least for small bore gasoline engines. We are exploring the possibilities of funding for this application with investigators at Southwest Research Institute.

Over the course of this project, we also developed two numerical models to aid our understanding of railplugs and their effects on the subsequent combustion process. The first model was used to simulate the plasma formation and jet ejection processes. We showed that we could accurately predict all of the jet characteristics. We then used the results of this model as input to a multidimensional engine model (KIVA-II). Our goal with this second model was to improve our understanding of how railplugs improve the burning rate of lean burn engines. We found that this is due both to the large "ignition kernel" generated (the plasma jet) and to the inducement of bulk flow in the unburned gas by the high velocity jet. While we had shown this previously in our bomb experiments, the bomb experiments used quiescent mixtures whereas the mixture in an engine is both turbulent and has a bulk flow component. It was not obvious, until this second model was completed, that the jet issuing from a railplug was sufficiently energetic to impose such effects in an engine environment. We now know that railplugs do have this effect in an engine.

Our various tasks are discussed in more detail in the following sections, essentially in the order in which they were discussed in the original proposal. Durability, which was not included in the original proposal, is discussed last. The papers we have written are included in the appendices for additional information.

3.0 FUNDAMENTAL RAILPLUG EXPERIMENTS

In our initial tasks, we examined the performance of railplugs in a non-engine environment. Three papers resulted from these tasks, each of which is summarized below.

3.1 Initial Fundamental Studies

Initially, we examined the performance of parallel rail railplugs (Hall et al., 1991). This is the geometry used for railguns (e.g., Figure 1). The first generation of driver electronics was used (Figure 4).

In these experiments we showed that the Lorentz force is significant even for these small, low current and low energy (compared to a railgun) railplugs. Plasma exit velocities of about 300 m/s were measured for atmospheric pressure firings. In other atmospheric pressure experiments, we found that current pulses that are too short result in rapid deceleration of the plasma while it is still within the railplug cavity. The reason for this behavior is as follows. There is a magnetic inductance associated with the magnetic field produced by the current flow. After the current begins to collapse, the magnetic field seeks to maintain its strength. It does this by removing kinetic energy from the plasma, exerting a Lorentz force on the plasma armature in the opposite direction, a kind of motor/generator effect. The result is the generation of eddy currents in the plasma which rapidly decelerate it. A typical current history is shown in Figure 7. This was our first indication that the current pulse shape must be matched to the geometry of the particular railplug under study: the "electronics matching" issue.

We also measured the rate of pressure rise of a lean methane/air mixture (a fuel-air equivalence ratio, ϕ , of 0.85) in a combustion bomb. This is the leanest condition for which ignition is assured using a conventional spark plug at this pressure (50 psig initially) and initial temperature (ambient). The combustion bomb is described in detail in this paper (Hall et al., 1991). This bomb had a cylindrical combustion chamber 79 mm in diameter (about the same as the bore of a typical engine cylinder) and 2.54 cm in width. Optical access was provided through two quartz windows which gave optical access to the entire chamber for the laser Schlieren and laser shadowgraphy that was done to visualize the propagating flame. The Schlieren and shadowgraph systems are also discussed in detail in

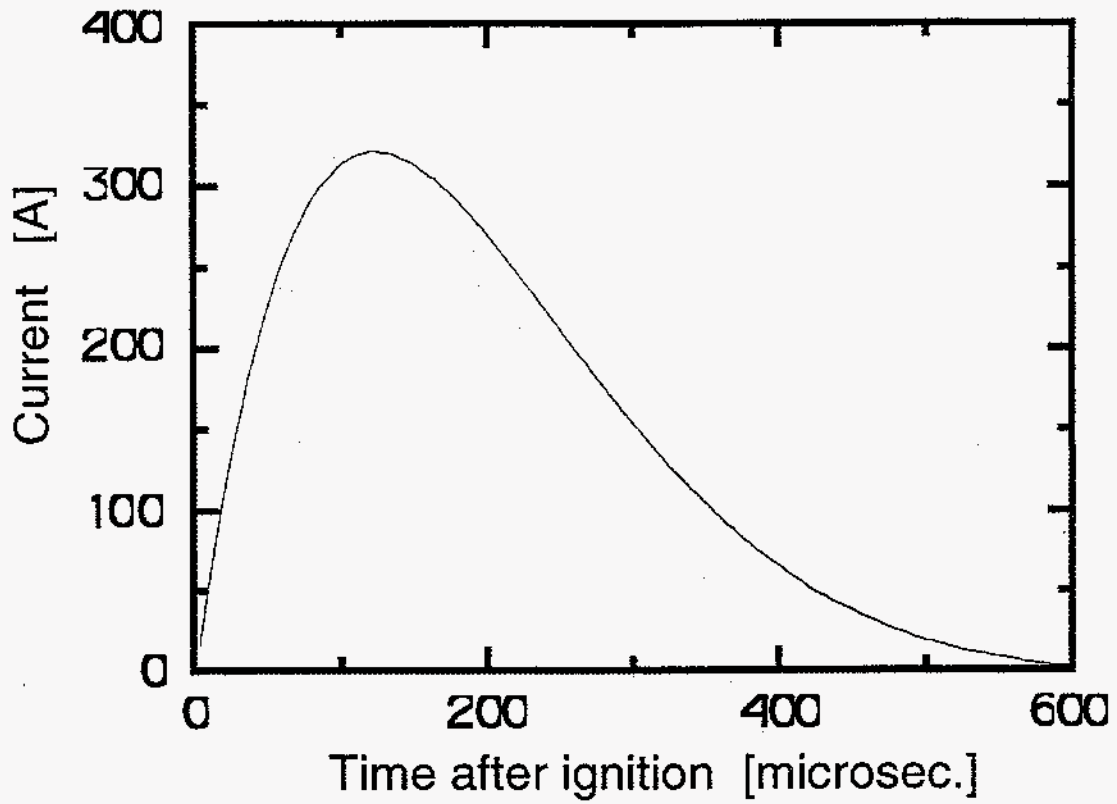


**Figure 7. Typical follow-on circuit current history
(this one was specifically measured for the transparent railplug tests).**

this paper. The bomb also had eight ports located around the circumference of the vessel provided access for the gas intake and exhaust, a pressure transducer, a spark plug, and a railplug.

We compared combustion using a parallel railplug with that using a surface gap ignitor with the same energy as the railplug and also compared to a spark plug using conventional energy. The differences between the railplug, the spark plug, and a surface gap ignitor in combustion duration and ignition delay can be seen in Figure 8, which shows pressure histories for nine firings of each ignitor. Some shot-to-shot variation in the pressure development for each case can be seen in the figure. This was probably due primarily to slight differences in equivalence ratio. The time to peak pressure is approximately cut in half by the railplug while the "ignition delay" is dramatically reduced by the railplug. With the spark plug, almost 10 msec pass before a distinct pressure rise is discernible; with the railplug, however, the pressure begins to rise almost immediately after ignition. The pressure high energy histories of the surface gap ignitor powered by the same electronics and supplied the same power as the railplug are only slightly faster than the conventional spark plug, but are substantially slower than with the railplug. The reasons for the increased rate of combustion using railplugs were revealed by imaging, as discussed in the next paragraph.

Schlieren images comparing railplug with spark plug ignition in the combustion bomb are shown in Figure 9. The spark plug images were taken with the spark plug located at the 9:00 position while the railplug images were taken with the railplug at the 7:30 position on the circumference of the bomb. A highly turbulent jet-like plume produced by the railplug is evident shortly after ignition. The flame front resulting from spark plug ignition remained laminar, and propagated very slowly compared to that resulting from the railplug. The faster rate of flame propagation resulting from the railplug is caused by two factors: the railplug both generates turbulence at the flame surface and also induces a bulk flow in the unburned gases due to the high velocity of the jet. Thus, the flame propagates faster and preferentially in the direction of the jet axis. This preferred direction of flame propagation is not found with conventional or surface gap ignitors.

Finally, we examined the effects of energy on the rate of pressure rise in the bomb when parallel railplugs are used. We found the fastest flame propagation at an intermediate energy. This was our second indication that electronics matching is important.

3.2 Continued Fundamental Studies

In our second paper (Faidley et al., 1992), we compared parallel rail with coaxial rail railplugs. Both railplugs were instrumented with fiber optics to measure the time required for the plasma to pass that measuring point. We found that the parallel geometry provided better performance (i.e., faster jet velocities). However, these railplugs were very difficult to fabricate, so we focused our remaining studies on the coaxial design. Following this decision, most of the railplugs we used thereafter were made for us by Champion Spark Plug Company using standard spark plug production parts. This means that railplugs should cost little more than conventional spark plugs. In this same paper, we reported our first durability results. We used coaxial railplugs manufactured by Champion and referred to as the Champion 689 railplug. This railplug had a tungsten center rail of 0.052 inch diameter. For repeated firings in air at 200 psig, only about 20,000 shots were obtained before we noted an erratic current history for the follow-on circuit. We defined this condition as failure, although it is not obvious that this would affect engine performance.

3.3 Final Fundamental Studies

In our last paper regarding our fundamental studies (Matthews et al., 1992), we compared the performance of various coaxial configurations and also examined the effect of the current pulse shape delivered by the follow-on circuit. The same type of electronics driver developed for the initial studies was used (as in Figure 4) but with no intentional

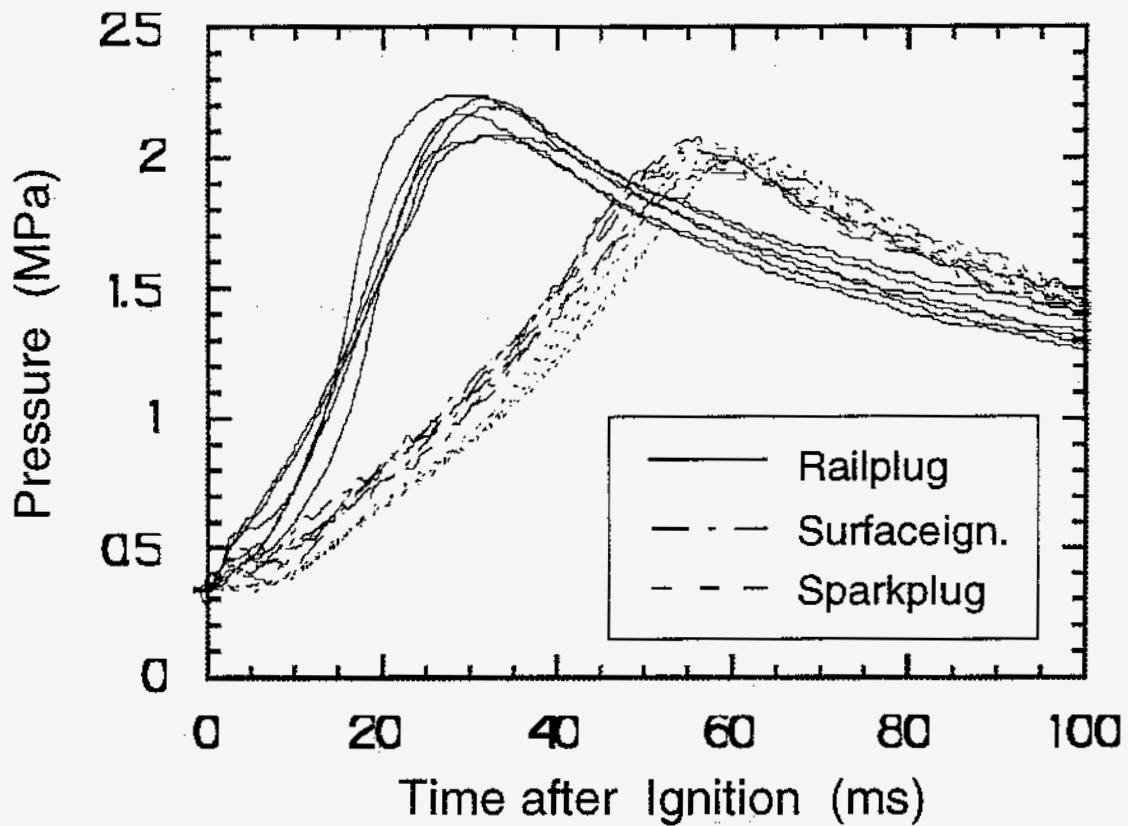
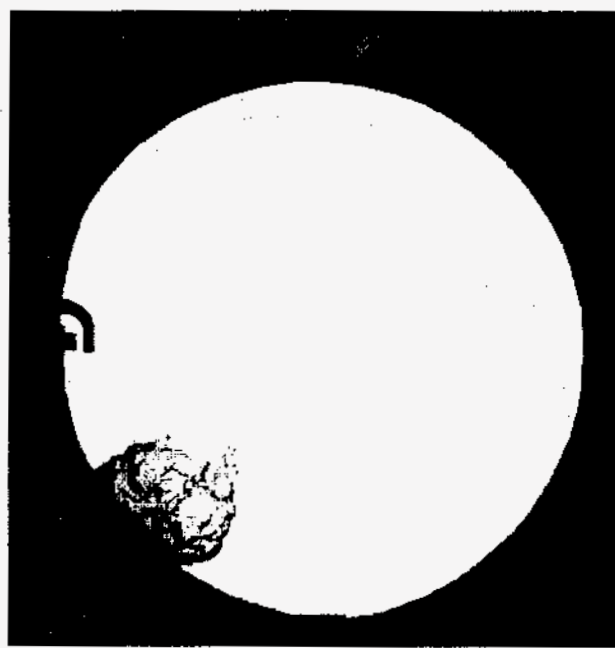
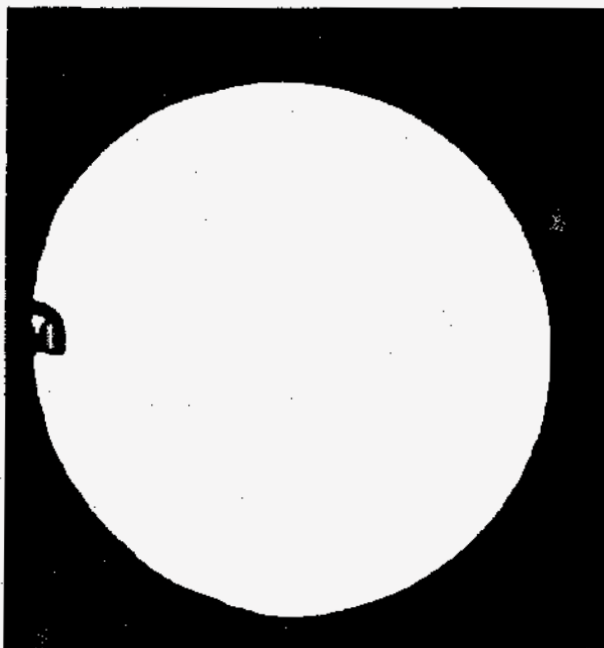
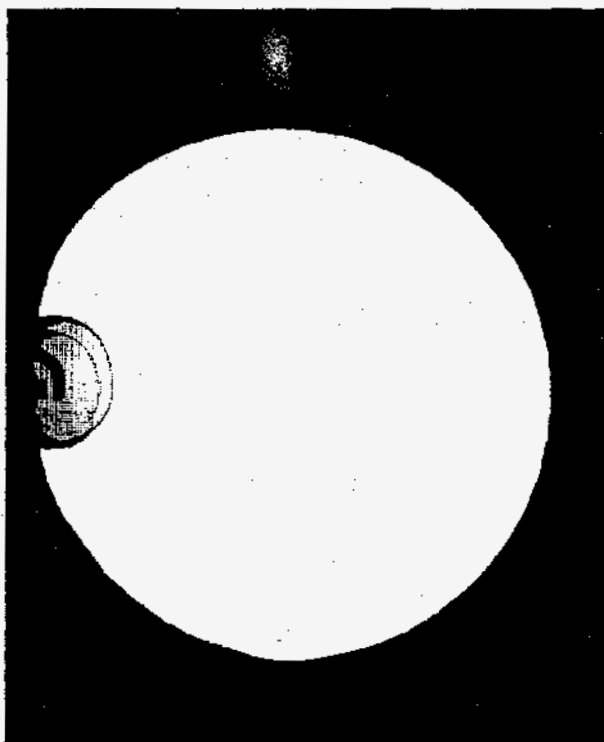


Figure 8. Pressure histories during combustion after ignition using railplug, spark plug, and surface gap ignitors in the constant volume combustion vessel.



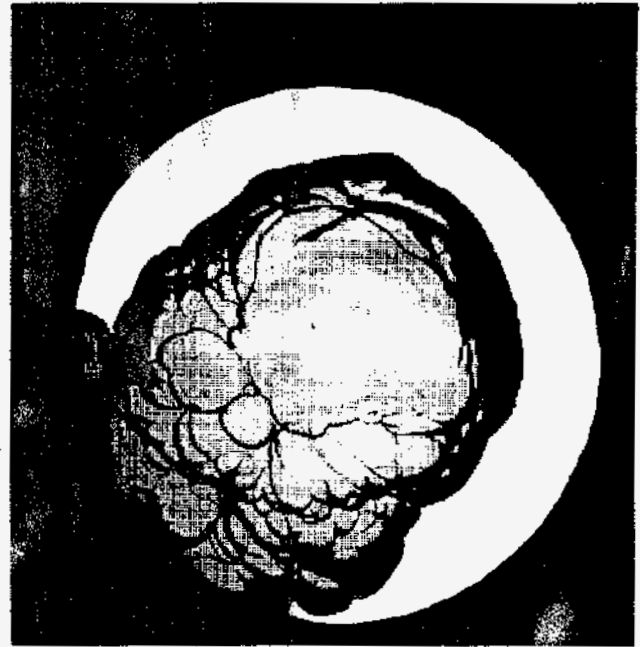
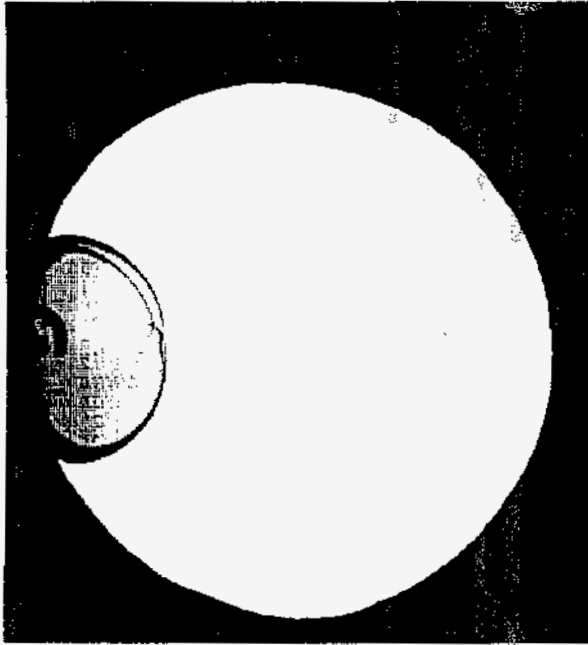
a



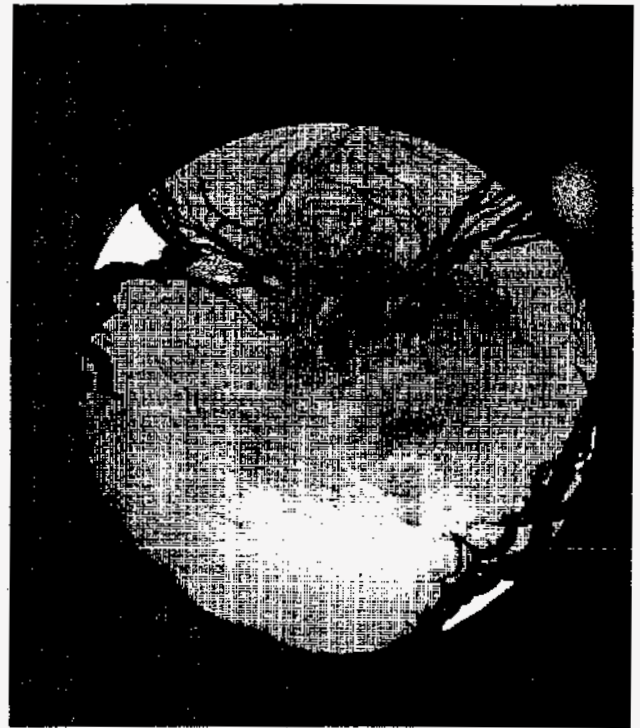
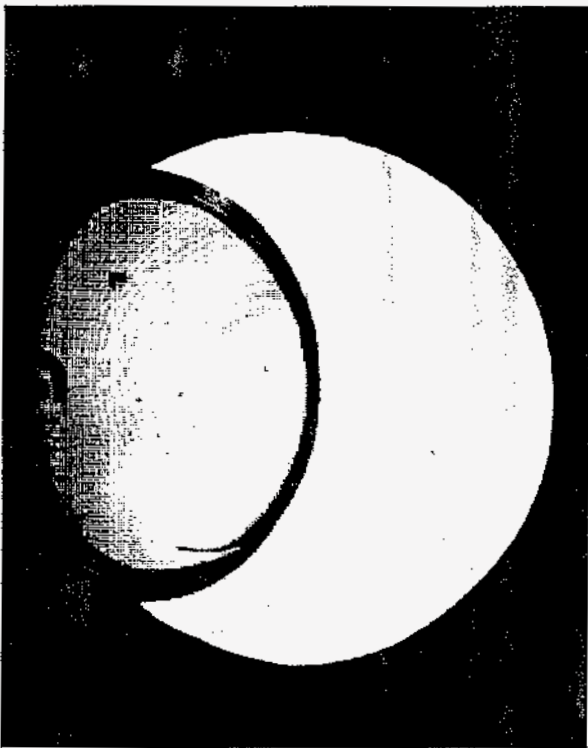
b

Figure 9. Schlieren images of flame propagation in the combustion vessel comparing spark plug (left) with railplug (right) ignition for four times after ignition: a) 0.3 msec., b) 4.6 msec., c) 7.9 msec., and d) 16.6 msec. Note: images (c) and (d) are on the next page.

19
20



c



d

Figure 9 (continued). Schlieren images of flame propagation in the combustion vessel comparing spark plug (left) with railplug (right) ignition: a) 0.3 msec., b) 4.6 msec., c) 7.9 msec., and d) 16.6 msec. Note: images (a) and (b) were on the previous page.

inductance in the follow-on circuit. Performance was judged by the rate of pressure rise of a lean mixture in the combustion bomb described previously (Subsection 3.1). Coaxial railplugs (as illustrated in Figure 3) were evaluated for the reasons discussed in Subsection 3.2. Some of the coaxial railplugs tested were constructed at the University of Texas while others tested were fabricated by Champion using production spark plug parts. Thus, the size of all of these railplugs is similar to that of a spark plug. For these studies, the initial pressure in the bomb was 200 psig, which is approximately that in an engine at the time of ignition.

Figure 10 illustrates the effects of the current pulse shape on the pressure history in the bomb for one of the coaxial railplugs tested. Because we had earlier found that inductance impeded plasma acceleration, our primary means available for shaping the current pulse was via the capacitance. The equivalence ratio for these tests was 0.6, which was too lean to obtain ignition with a spark plug. The pressure histories reported are averages over three experiments, which were found to be repeatable. The delivered energy was 0.9 J in all cases. For this particular railplug, a capacitance of 130 μF in the follow-on circuit yielded a current pulse that was too short as assessed from the low rate of pressure rise illustrated in Figure 10. A capacitance of 260 μF appears to be a much better electronics match, while 390 and 520 μF yield pulse durations that are too long. Similar matching studies were done for the other railplugs examined and the "best" capacitance for each railplug was used for all further experiments. However, it should be pointed out that the available follow-on circuit only allowed capacitance choices in 130 μF increments, with a minimum of 130 μF . Thus, the "best available match" used for these studies was not necessarily the optimal capacitance for any given railplug.

The pressure histories for all of the railplugs examined are compared to that resulting from spark ignition in Figure 11. The equivalence ratio used was 0.75, which was sufficiently rich for spark ignition, thereby allowing comparison with the pressure history resulting from ignition by a spark at the same energy level (0.9 J delivered). For each railplug, the curve shown is that obtained with the best electronics match. As shown in Figure 11, all of the railplugs examined resulted in faster combustion than that which results from high energy spark ignition. This proves that the railplug effect cannot be attributed solely to the additional energy delivered to the ignitor. Rather, the plasma velocity is also important because it increases the rate of combustion (via creation of turbulence and inducement of bulk flow in the unburned gases, as discussed earlier).

The results shown in Figure 11 confirmed our expectation that the railplug geometry has a significant effect on the combustion process. A measure of the performance of each railplug design was sought for design optimization. This design parameter can be derived from the expression for the Lorentz force, which as previously shown to approximately equal:

$$F = \frac{1}{2} L' I^2 \quad (3)$$

Assuming that the mass of the armature (the plasma) is constant, Newton's Second Law of Motion is:

$$F_{\text{net}} = m a \quad (7)$$

For the present purposes of a simple parameterization, thermal expansion and drag are neglected or, equivalently, it is assumed that these two terms cancel. Then, combining Equations 3 and 7 and rearranging yields:

$$a = \frac{1}{2} \frac{i^2 L'}{\rho V} \quad (8)$$

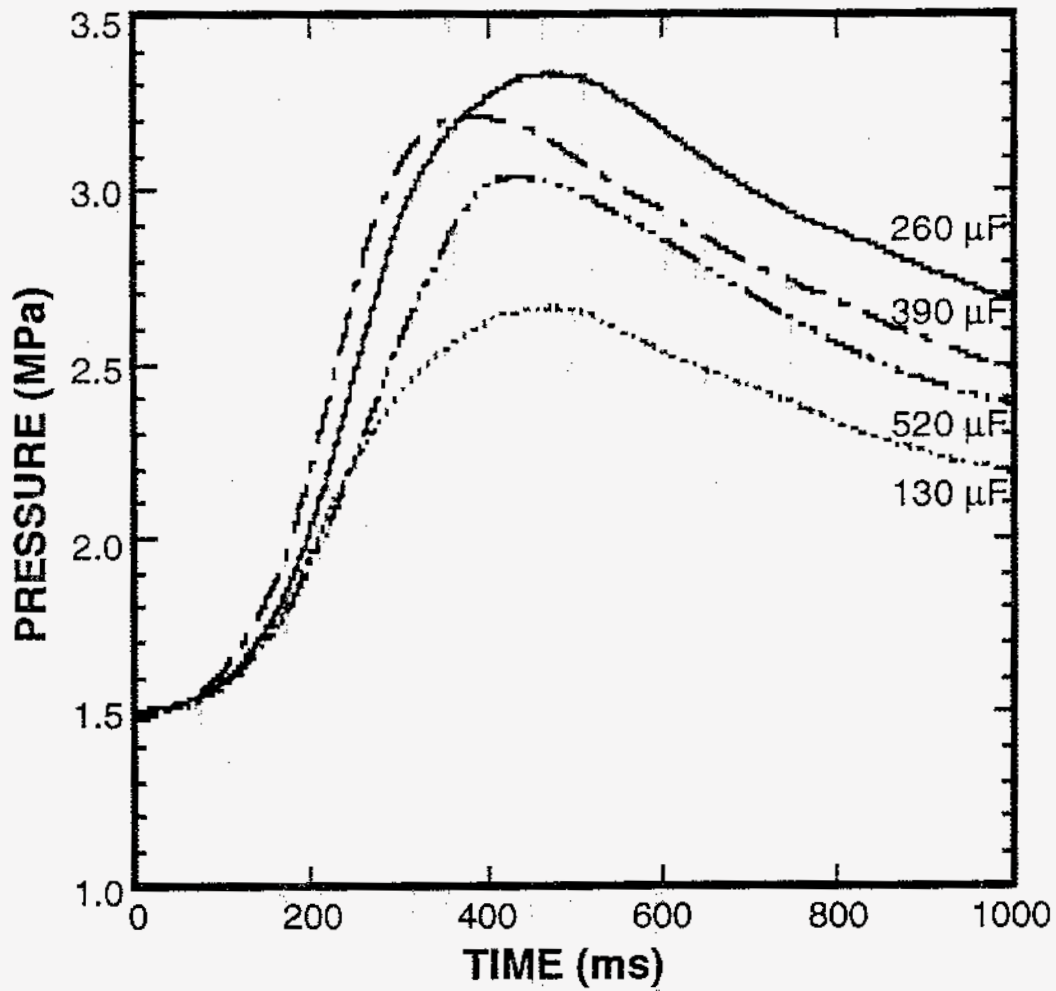


Figure 10. Pressure histories in the bomb for various capacitances in the follow-on circuit for the UT-L railplug with $\phi = 0.60$ and 0.9 J delivered.

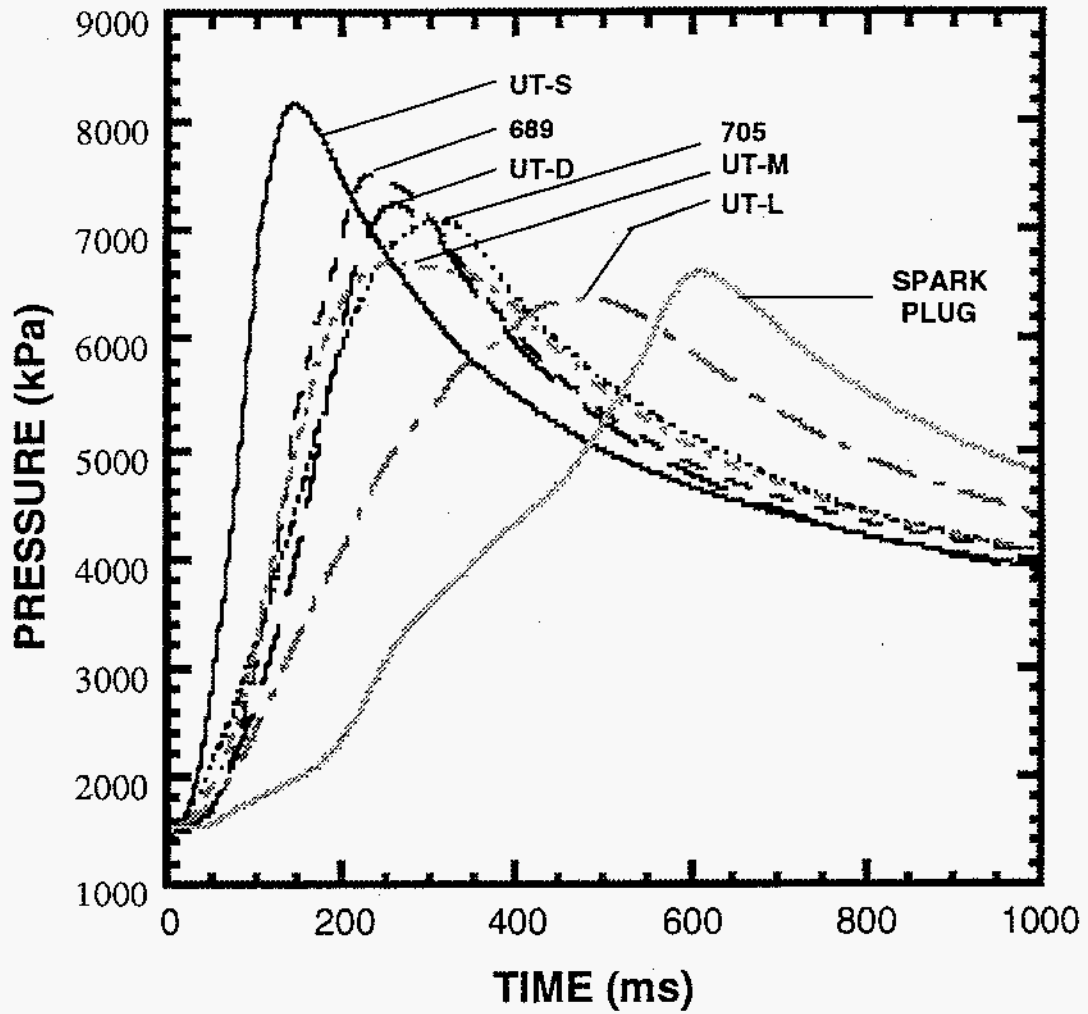


Figure 11. Pressure histories in the bomb for various railplugs with matched electronics for $\phi = 0.75$ and 0.9 J delivered.

Even though simplifications have been made to obtain Equation 8, the inductance gradient (L') and the trapped volume (V) are solely functions of the geometry, and therefore it was believed that L'/V should be a useful parameter for railplug design. This belief was confirmed by the tests illustrated in Figure 12, which is a graph of the rate of pressure rise resulting from each railplug geometry versus the value of L'/V for that railplug design. As expected, the results correlate linearly with L'/V . The data for the three railplugs that have the same L' (UT-L, UT-M, and UT-S) are linear with a correlation coefficient of 0.997. When the data for the remaining railplugs are included, the line fit has a correlation coefficient of 0.932. Therefore, although other factors may have some effect, it appears that L'/V dominates the geometry effects, at least as far as the rate of combustion is concerned.

One of the easiest methods available for achieving a high value for L'/V is to use a small center rail diameter. However, we later found that these had poor durability due to the small cross-sectional area available to conduct heat away from the center rail. Another easy method is to make the cavity shorter, but the extreme of this is a surface gap ignitor, for which one would be electromagnetically accelerating the plasma starting at zero velocity over zero length. This illustrates the shortcomings of the simplified model presented as Equation 8: some length is needed to allow acceleration. Perhaps the main advantage of a railplug over a plasma jet ignitor is that the arc moves, thus distributing the electrical energy over more surface area to decrease rail erosion. This cannot occur with a rail length of zero. However, our recent studies are pointing us toward shorter rails to enhance durability, since we are now focused on lower energies which means shorter current pulses, which require shorter rails to get a proper match between the current pulse shape and the railplug geometry.

Here, it should be noted that the fact that L'/V appears to be a suitable measure of "goodness" of railplug design indicates that the parallel rail design should be superior, since this design results in an increase of L' by about a factor of 2 and parallel railplugs can also be designed with a much smaller trapped volume. However, this would require significant advances in abilities to fabricate parallel railplugs.

4.0 RAILPLUG MODELING TASKS

Two types of numerical model were developed over the course of this project: one for the plasma jet ejection from a railplug and a second for the effects of railplugs in an SI engine. Each of these are discussed in the following subsections.

4.1 Railplug Plasma Jet Modeling

In this work (Ellzey et al., 1993), a multidimensional numerical model of a parallel railplug issuing into ambient air was developed. The governing equations for this simulation are:

Mass Conservation:

$$\frac{\partial \rho}{\partial t} + \nabla \cdot (\rho \vec{V}) = 0 \quad (9)$$

Momentum Conservation:

$$\frac{\partial \rho \vec{V}}{\partial t} + \nabla \cdot (\rho \vec{V} \vec{V}) = -\nabla p + \vec{J} \times \vec{B} \quad (10)$$

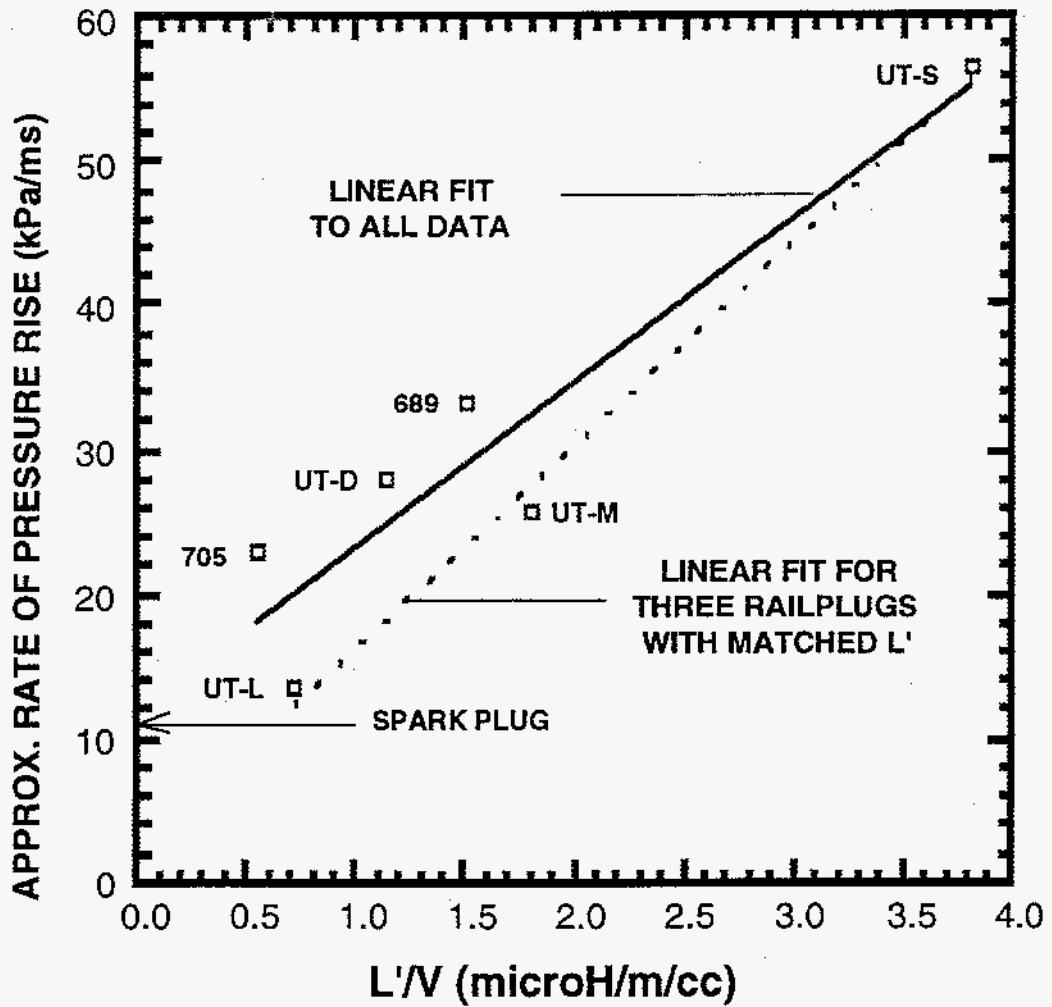


Figure 12. Effect of L'/V on the approximate rate of pressure rise (from Figure 11).

Energy Conservation:

$$\frac{\partial \rho e}{\partial t} + \nabla \cdot (\rho e \bar{V}) = -\nabla \cdot (p \bar{V}) - \nabla \cdot \bar{q} + (\bar{J} \times \bar{B}) \cdot \bar{V} + \frac{J_x^2}{\sigma} + \frac{J_y^2}{\sigma} \quad (11a)$$

where ρ is the fluid density, \bar{V} is the fluid velocity, p is the pressure, \bar{q} is the radiative heat flux, J is the current density, B is the magnetic induction, and e is the total energy (internal and kinetic) density. In the momentum and energy equations, all the viscous terms are neglected. The Lorentz force can be determined from Maxwell's equations and Ohm's Law but here this force was assumed to be constant across the plasma. Also, to further simplify the calculations, it was assumed that the radiative heat loss in the energy equation balanced the Joule heating terms. That is:

$$\nabla \cdot \bar{q} = \frac{J_x^2}{\sigma} + \frac{J_y^2}{\sigma} \quad (12)$$

This reduces the energy equation to:

$$\frac{\partial \rho e}{\partial t} + \nabla \cdot (\rho e \bar{V}) = -\nabla \cdot (p \bar{V}) + (\bar{J} \times \bar{B}) \cdot \bar{V} \quad (11b)$$

The relationship between internal energy and pressure is given by:

$$u = \frac{p}{\gamma - 1} \quad (13)$$

where γ is the ratio of specific heats and

$$u = e - \frac{1}{2}(V_x^2 + V_y^2) \quad (14)$$

The temperature is calculated through the equation of state:

$$p = nkT \quad (15)$$

where n is the number density and k is Boltzman's constant. In the computations, Equations 9-11 were solved using Flux-Corrected Transport which is an explicit, finite-difference algorithm and has been shown to maintain steep gradients such as those in shocks.

Modeling spark breakdown and arc formation have long been problems that have eluded modelers. For this reason and since our primary interest was in the interaction of the plasma jet with the surrounding gases after the jet exits the railplug cavity, not in the details of the arc initiation processes, the calculations were started 30 μ s after the plasma was formed. Shadowgraph images were used to determine the initial plasma volume at this time. The plasma temperature at this time is also needed and was determined by calculating the percentage of the stored energy that must have been deposited as thermal energy at this time so as to yield agreement of the predictions with experimental data for a baseline case. This efficiency was not changed for any of the other cases examined.

The railplug simulated is a transparent parallel railplug used for experiments described earlier in this final report. The rails were enclosed between microscope slides to

form a cavity. The rails were separated by 5.0 mm and the distance from the spark gap to the cavity exit was 2.6 cm. To minimize the computational time requirements, a cylindrical geometry with a cross-sectional area the same as that of the actual railplug was assumed, and the axisymmetrical form of the governing equations was used in the calculations.

Comparisons were made between the predictions and the experimental results from shadowgraph images. Thus, predicted density contour plots at various times after initiation were compared to shadowgraphs for various stored energies. These results are summarized in Figure 13. Both the velocity of the shockwave that precedes the plasma and the velocity of the plasma front are both predicted very well. The predictions at the railplug exit for the mass flux and the temperature were later used as boundary conditions in models for railplugs in an engine, as discussed in the next subsection.

4.2 Multidimensional Engine Modeling

This work has not yet been published but is available in the dissertation of a PhD student who worked on the railplug project (Zhao, 1994). Engine combustion with railplug ignition was compared to combustion as initiated with a conventional spark plug via simulations using the KIVA-II code, which is very widely used for engine simulations. However, KIVA does not include model that is suitable for simulating combustion in an SI engine. Thus, predictions were made using two different combustion models: the Coherent Flame Model and the Fractal Flame Model, the latter of which was developed at the University of Texas.

Because it normally takes about six months to load a combustion chamber geometry into KIVA, we were not able to directly simulate our railplug engine experiments. Instead, we simulated a different engine for which we had already loaded the combustion chamber geometry into KIVA. We had already proven our ability to predict combustion in this engine using both combustion models and using conventional spark ignition (e.g., Zhao et al., 1994). We examined a two equivalence ratios at 1200 rpm. Results for only one combustion model are summarized below. The results for the other cases are available in the dissertation (Zhao, 1994).

It was assumed that the large flame kernel with railplug ignition could be simulated as the result of a concentrated and simultaneous multi-point ignition. The potential effects of the plasma jet on the turbulence in the engine cylinder was neglected. The railplug was centered along the axis of the engine cylinder with its muzzle being in the plane of the bottom surface of the cylinder head, as was the case for the spark plug used in experiments using this engine during experiments carried out by others. A large flame kernel was initiated by setting a number of computational cells as the ignition sites close to the railplug exit. Flame kernel formation at each ignition site was treated in the same way as for a single spark ignition.

Comparisons between railplug ignition and the spark ignition included 1) cylinder pressure histories, 2) burned mass fraction histories, 3) density contours as a function of crank angle after ignition, and 4) temperature contours as a function of crank angle after ignition. The cylinder pressure histories at a slightly lean equivalence ratio are shown in Figure 14 and the corresponding burned mass fraction profiles are shown in Figure 15. Both illustrate that combustion is much faster and that the ignition delay has been eliminated using railplugs. This agrees with our results in both bomb experiments and engine experiments. Figures 16 and 17 give similar information for combustion near the lean limit, $\phi = 0.7$. At this very lean condition, the burning rate was also increased by using railplug ignition. Temperature contour plots for this case are provided in Figure 18.

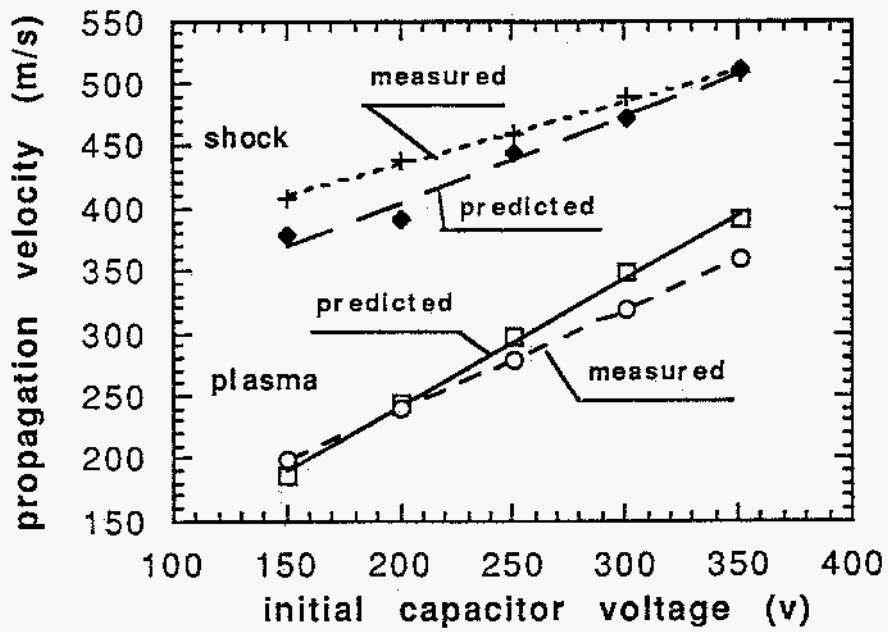


Figure 13. Predictions of the shock front velocity and of the plasma front velocity in comparison to experimental measurements for a parallel railplug.

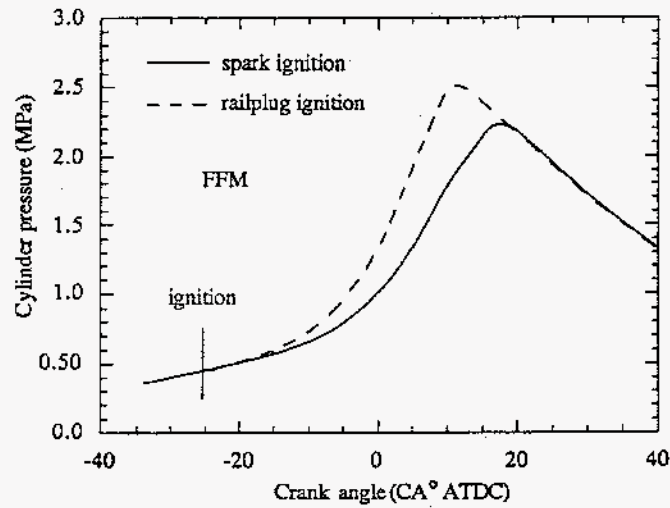


Figure 14. Comparison between cylinder pressure histories for spark ignition and railplug ignition for the IFP engine at 1200 rpm with $\phi = 0.9$.

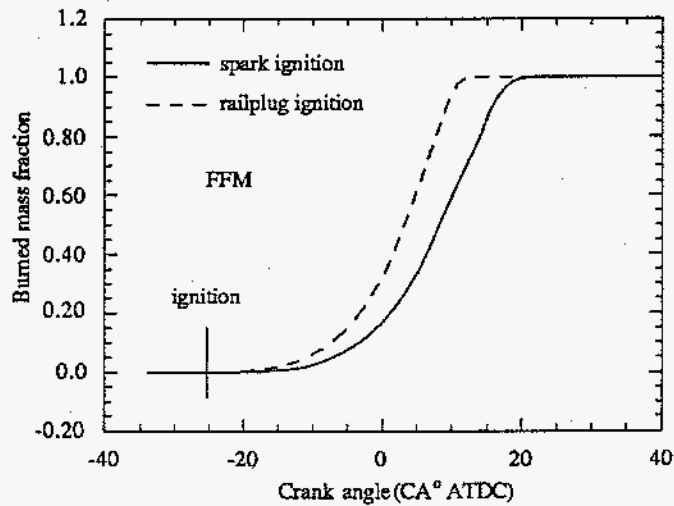


Figure 15. Comparison of burned mass fraction profiles for spark ignition and railplug ignition for the IFP engine at 1200 rpm with $\phi = 0.9$.

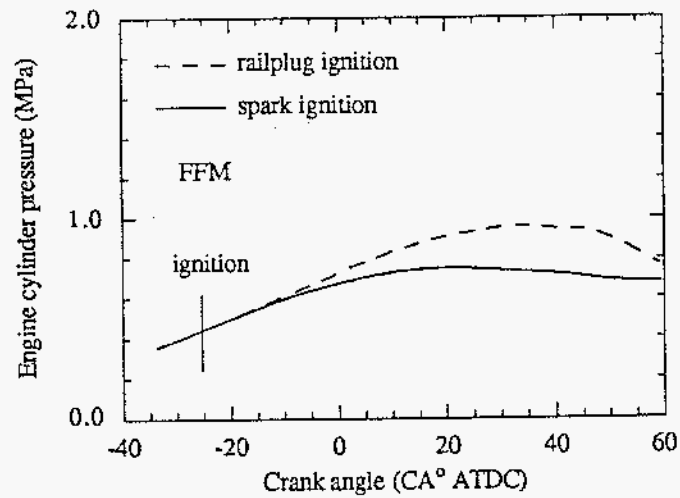


Figure 16. Comparison between cylinder pressure histories for spark ignition and railplug ignition for the IFP engine at 1200 rpm with $\phi = 0.7$.

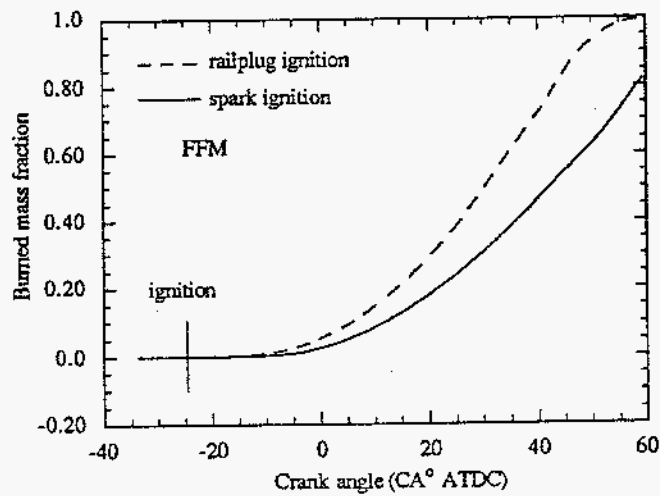
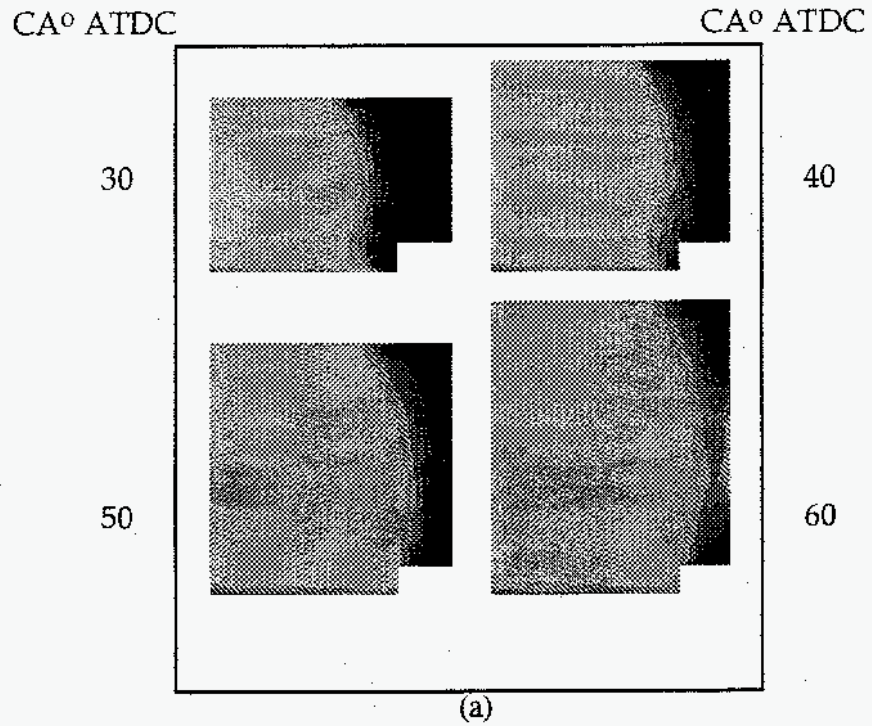
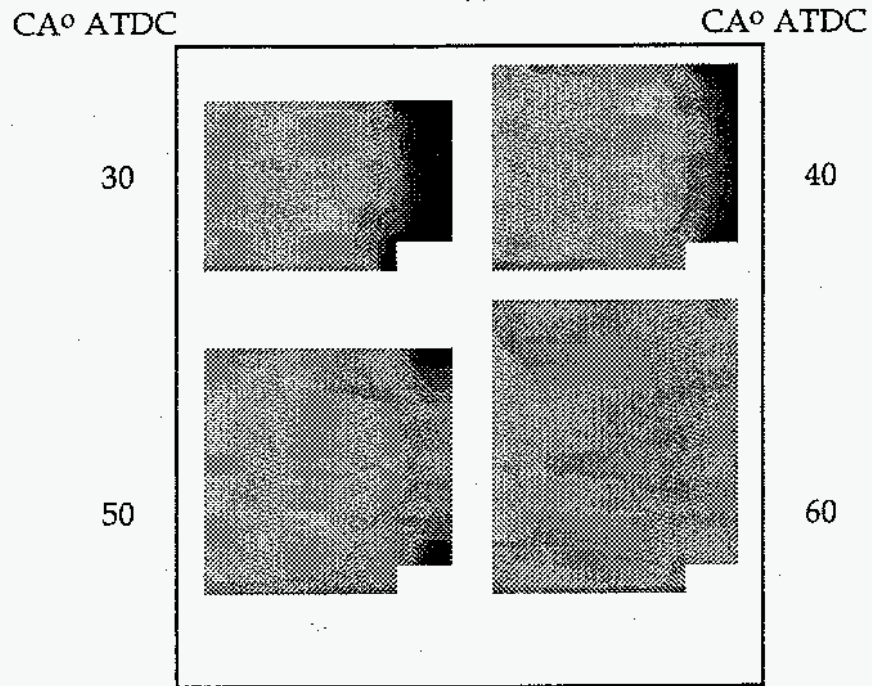


Figure 17. Comparison of burned mass fraction profiles for spark ignition and railplug ignition for the IFP engine at 1200 rpm with $\phi = 0.7$.



(a)



(b)

Figure 18. Comparison of temperature contour plots between (a) spark ignition and (b) railplug ignition calculated for the IFP engine at 1200 rpm with $\phi = 0.7$ ($T_{\max} = 2400$ K, $T_{\min} = 800$ K).

5.0 PROOF OF PRINCIPLE FOR EXTENSION OF THE DILUTION TOLERANCE OF SPARK IGNITION ENGINES

Dilution of the fresh charge is used to control NO_x emissions from SI engines. This can be achieved either via excess air, which provides an efficiency benefit, or via exhaust gas recirculation, which allows use of a conventional oxygen sensor for closed loop control and also allows use of a conventional three way catalyst. In either case, increasingly stringent emissions standards are requiring more dilution. However, excessive charge dilution increases cyclic variability, especially for low speed, low load operating conditions. This increase in cyclic variability is due to slow burn, partial burn, and misfire problems that occur when the charge is diluted too much. We wished to prove that railplugs can extend the dilution tolerance of SI engines. This task consisted of three parts, each of which is discussed in the following subsections.

5.1 Initial Results in a Research-Type Engine

Initial tests were performed to demonstrate the potential of railplugs for improving the combustion stability of dilute mixtures. A coaxial railplug developed and fabricated at the University of Texas, that was similar to the Champion 689 (illustrated in Figure 3), was tested in a high speed CFR engine (Matthews et al., 1992). This single cylinder research engine is mechanically fuel injected and has a variable compression ratio. The cylinder pressure measurement techniques are discussed in detail in this paper are not repeated for brevity. To roughly simulate idle conditions (for which cyclic variability is most noticeable), these initial engine tests were performed at 1000 rpm with a compression ratio of 7.5:1 and a volumetric efficiency of 54%. The railplug had a 1.52 mm (0.060 in.) tungsten center rail with a 3.175 mm (0.125 in.) ID, stainless steel, annular rail. The initiation gap was 0.635 mm (0.025 in.) and the effective rail length was 12.7 mm (0.5 in.). Thus, this railplug had an L/V of 1.9 $\mu\text{H}/\text{m}/\text{cc}$. The follow-on circuit had a capacitance of 780 μF and an intentional inductance of 10 μH . No attempts to match the electronics to the railplug geometry were made and, given our current understanding of matching as discussed previously, it appears that the two were not well matched. The delivered energy was about 5.5 J, which was within about an order of magnitude of our long-term goal of 0.5 J. The ignition system used for the spark plug was the same as the breakdown system used for the railplug. It consisted of a standard automotive coil and an Echlin TP-45 ignition module which was triggered by a signal from the stock CFR magneto. The spark plug gap was 0.89 mm (0.035 in.) and the delivered energy is estimated as no more than 0.1 mJ.

The initial engine results are illustrated in Figure 19, a graph of the Coefficient of Variability (the standard deviation normalized by the mean) of the indicated mean effective pressure as a function of the equivalence ratio. The COV of IMEP is routinely used as a measure of cyclic variability. All of the spark plug data were acquired with the ignition timing at MBT, which was set using the spark advance that resulted in the location of peak pressure at 17 ATDC. Only two data points for the railplug were obtained due to the poor durability of this particular design. This engine was not designed to operate lean, as obvious from the fact that the Lean Stability Limit (the equivalence ratio at which the COV of IMEP is 10%) occurs at the relatively high equivalence ratio of about 0.9. These results indicate the potential of railplugs to improve the combustion stability of dilute mixtures, since the COV using a spark plug was over 20% at $\phi = 0.81$ while the COV was less than 5% using the railplug at this equivalence ratio. However, the data acquisition system used was only capable of storing pressure traces for 40 cycles. For valid statistical calculations (such as the COV), at least 100 cycles and preferably over 500 cycles are needed. Thus, a better data acquisition system was obtained for the additional studies discussed in the next subsection.

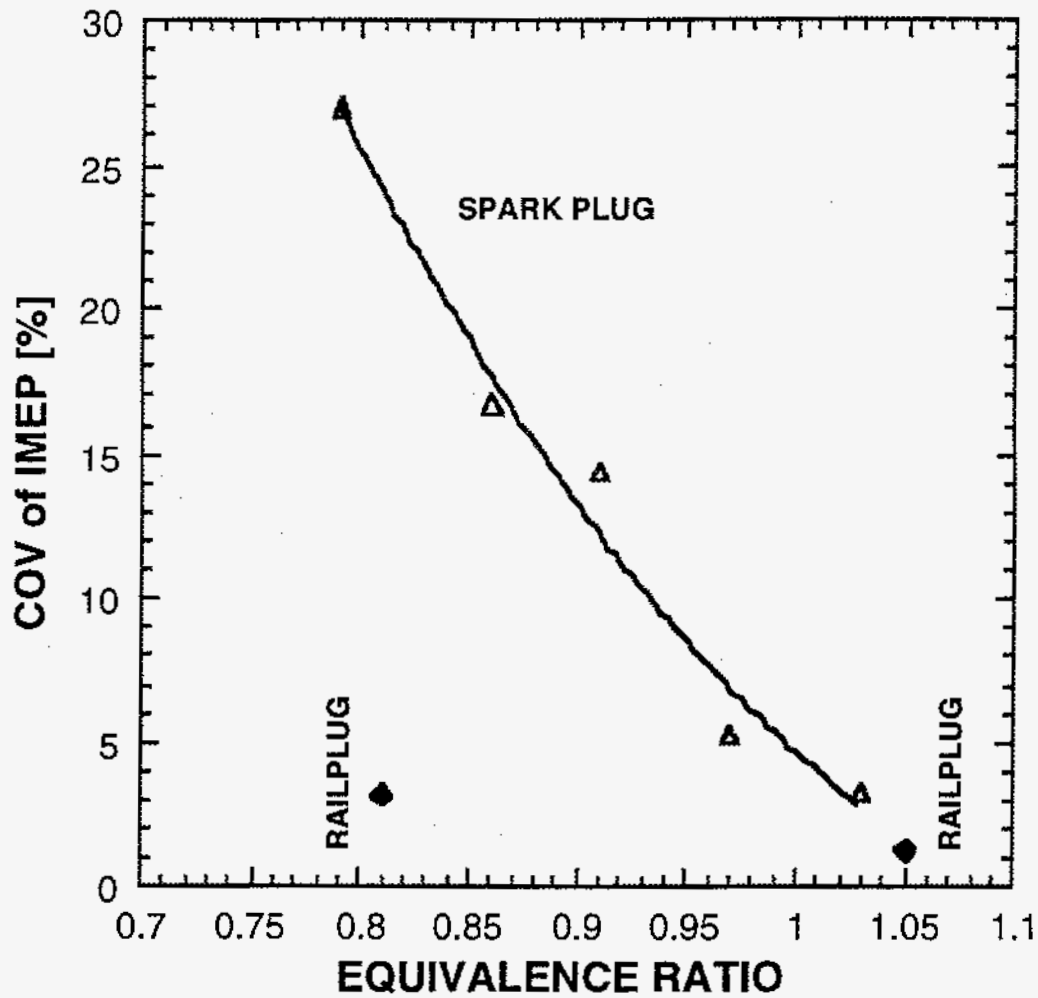


Figure 19. Comparison of combustion stability using a spark plug and a railplug in a CFR at 1000 rpm, 7.5:1, and a volumetric efficiency of 54%.

5.2 Further Lean Limit Studies

The initial tests discussed in the prior subsection indicated that railplugs had potential for extending the dilution tolerance of SI engines but the value of the results was limited by the limitations of the instrumentation available at that time. Thus, additional tests were run using the same engine but with new instrumentation and under different operating conditions. In our second set of tests (Zheng et al., 1993), the dilution tolerance of our CFR engine was evaluated via comparisons of a railplug, a conventional spark plug, and a wide gap spark plug. The experimental system used for these studies is discussed in the following subsection, followed by presentation of the experimental results.

5.2.1 Experimental System

Again, care was taken to insure accurate pressure signals, as discussed in this paper in more detail. The cylinder pressure data were acquired using a DSP Technology combustion event analyzer with DSPT model 4325 real time processor. This data acquisition system allowed automatic determination of the indicated mean effective pressure (imep), location of peak pressure (LPP), mass burned fraction profiles, percent misfiring cycles, and COV of imep. All results were averaged over 500 cycles (in contrast to the limit of 40 cycles with the previous instrumentation).

Howell Hydrocarbons EEE standard unleaded gasoline (Indolene) was used for all tests. For this fuel, the stoichiometric air/fuel ratio is 14.55. For each experiment, the air/fuel ratio was determined from the exhaust gas using a Horiba AFR Analyzer, model MEXA 101λ. The output from this instrument was automatically logged by the DSP data acquisition system and averages were taken over the same 500 cycles as were the other data.

As discussed in the previous subsection, our initial engine tests (were performed at 1000 rpm with a compression ratio of 7.5:1 and a volumetric efficiency of 54%. A different set of operating conditions was used for the second set of tests. General Motors uses three standard conditions for evaluation of their engines. These are: (1) an idle simulation condition of 700 rpm with 210 kPa imep; (2) a mid-speed, mid-load condition of 1300 rpm with 390 kPa imep; and (3) a high load point of 2200 rpm with 520 kPa imep. Ford uses a single "world point" to evaluate their engines: 1500 rpm at 262 kPa bmep (brake mean effective pressure). Chrysler also uses a single world point that is similar to Ford's world point: 1600 rpm at 241 kPa bmep. Because the Ford world point, the Chrysler world point, and the mid-speed GM point are similar, the mid-speed GM test condition was chosen for these studies because this operating condition is of more universal interest. The compression ratio was set at 8.5:1 for all of these tests.

Experimentally determining MBT (minimum advance for best torque) ignition timing for constant imep, constant speed tests is problematic, especially with the low torque output of this single cylinder engine for these operating conditions. MBT timing should coincide with the timing that minimizes the indicated specific fuel consumption (isfc), since both indicate maximum thermal efficiency. For all three ignitors, timing sweeps were performed at 1300 rpm and an imep of 390 kPa and the isfc was monitored to determine the location of peak pressure (LPP) that coincided with the minimum isfc. These tests resulted in a relationship for the desired LPP (to simulate MBT) as a function of the equivalence ratio:

$$LPP = 12.7 - 22.7\phi + 29.22\phi^2 \quad (16)$$

For all tests, the LPP was set to within 1 CA of this desired value. For all three ignitors, the isfc decreased monotonically as the mixture was leaned from stoichiometric to AF = 20 with the LPP set at each equivalence ratio as per Equation 16.

As discussed previously, the ratio of the railplug's inductance gradient (L') to the volume enclosed between the rails (V) is a useful measure of the effects of railplug

geometry on railplug performance. Increasing L/V yields a faster combustion process. In our preliminary engine studies (Subsection 5.1), we used a railplug fabricated at The University of Texas that had an L/V of $1.9 \mu\text{H}/\text{m}/\text{cc}$. For the present experiments, a Champion 727 railplug was used. This railplug has an L/V of only $0.5 \mu\text{H}/\text{m}/\text{cc}$ but was chosen for this study due to its good durability. We are continuing to study techniques to develop railplugs that have high L/μ but also have durability that is superior to the Champion 727. The results of our durability investigations are discussed in Section 8.

The spark plug used for the comparative tests was a Champion N12YC. Most of the data were acquired using a spark gap of 1.8 mm (0.070") because wider gaps yield improved combustion stability. Some data was also acquired using a more conventional spark gap of 0.9 mm (0.035"). The ignition system used for the spark plug was the same as the breakdown system used for the railplug which was triggered by a signal from the stock CFR magneto.

For both the normal gap and wide gap spark plugs, the delivered energy was 35-40 mJ. For all of the railplug tests, the delivered energy was 2.5 J. This is less than half the energy delivered during our initial engine tests and is within a factor of 5 of our long-term goal of 0.5 J.

For our initial engine tests, we did not "match" the railplug electronics to the railplug geometry. The electronics were matched to the Champion 727 geometry for this second set of tests. No intentional inductance was used in the follow-on circuit and the overall system was left the same from test to test except for the matching study, during which the capacitance of the follow-on circuit was varied. The optimum match for this railplug was found to be a capacitance of $100 \mu\text{F}$. This capacitance provided the shortest interval between ignition and the location of peak pressure, and thus yields the fastest combustion process.

5.2.2 Engine Results

The results of this set of experiments are illustrated in Figure 20, a graph of the COV of the imep as a function of the equivalence ratio. There is little difference between the three ignitors, as far as combustion stability is concerned, for mixtures as lean as $A/F \approx 20$. For leaner mixtures, the differences between the three ignitors become noticeable. The Lean Stability Limit (LSL, the air/fuel ratio at which the COV of imep is 10%) of the conventional gap spark plug occurs at $A/F \approx 22$. Use of a wide gap extends the lean limit by about 1.5 air/fuel ratios to $A/F \approx 23.5$. Near the LSL for the wide gap spark plug, at $A/F \approx 23.1$, the COV for the wide gap spark plug is 9.5 while it is only 6.5 for the railplug. At the time this paper was written, time did not allow exploration of the LSL for the railplug. In later studies, we found that we could not attain sufficient spark advance to keep the LPP at the appropriate value (from Equation 16) for significantly leaner mixtures, so that it was not possible to quantitatively determine how much additional dilution tolerance was afforded by railplugs. However, the results presented in Figure 20 have proven sufficient to demonstrate that railplugs can extend the LSL significantly.

Earlier studies (Edwards et al., 1983) in a similar engine but for different operating conditions demonstrated that a plasma jet ignitor could extend the LSL from $\phi=0.7$ for a standard spark plug to $\phi=0.62$ using a plasma jet ignitor with an energy of 0.70 J. It was also shown that use of a surface discharge ignitor with 0.70 J extended the LSL only to $\phi=0.67$, thus demonstrating that energy is not the dominant factor. Our results using 2.5 J showed that we can extend the LSL to at least $\phi=0.60$. Our goal is to shift the LSL to $\phi=0.57$ ($A/F=26:1$ for gasoline) using 0.5 J. Because it has been shown, both in our previous work and in earlier work by others, that energy is not the dominant factor, and because the Champion 727 does not have high L/V , and because we are already close to our goals, we believe that development of better railplug geometries will allow us to achieve our goal using lower energies. Work continues in this area.

The percent cycles that produced an imep that was less than 85% of the average imep is shown in Figure 21. Slow burn cycles produce an imep that is 46-85 percent of the

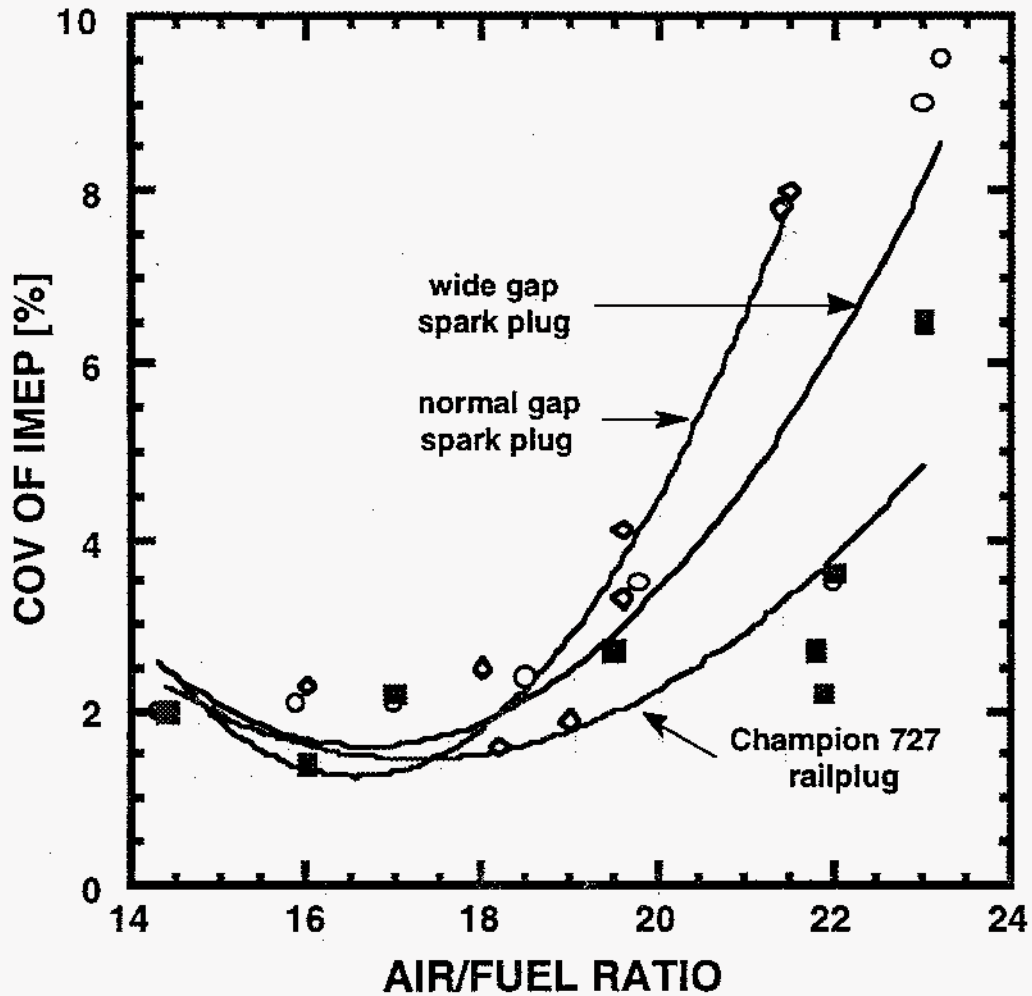


Figure 20. Effect of the air/fuel ratio on the combustion stability for three ignitors. 1301 ± 6 rpm, imep=390 kPa $\pm 2.8\%$. The second order least squares curve fits used to illustrate the trends show an unintentional and nonphysical minimum.

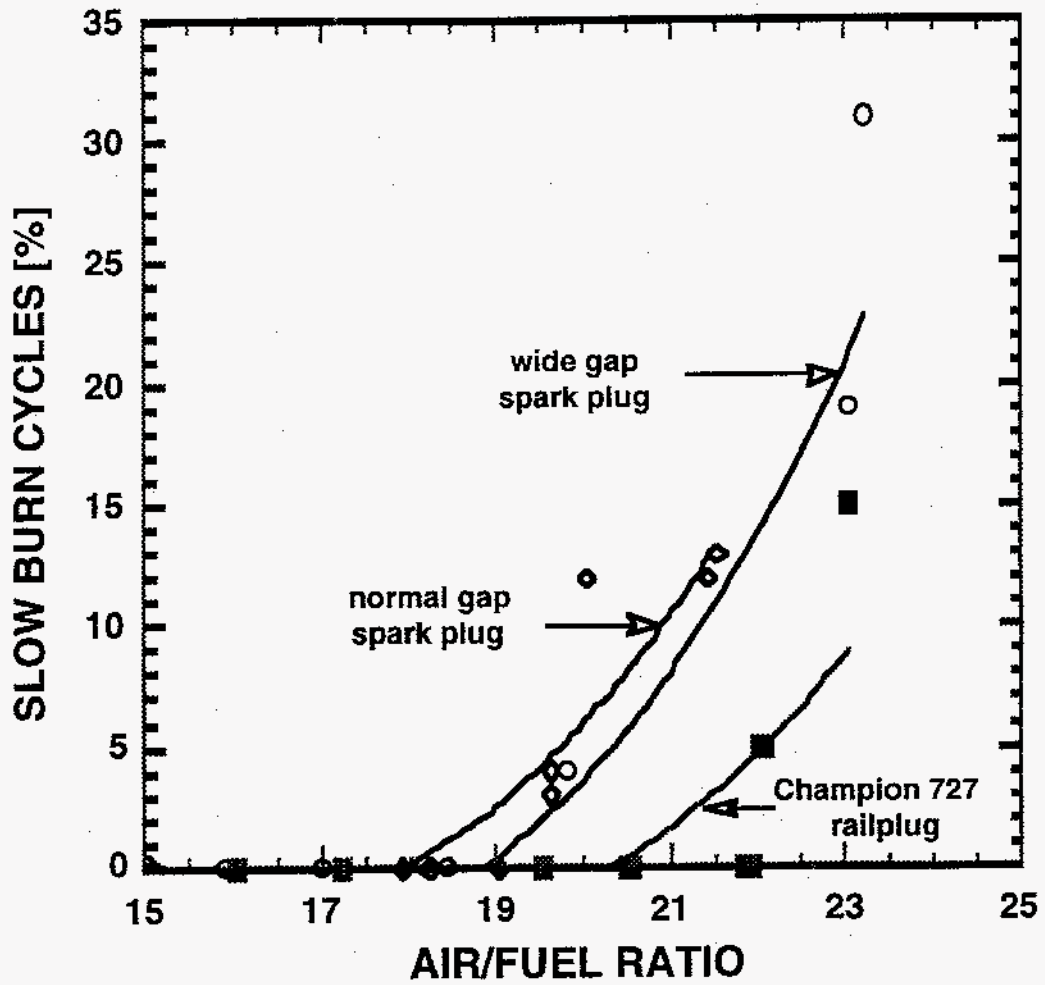


Figure 21. Effect of the air/fuel ratio on percent slow/partial burn cycles for three ignitors. 1301 ± 6 rpm, $imep=390 \text{ kPa} \pm 2.8\%$. Curves are second order least squares fits to data.

average imep, partial burn cycles produce an imep that is less than 46% of the mean imep, and misfire cycles have $\text{imep} \leq 0$ (Heywood, 1988). The railplug produced no partial burn or misfire cycles while the normal gap and wide gap spark plugs produced only one misfire and up to two partial burn cycles over 500 cycles for the leanest mixtures ($A/F=21$). Thus, the data shown in Figure 28 may be interpreted as primarily percent slow burn cycles. Slow burn cycles begin to appear at the same air/fuel ratio at which the COV differences between the ignitors become apparent, $A/F=20$. This figure demonstrates that the railplug significantly decreases the slow burn problems that are encountered as the mixture becomes diluted. Again, no partial burn or misfire cycles were encountered with the railplug, and the air/fuel ratio at which at least 5% of the cycles resulted in slow burn was pushed from $A/F=19.5$ for the spark plugs to $A/F=22$ for the railplug.

Mass fraction burned information for near-stoichiometric combustion is provided in Figure 22, which is a histogram depicting the three regimes of combustion. The three regimes are: kernel formation (0-2% burned), early flame growth (0-10% burned), and fully developed flame propagation (10-90% burned). The duration of combustion is normally defined as the crank angle interval for 0-90% burned, and is also shown in Figure 22, as is a comparison of the COV of imep. In comparison to the normal gap spark plug, the wide gap spark plug decreases the duration of kernel formation and early flame growth, has no effect on the fully developed turbulent flame propagation phase, and yields a decreased overall duration of combustion. The railplug decreases the duration of all phases of combustion as well as the overall duration of combustion in comparison to both spark plugs.

Mass fraction burned histories at $A/F=22$ are provided in Figure 23. Interestingly, although operation of the railplug with the same timing as the spark plug results in an earlier and higher peak pressure and a shorter duration of combustion (graphs are provided in the paper but are not reproduced here for brevity), the rate of the fully developed turbulent propagation phase of combustion is slower. We believe that this is because the railplug-ignited flame enters the fully developed phase of combustion earlier (at 30 °BTDC), when the turbulence intensity, u' , is higher. Because flame strain typically scales with $(u')^{3/2}$ (e.g., Herweg and Maly, 1992; Abdel-Gayed et al., 1989), the flame is strained harder with earlier ignition, thereby slowing down the main phase of the combustion process of this very weak mixture. Railplug operation with retarded timing (by ~15 CA°) to achieve the same LPP and imep as for the wide gap spark plug does not exhibit this trend because this weak flame enters the fully developed phase of combustion later in crank angle degrees. That is, railplug operation with the timing set to yield the same LPP and imep as for the wide gap spark plug results not only in a lower COV of imep but also a shorter duration of combustion.

5.3 Application to a Production SI Engine

Although discussions with various members of our External Advisory Board indicated that our single cylinder work (discussed in the preceding subsections) was sufficient to demonstrate that railplugs are effective in extending the dilution limit, we had originally proposed to also demonstrate this in a production engine. Such a study is of value because: (1) the single cylinder engine is not representative of modern engine designs, (2) many of the manufacturers are now favoring high EGR rates for NOx control rather than lean burn, and we wished to demonstrate that railplugs would be equally effective for extending the dilution tolerance for this type of dilution, and (3) we did not measure emissions or specific fuel consumption in the single cylinder engine tests because we planned to do this in the multicylinder engine tests.

A 2.2 liter GM port fuel injected four cylinder production engine was obtained for testing of railplug in a production engine. Results for variable high exhaust gas recirculation rates were to be compared for wide gap spark plugs and railplugs. The engine was setup on a dyno and the railplug electronics were built. Initial testing on debugging the

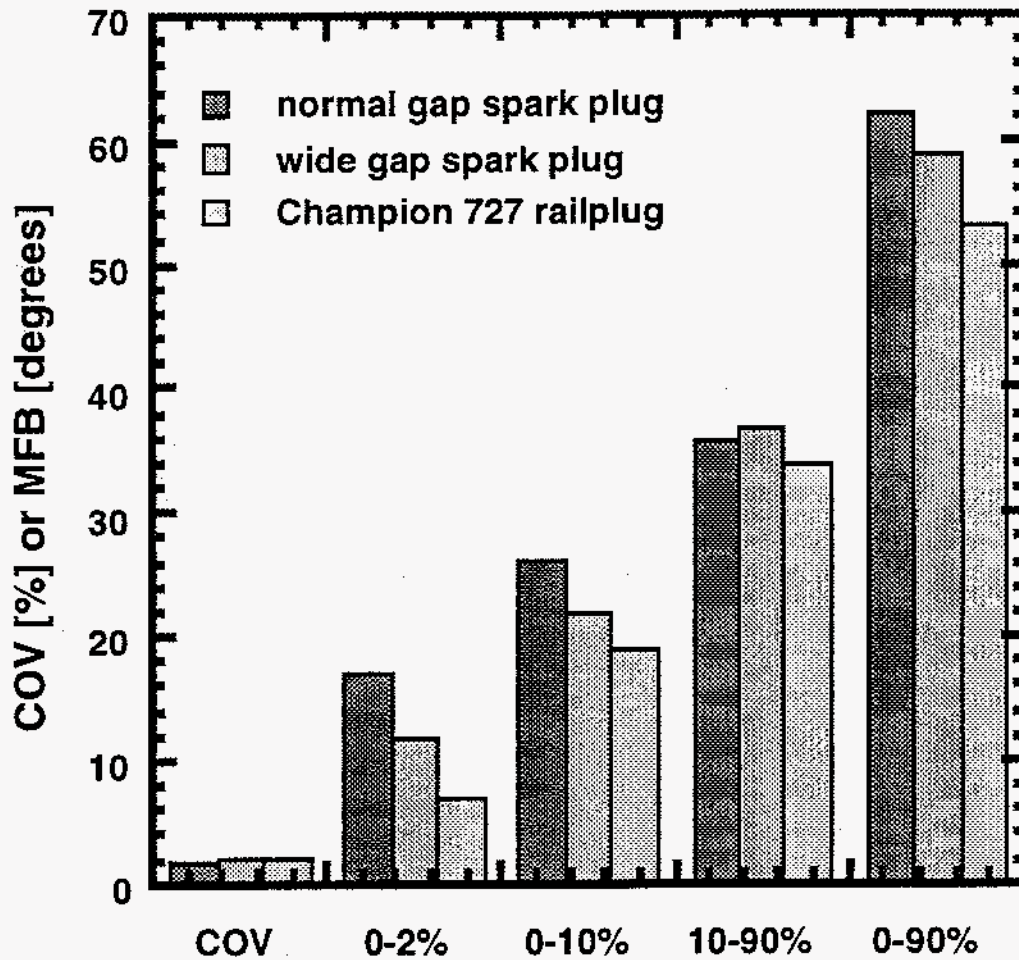


Figure 22. Comparison of the phases of combustion for a near-stoichiometric mixture (otherwise, same conditions as Figure 21).

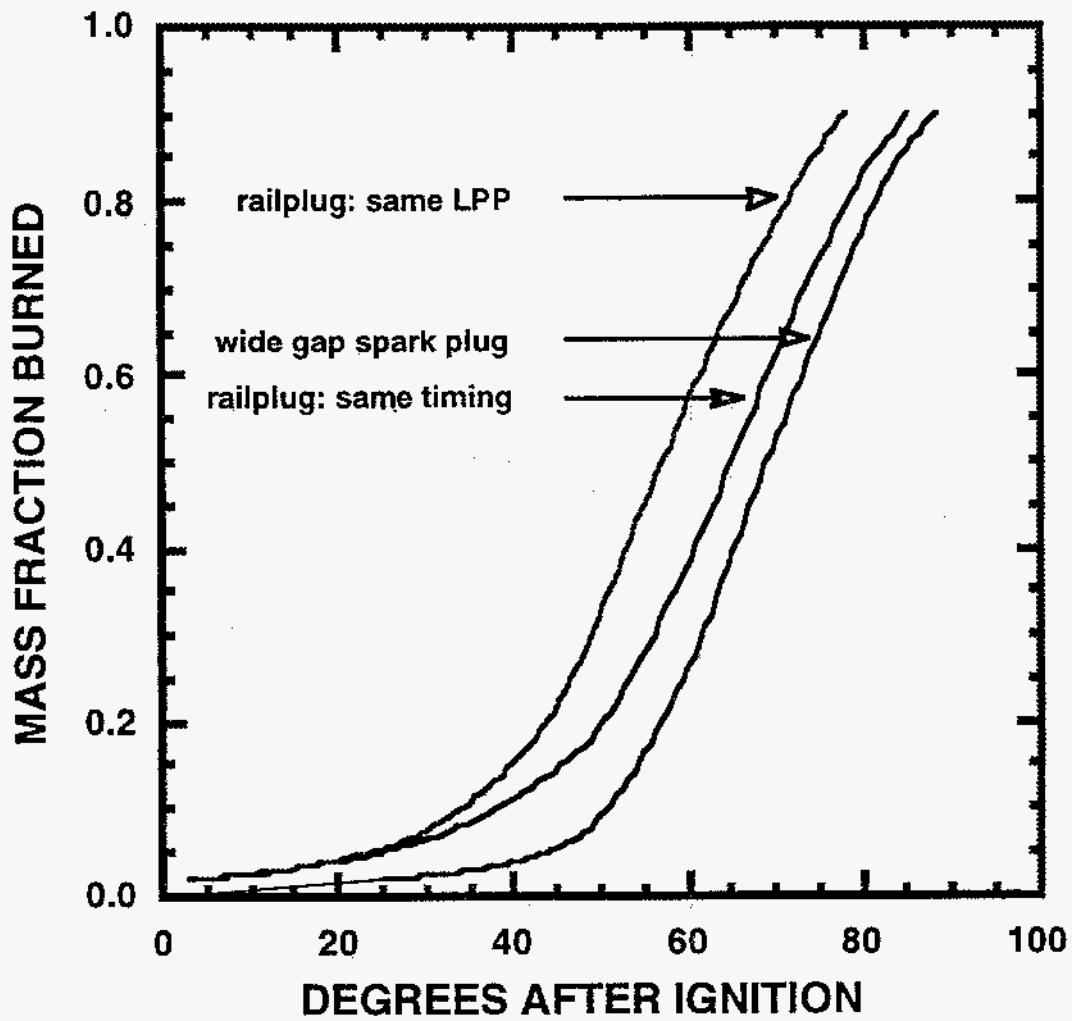


Figure 23. Comparison of the mass burning rates for $A/F=22$.

system began, but we encountered severe problems with the dyno controller. We had not finished repairing this system before the program ended. However, we did operate this engine with railplugs at an idle condition to demonstrate that the four cylinder power supply worked properly.

Again, it should be noted that the addition of durability testing - which was not included in the proposed work - limited the manpower that we could devote to this task. This fact, together with our dyno control problems, caused this task to fall behind schedule..

6.0 PROOF OF PRINCIPLE: DIESEL COLD START

Tests were performed to study the potential of railplugs for reducing the time to start a diesel engine (Shen et al., 1994). An indirect injection diesel engine was chosen because these engines have an access hole (the glow plug hole) in which we can install railplugs and because this is the type of diesel engine used in virtually all light duty diesel vehicles in the U.S. Even though we tested railplugs in an IDI diesel, it is believed that successful use of railplugs as a cold start aid for this engine is evidence that railplugs can be an effective cold starting aid for DI diesels as well. Glow plugs are used as cold start aids in these engines. At low temperatures, glow plugs require a pre-heat time before starting the engine. In addition, glow plugs have a cold start temperature limit below which the engine will not start. The experimental system used for these studies is discussed in the following subsection, followed by presentation of the experimental results.

6.1 Experimental System

Railplugs were tested in a 1992 VW ECO diesel engine with a bore and stroke of 76.5 mm and 86.4 mm respectively. This four cylinder IDI diesel has a total displacement of 1.6L and a compression ratio of 23:1. This engine has excellent cold start characteristics, making for a tough test for railplugs. The beginning of fuel injection under starting conditions is normally 6 °BTDC and is 10 °BTDC with the cold start timing device. The duration of injection is approximately 10 CA°.

The cold start tests were performed by replacing the glow plug in the number four cylinder with a railplug. This approach was used, rather than installing a railplug in all cylinders, because of the resulting decreased expense and complexity. The exhaust port temperatures were monitored to indicate whether or not combustion had been initiated in the corresponding cylinder. The railplug directly replaced the glow plug in the same hole, as illustrated in Figure 24. As shown in this figure, the end of the railplug is flush with the prechamber wall. In contrast, the original glow plug extends into the prechamber to near the centerline of the fuel spray.

The stock glow plugs are a quick glow system which the manufacturer specifies has a minimum ambient temperature for successful cold start of -24 °C. The required glow plug pre-heat time at this temperature is approximately 8 seconds.

The railplugs used in this study were fabricated at two separate facilities: at Champion Spark Plug Company and at the University of Texas' Center for Electro-Mechanics (CEM). The Champion railplugs had ceramic bodies, while the CEM railplugs had insulators made of G-10. Both tungsten or nickel center rail materials were examined. Several outer rail designs were tested.

The breakdown circuit used for this cold start investigation consisted of a Delco CD ignition system which was triggered using a Hall effect sensor and one or two magnets on the camshaft sprocket. The follow-on circuit consisted of several 50 µF capacitors and a charging unit. The charging unit consisted of a full wave rectifier, a voltage doubler, and a 140 % variable transformer. With a 120 V AC input, the maximum capacitor charging voltage is 475 VDC.

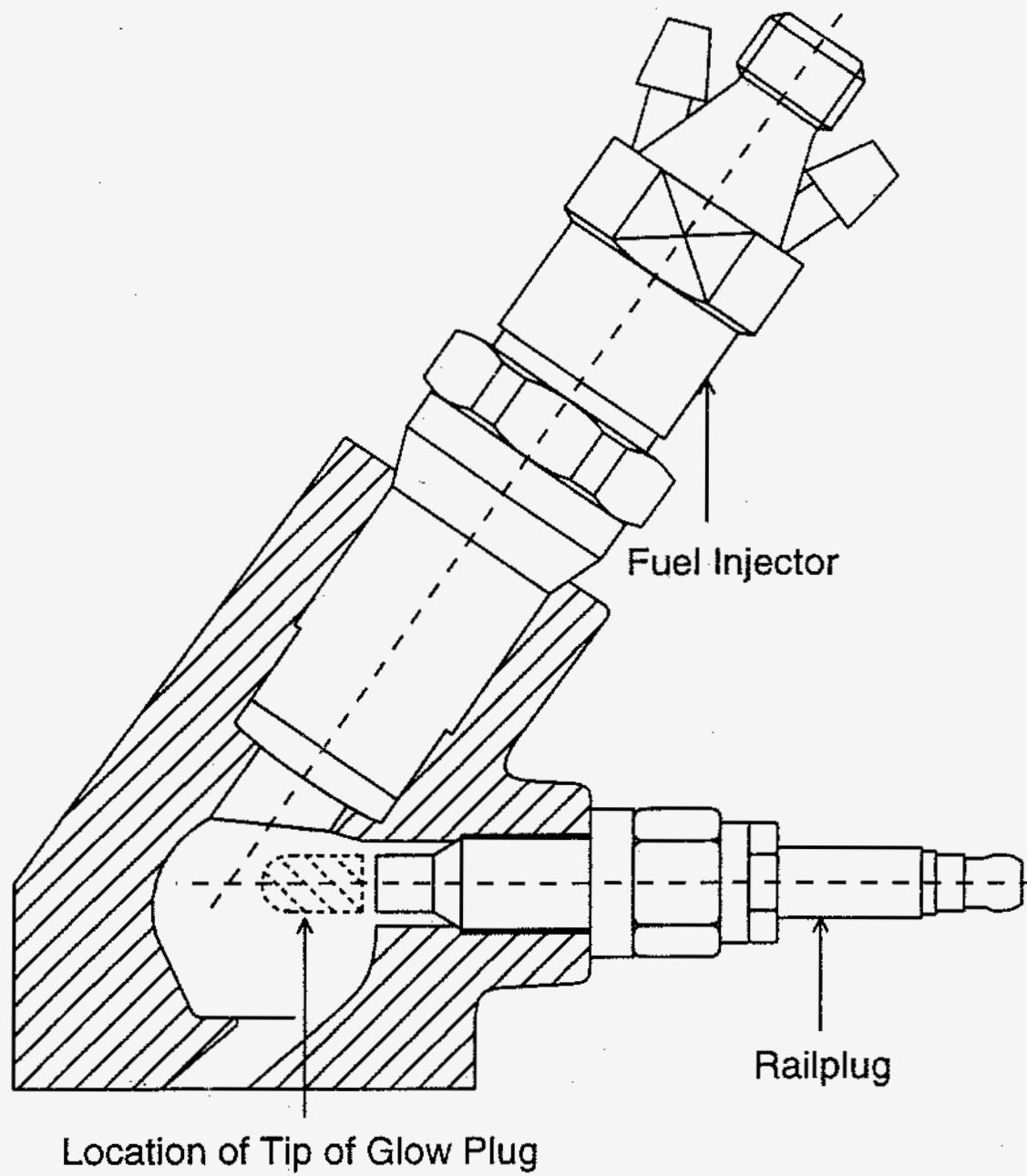


Figure 24. Schematic of railplug, glow plug, and fuel injector locations in the IDI diesel prechamber.

Type K thermocouples were used to monitor chamber and coolant temperatures in addition to each of the four exhaust port temperatures. It should be noted that the data acquisition system used was relatively slow (data points on each channel are approximately one second apart), so there is some scatter inherent in the data, especially in the engine rpm during cranking, since the rotational speed varies throughout a revolution and the data acquisition system does not take data that is phased to crank position.

The engine, along with the batteries and fuel, were located inside an environmental chamber. The environmental chamber is capable of attaining -29°C with the working fluid that we used (R 502). The fuel used was a federal specification VV-F-800 DF-A Arctic grade diesel fuel with a cloud point maximum of -51°C . The engine oil used was Mobil DELVAC 1; a high performance diesel synthetic motor oil for sub-zero temperature service.

6.2 Engine Results

Several railplug geometries and materials were examined. The first successful results were obtained with railplug design B which has a value of L/V that is relatively low compared to subsequent railplug designs. The tests using this design were conducted at -6°C , which is below the temperature at which this engine will not start without use of some starting aid. As usual, the railplug was installed in the number four cylinder and the glow plugs were disconnected for cylinders 1-3. The railplug follow-on electronics were set to 150 V and 520 μF , yielding 5.85 Joules stored (notes: 1) the effects of energy are discussed later, and 2) we have not yet attempted to generate efficient electronics, so delivered energy would be more meaningful but has proven difficult to measure accurately). The timing was set to fire the railplug once at 6 CA° BTDC. Figure 25 shows that the exhaust temperatures for those cylinders without a starting aid (#s 1-3) decreased throughout about the first 30 seconds of cranking due to the thermal energy used to evaporate the fuel. In contrast, the exhaust temperature of the railplug-equipped cylinder (#4) was about constant for approximately the first 20 seconds, indicating partial combustion. After 20 seconds, the exhaust temperature of the railplug cylinder began to rapidly increase and the engine speed increased from 200 rpm to 400 rpm. This indicates that the railplug cylinder was firing normally. After 31 seconds of cranking, the exhaust temperatures in the third, second, and first cylinders began to increase in that order and the engine speed increased from 400 rpm to 1100 rpm (off the scale of Figure 25). That is, a single railplug successfully started this engine at -6°C , with heat transfer from the started railplug cylinder leading to eventual starting of adjacent cylinders. With regard to the results that will be discussed below, it should be noted that the exhaust temperatures reach a peak of 40-50 C when the engine has started.

Subsequent tests used railplugs with a higher L/V and temperatures of -29°C . The most significant of these are discussed below.

As noted above, a delay between the start of cranking and the beginning of the increase in exhaust temperature was generally noted in these early tests. However, since we are forcing ignition rather than relying on autoignition, there is no obvious reason for this delay. Because we suspected that heat transfer to the cold rails might be delaying generation of an effective plasma jet until the rails became heated, experiments were conducted in which the railplug was pre-fired at 5 Hz for 2 seconds to preheat the rails before attempting to start the engine. However, it was later discovered that the follow-on circuit was not consistently triggered after breakdown at each firing of the railplug, and therefore the plasma was not being accelerated into the combustion chamber. Once this problem was solved, tests were run with and without pre-firing, and the pre-firing was shown to be unnecessary. That is, achieving consistent follow-on resulted in elimination of the delay and the exhaust temperature would rise without any delay.

The timing of the forced ignition by the railplugs could be varied to optimize the injection of the plasma through the fuel injection spray. The follow-on circuit capacitance was 200 μF charged to 250 V. Railplug design E was used for these tests. As shown in Figure 26, this design allows successful ignition, again resulting in an increase in the

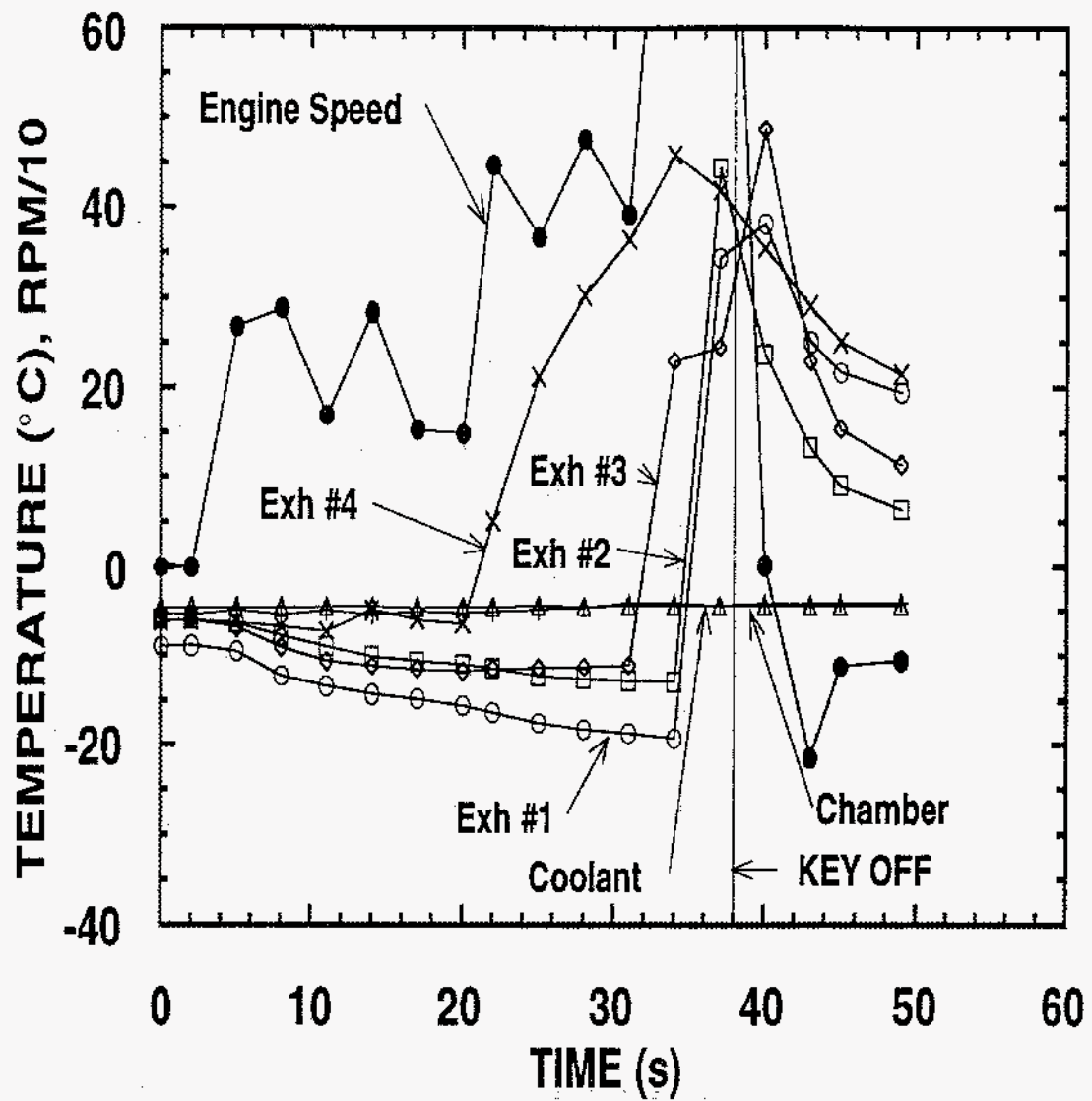


Figure 25. Initial diesel cold start tests at -6°C . Railplug design B was used with a follow-on circuit consisting of $520\ \mu\text{F}$ capacitors charged to 150 V. A single railplug in Cylinder #4 successfully started the engine.

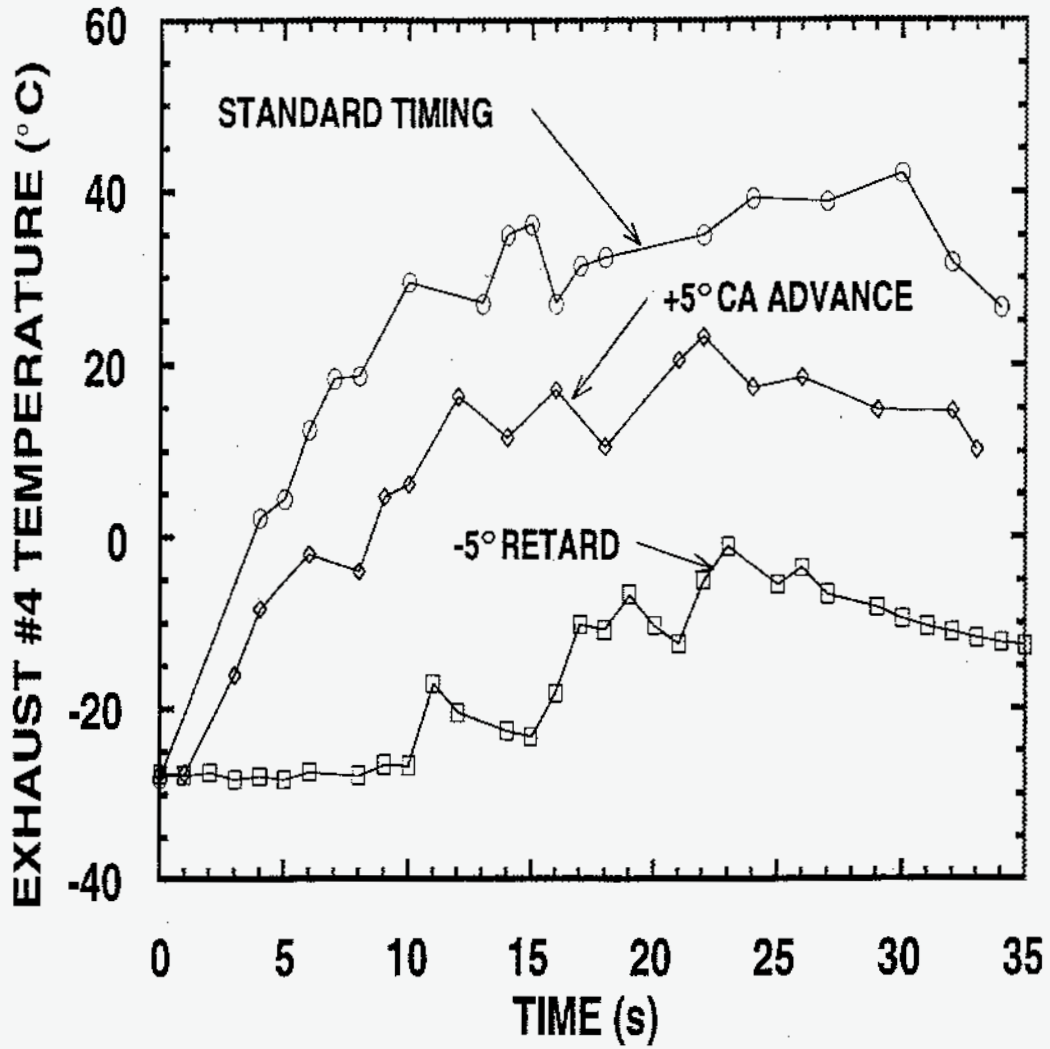


Figure 26. Effects of ignition timing using only one railplug shot per cycle. Railplug design E was used with a follow-on circuit consisting of 200 μ F capacitors charged to 250 V.

exhaust temperature to 30 °C, thus indicating that the engine would start if equipped with railplugs in all four cylinders. Figure 26 shows that with the standard timing, which was spark onset at the beginning of fuel injection, the exhaust temperature increased to 30 °C in 10 seconds. Advancing the timing to 5 CA° before the beginning of fuel injection results in an increase of the exhaust temperature to only 18 °C in 12 seconds. Retarding the timing by 5 CA° to yield spark onset in the middle of fuel injection yields an increase of the exhaust temperature to only 0 °C in 13 seconds after a 10 second delay. Thus, the optimum timing is railplug firing at the beginning of fuel injection.

The effects of both stored energy and "electronics matching" were also investigated. In our previous studies of railplug ignition of premixtures in both a bomb and an SI engine, it was shown that the follow-on circuit electronics must be matched to the railplug geometry under study. Thus, electronics matching was also studied in the diesel cold start tests. The current pulse was shaped by the capacitance of the follow-on circuit and no intentional inductance was used in the follow-on circuit. Tests were run at 50, 100, and 200 μF of capacitance and 150, 200, and 250 volts, yielding stored energies ranging from ~0.6 J - 6.25 J. Railplug design D was used because railplugs of designs C or E were not available for these tests. Two firings per cycle (one at the beginning of injection, the other 10 CA° later) were used because it was shown earlier (as discussed in the paper) that railplug design D is not effective unless double shots are used. Figure 27 shows the results from these tests. As illustrated by the top four curves in Figure 27, for stored energies at or above 2 Joules - with the exception of the 150 V, 200 μF case (2.25 J stored) - the rate of exhaust temperature rise is approximately independent of energy or pulse shape. The result at 150 volts and 200 μF is due to the slow rate of current rise and/or long duration of the current pulse of the 200 μF capacitors at this voltage, as illustrated by the improved results using the same voltage but a lower capacitance (100 μF) even though this also results in decreased stored energy (1.13 J compared to 2.25 J). All of the tests using 50 μF resulted in a relatively slow rate of exhaust temperature rise, probably due to a current pulse that is too short. Thus, it appears that "matching" is more important than stored energy, and that 1-2 J stored is sufficient. Again, it should be noted that we have not attempted to develop efficient electronics, and thus less stored energy may be feasible once more efficient electronics are developed.

7.0 DURABILITY

Examination of durability was not included in the proposed research. However, our External Advisory Board encouraged us to examine the durability of railplugs because alternative ignitors not only must prove to be advantageous, but must also demonstrate acceptable durability.

It is expected that several characteristics should allow railplugs to achieve acceptable durability: 1) the energy is deposited over a large surface area, 2) the arc is accelerating down the rails leaving little time available for erosion, 3) the arc is initiated with currents equivalent to those of spark plugs (the plasma initiation gap is about the same as a spark gap or smaller) and then the current is ramped up to higher levels as the arc accelerates down the rails, and 4) suitable materials can be used near the breech end (i.e., the plasma initiation end) of the railplug where wear rates are highest (since the arc begins with a velocity of zero). Also, durability is expected to improve as less energy is delivered to the railplug.

However, for coaxial railplugs, such as those used in most of our studies, it is difficult to cool the center rail and this has proven to be an additional factor that affects durability. Failure of the coaxial railplugs generally occurs due to material removal from the center rail beginning at the plasma initiation point and extending to a location about 3-4 mm downstream, with almost no erosion further downstream and no significant wear on the outer rail. It is believed that the center rail is becoming too hot in this high erosion region because the arc is established here and initially has a velocity of zero. Cooling of the

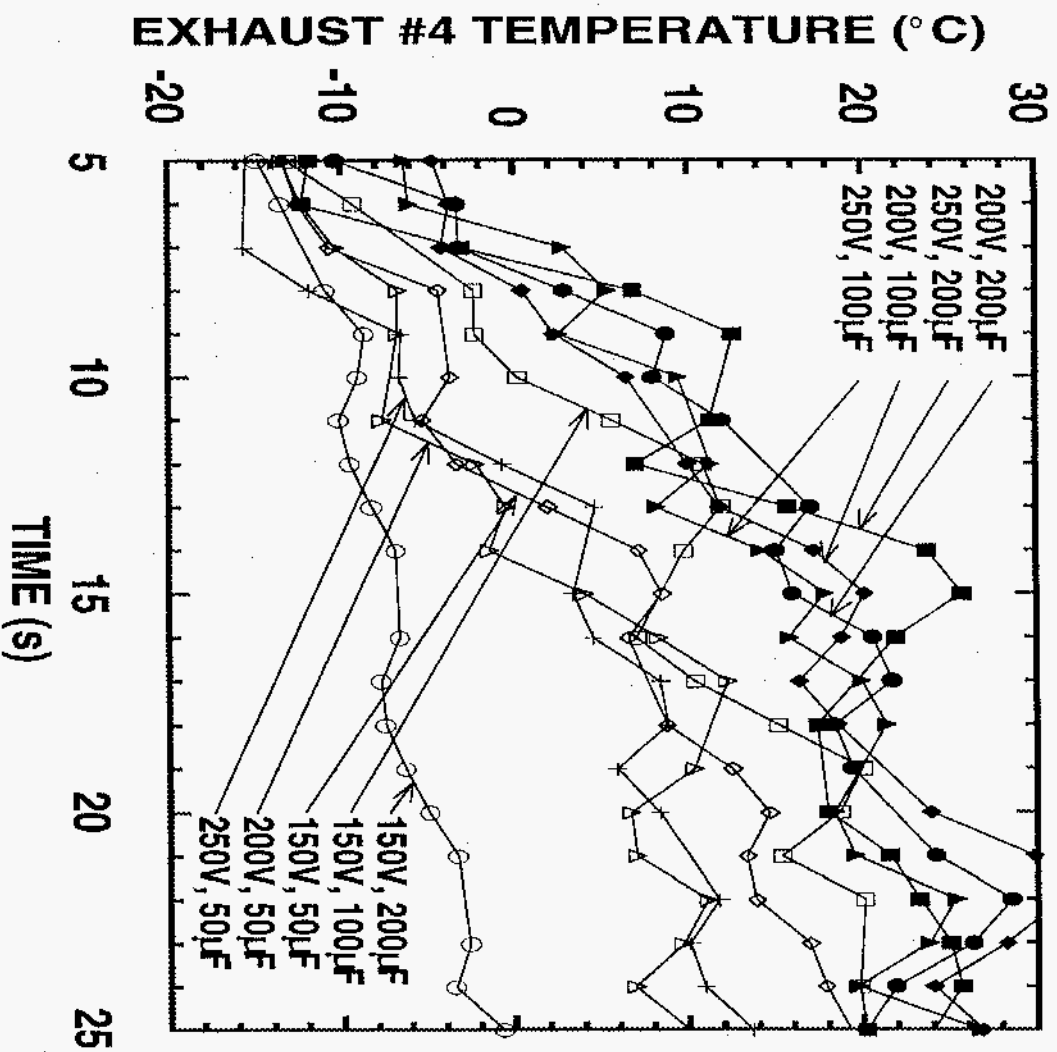


Figure 27. Effects of follow-on circuit electronics settings and stored energy using railplug design D.

center rail can be enhanced through materials selection for the center rail and/or by designing the center rail to have a large cross-sectional area for heat flow into the ceramic.

7.1 Initial Studies

The initial durability tests ((Matthews et al., 1992) were performed in a high pressure vessel filled with air. The pressure vessel was not evacuated and refilled between firings. The test pressure was 1480 kPa (200 psig). Two types of coaxial railplugs were examined: the Champion 705 and the Champion 689. The railplugs were fired at a rate of 18.33 Hz, which corresponds to an engine speed of 2,200 rpm for a four-stroke engine.

The combined effects of the cross-sectional area and rail material on durability are shown in Table 2. The major differences between these coaxial railplugs is the diameter and material of the center electrode. In comparison to the Champion 689, the cross-sectional area available to conduct heat out of the center rail of the Champion 705 is about 3.7 times larger. Also, the Champion 689 has a tungsten center rail while that of the Champion 705 is a high nickel (95.5%) alloy. The thermal conductivity of nickel is about twice that of tungsten. Therefore, it might be expected that the Champion 705 railplug would have about 7 times the durability of the 689 based solely on the product kA . However, as shown in Table 2, the 705 railplug lasts 25 times longer under these conditions. This indicates that other factors are equally important as far as durability is concerned. As one example, although tungsten has a high melting point, it is also susceptible to metal removal through oxide transport. Therefore, it is believed that additional durability can be attained once all of these other factors are identified and included in the railplug design process.

Table 2
Initial Tests of the Effects of Design on Railplug Durability
(at 1.0 J delivered)

Coaxial Railplug	OD* (mm)	material	k** (W/cm-K)	kA (W-cm/K)	time (hr:min)	No. Firings
Champion 689	1.32	W	0.899	0.049	0:07	7,770
Champion 705	2.54	95.5% Ni	1.7	0.344	3:00	198,000

* - of center rail

** - of pure tungsten or nickel at 25 C and 101 kPa

The effects of delivered energy on railplug durability were also studied in these initial tests. As illustrated in Figure 28, railplug durability increases almost exponentially with decreasing energy. Because of the limited electrical power available for peripheral equipment (e.g., power seats, electric window defroster, etc.) operation while the engine is idling, one goal of this project is to develop an effective railplug that requires only 0.5 J delivered, at least at idle (at other speeds and loads, the delivered energy will be a function of the tradeoffs between the railplug performance, brake specific fuel consumption, and durability). These initial results, as expected, indicated that this goal also aids electrode durability. At 0.5 J delivered, the lifetime (as defined by this testing technique) of the railplug used for this study was 300,000 firings.

At the time of these tests, the lifetime of railplugs was about a factor of 250 below our long-term goal. However, the characteristics listed above indicate that reasonable lifetimes should be attainable. This potential was explored in more detail in subsequent tests, as discussed in the following subsection.

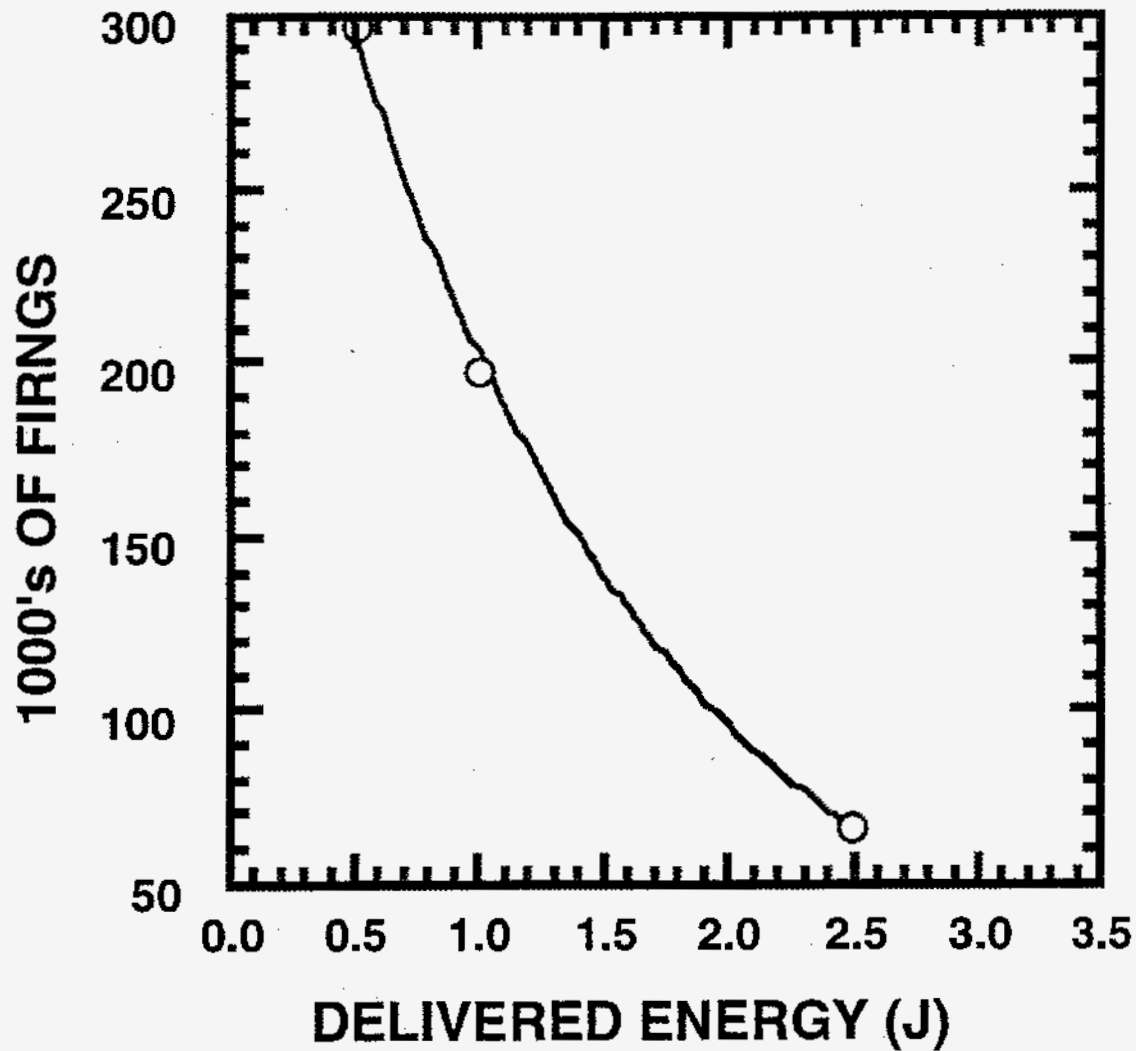


Figure 28. Initial study of the effects of energy on railplug durability in a bomb filled with air at 1480 kPa. Champion 705 with a nickel center rail. Exponential fit to data shown ($R=0.9995$).

7.2 Erosion Studies

As discussed above, for a railplug the combined effects of electromagnetic and thermodynamic forces drive the plasma into the combustion chamber. As importantly, the electromagnetic force results in movement of the arc over the length of the rails. Since the arc is not stationary as in the case of the plasma jet ignitor, electrode erosion should not pose the same difficulty as has prevented the application of the plasma jet ignitor. Again, for the railplug, durability problems are expected to be less severe since 1) the energy is deposited over a much larger surface area, 2) the arc is accelerated down the rails leaving little time available for erosion, 3) the arc can be initiated with currents equivalent to those of spark plugs (the plasma initiation gap is about the same as a spark gap) and then the current can be ramped up to higher levels as the arc accelerates down the rails, and 4) suitable materials can be used to reduce erosion rates in the high wear areas.

In spite of the factors that promise extended durability of railplugs in comparison to plasma jet ignitors, durability remains a critical issue if railplugs are to be successful. However, one difficulty in assessing the durability of railplugs is the lack of a standardized test procedure for evaluation of spark plug life. Thus, our early railplug durability tests, discussed in the previous subsection, focused on "time-to-failure" tests in which a railplug was fired repeatedly in a pressurized chamber - without a combustible mixture - until the railplug failed. A problem with this type of testing came with the definition of "failure". Because a combustible mixture was not used in these tests, conventional measures of failure, such as misfiring, could not be used. Catastrophic failures, such as shorting out of the railplug, were obviously easy to identify. Otherwise the test would be discontinued, and durability thereby defined, when fluctuations in arc current (from one firing to the next) were noted. However, it could not be determined if such fluctuations in arc current would have a significant impact on the performance of the railplug in an operating engine.

The previous comparisons between two railplugs that had different center rail materials and diameters indicated that durability is strongly influenced by the ability to conduct heat away from the center rail but that other factors (that were not identified) appeared to have an even stronger effect. These other factors are believed to be related to material properties in addition to the thermal conductivity, such as the melting point.

In our initial durability studies, three modes of railplug failure were identified:

- 1) railplug shorting (recently determined to stem from a problem with the driver circuit),
- 2) tip initiation (the arc jumping at the muzzle end rather than at the initiation gap, which has been cured by radiusing the muzzle end of the center and outer rails), and
- 3) excessive wear for a length of about 3 mm in the vicinity of the plasma initiation gap.

This last factor motivated the study of materials effects (Chiu et al., 1994). Because of this, we felt it was valuable to examine the fundamentals affecting the erosion rates of railplug electrodes, rather than simply run them to failure as in our prior study. It was believed that this fundamental study, comparing different materials and power supply configurations, would give us the background needed to construct long-life railplugs. The effects of pressure, delivered energy, and voltage at constant delivered energy were studied while using various electrode materials.

7.2.1. Experimental Set-up

We constructed a special electrode holder that formed a parallel electrode railplug. This setup allowed us to quickly and non-destructively remove electrodes for evaluation. Also, as opposed to the standard coaxial railplug, the anode and cathode in this holder are geometrically identical, making for a consistent comparison of erosion between the two. The electrodes were weighed before and after each test. During pressurized testing, the railplugs were fired in a chamber that was pressurized from a bottle of compressed breathing air. The air entered from one end of the chamber and exited on the opposite end, thereby providing a small flow rate (~470 standard cc/min or ~7 air changes per hour) to prevent the build up of a substantial ozone concentration. In all tests, the energy delivered to the railplug was determined from the numerical integration, over time, of the measured

current multiplied by the measured voltage. A counter indicated the total number of firings delivered through the course of the test.

Two different circuits were used to fire the railplug, a standard automotive coil in parallel with the railplug follow-on capacitors-referred to as the "parallel" or "low voltage" circuit-and a triggered spark gap or over-voltage circuit-referred to as the "series" or "high voltage" circuit. The terms "low-voltage" and "high-voltage" refer to the energy storage capacitors, not the breakdown requirement, which was the same in either case. Figure 5 shows the low voltage system, where the pulse transformer is equivalent to an automotive ignition coil. Figure 6 shows the high voltage system, in which the power supply provides both the high voltage needed for breakdown and the high current (in this case, at high voltage) required to generate the Lorentz force. These two systems provide the capability of comparing widely varying capacitance/voltage combinations. This was considered an important parameter because the work by Smy and coworkers (1985) on plasma jet igniters showed a decrease in plug erosion with the use of a high voltage system. The low voltage system has a peak current of 270 amps at 40 μ s and the follow-on current pulse has a duration of 200 μ s. The high voltage system has a peak current of 1230 amps at 0.7 μ s and the follow-on current pulse has a duration of \sim 40 μ s. The high voltage system has a faster rate of current rise and a higher peak current, both of which should increase the acceleration of the plasma, thereby moving the plasma away from the initiation gap quicker and reducing the erosion near the initiation gap. All tests were performed at 20 Hz to simulate realistic engine firing rates.

7.2.2. Results of the Erosion Studies

The first set of tests were performed at atmospheric pressure and using 3 different delivered energy levels: nominally 0.5 J, 1.0 J, and 3.0 J. These tests were performed with the low-voltage power supply. A total of six different materials were tested, four of them common materials, and two of them "exotic" materials. The four standard materials were: tungsten (pure), Elkonite 10W3 (75% W, 25% Cu by weight), nickel (522 alloy, a Champion Spark Plug Co. electrode material), and copper (99.9%). The two exotic materials were a proprietary zirconium ceramic matrix composite (Zr-CMC) and pyrolytic graphite (PG). Pyrolytic graphite was selected because of its high melting point and high thermal conductivity (since it is highly anisotropic, care was taken to orient the material to take advantage of its high thermal conductivity in the direction parallel to the grain). The Zr-CMC has refractory-like properties that give it excellent high-temperature and thermal shock characteristics.

The results of the atmospheric pressure tests are summarized in Figure 29, in which erosion rates are presented in terms of volume loss rather than mass loss since this is the important parameter with respect to rail erosion. All data is normalized on a per firing basis. Tests were run for 30 minutes (36,000 firings) or to failure. None of the tests at 3.0 J lasted to 30 minutes except the Zr-CMC. Also, the pyrolytic graphite at 1.0 J did not last for 30 minutes. Tungsten showed very low erosion rates at all three energy levels, but in engine tests (discussed later) using coaxial railplugs with tungsten center electrodes, the railplugs did not perform as long as those with nickel electrodes. At 1.0 J delivered, Elkonite and copper had about the same low erosion rates followed in order of increasing erosion rates by nickel, Zr-CMC, and pyrolytic graphite. As expected, higher energy levels also increase erosion rates. In fact, of the four materials tested at all three energy levels, three (copper, tungsten, and Elkonite) exhibited rates of volume and mass loss that could be fit by exponentials with $R > 0.999$ while for nickel R was 0.968. The nickel data were fit slightly better by a straight line ($R=0.987$), while the other three materials were fit slightly worse by straight lines.

The second set of tests were performed at 790 kPa (100 psig) and again in air. Based upon the poor performance of the exotic materials during the atmospheric pressure testing, they were replaced with platinum and silver for the elevated pressure studies. Due to time constraints, copper and Elkonite were not tested at elevated pressure. The focus of

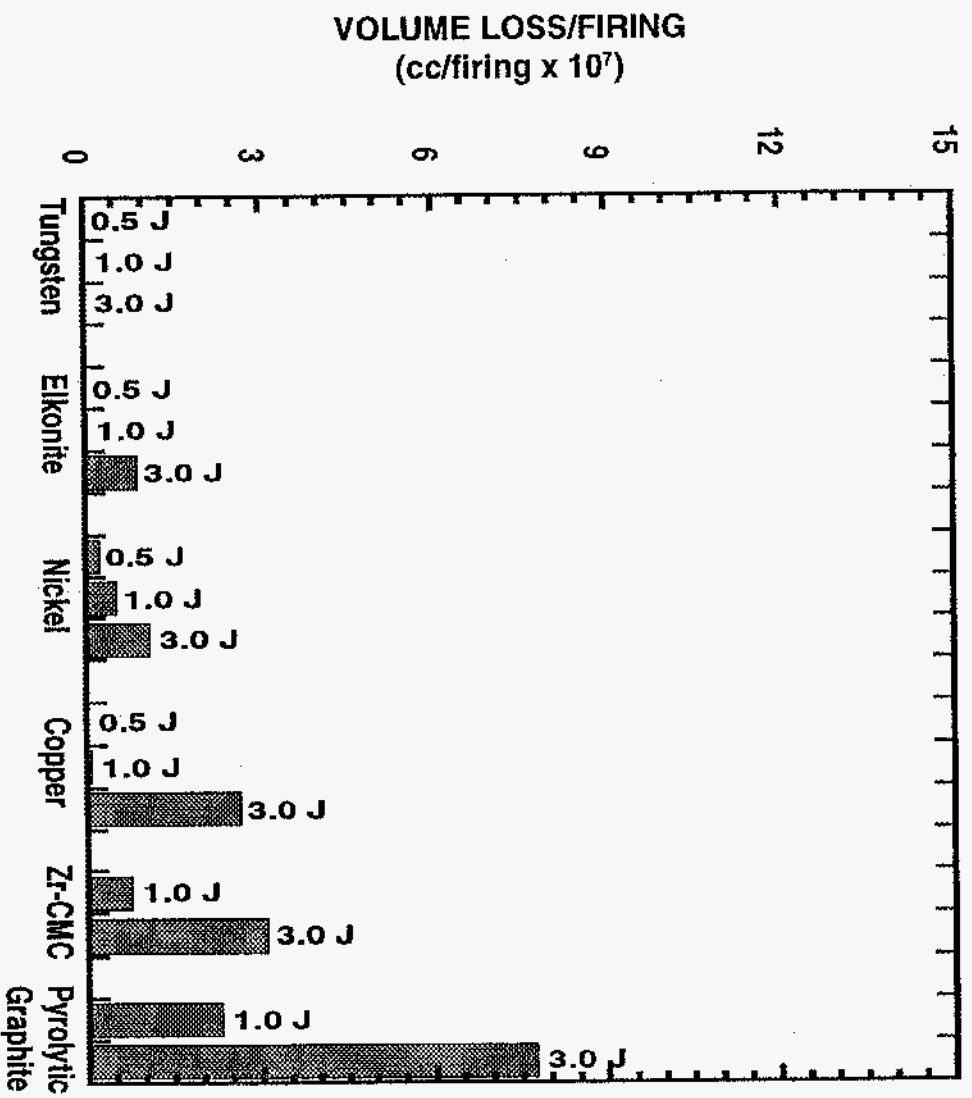


Figure 29. Erosion rates at atmospheric pressure. Volume loss is the sum of anode and cathode loss.

these tests was to evaluate the effect of voltage on electrical erosion. The tests were carried out with both low and high-voltage power supplies, maintaining the delivered energy to the plug at a constant 1.0 J in both cases.

The results of the 790 kPa (100 psig) testing are shown in Figure 30. In the pressurized testing, absolute erosion rates were much higher than in the atmospheric pressure tests, but these tests confirm the trend identified by Smy and coworkers (1985) of higher voltages yielding significant decreases in erosion rates. Silver had the lowest erosion rate followed in order of increasing erosion rates by tungsten, platinum, and nickel. Although Elkonite and copper were not examined in these high pressure tests, based upon comparisons of the materials that were tested at both low pressure and at elevated pressure, it is expected that both Elkonite and copper would exhibit relatively low erosion rates at 790 kPa, especially with the high voltage system.

Among the major conclusions drawn from these erosion tests were that silver and tungsten (and possibly Elkonite and copper) are good candidate materials from the perspective of electrode erosion. Tungsten's low erosion is believed to result from its high melting point, but is not a good material for ignitor applications due to its high-temperature oxidizing characteristics. Silver, copper, and - to a lesser extent - Elkonite, have high thermal conductivities. The high thermal conductivity of silver was responsible for its use as a spark plug electrode material in turbocharged Formula 1 engines due to the need "to get the tremendous heat generated by those engines away from the center electrode as quickly as possible" (Arkless, 1992). These are important conclusions because virtually all of the railplugs evaluated previously, including both engine testing and the prior durability study, had a nickel center rail - since this is a standard center electrode material available from Champion Spark Plug Company - but these results showed that it is not a good material for railplug center electrodes. Another major conclusion drawn from these erosion studies is that use of a high voltage firing circuit significantly reduces erosion rates. It was also found that the cathode erodes faster than the anode, so that the polarity used for railplug applications to engines is correct - the center rail is the anode. That is, because virtually all of the wear on a railplug is on the center rail, making this electrode the cathode would result in increased erosion rates.

7.3. Engine Studies

Durability tests were conducted in a 4-stroke SI engine (Chiu et al., 1994). We chose to measure durability in an engine, rather than firing railplugs in high pressure air as we did previously, for two reasons. First, tests in a pressure chamber do not reflect the temperatures and flows the railplug experiences in an engine, and it was believed that the dynamic events in an engine might influence durability. Second, the definition of railplug "failure" is more straightforward when an engine is being operated by a railplug than was the case for firings in air. In the engine experiments, the effects of delivered energy, current pulse characteristics, and materials were examined. Unfortunately, at the time this paper was completed we could only acquire one other material (in addition to the nickel rails most often used for our engine tests). This was a copper-cored nickel center rail; our erosion studies indicated that copper might be a preferable material. Time did not permit evaluation of use of a high voltage firing circuit. However, it is believed that the use of a high voltage system improves durability via the faster rate of current rise and higher peak current attained with the high voltage circuit. The fact that the current pulse shape also effects the performance of a railplug, even with a low voltage follow-on circuit, suggests the present study of the effects of current pulse shape (or electronics matching) on railplug durability in an engine.

The experimental system used for this study is discussed below, followed by presentation of the experimental results.

7)

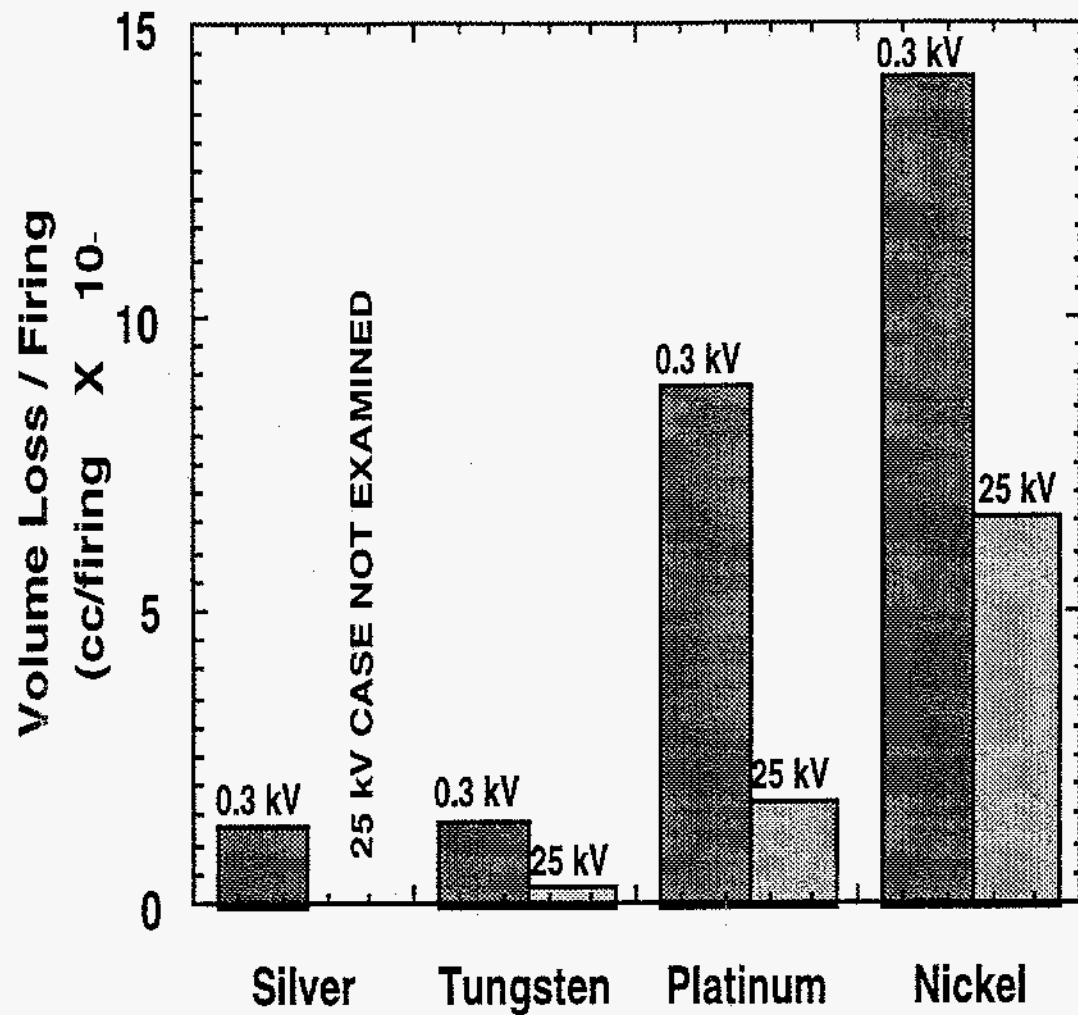


Figure 30. Total volume loss at 790 kPa (100 psi) for high and low voltage tests at 1.0 J delivered.

7.3.1 Experimental Setup

A motorcycle engine from a 1988 Kawasaki EX-500 was used for this experiment. The engine is a liquid cooled, two cylinder, 0.5 liter displacement, 4-stroke engine with spark plugs of 12 mm thread diameter and a 19 mm reach.

The engine was run with a railplug installed in one cylinder and the spark plug wire disconnected in the other cylinder. The engine was not loaded using a dynamometer, and thus the motoring cylinder was used to provide some load to the railplug-equipped cylinder. There was no change to the stock ignition timing, which was measured to be 12 °BTDC for the present operating condition. Unleaded pump gasoline was used as the fuel. Because of the interest in railplug applications to lean burn engines, the carburetor was leaned out as far as possible for these tests. The air/fuel ratio was ~15.8, as measured using a Horiba MEXA-544GE air/fuel ratio monitor.

The railplugs used were of the Champion 727 design, but were modified for 12 mm threads. The 727 is identical to the Champion 705 used in our initial durability investigation (discussed in Section 7.1) except for a somewhat smaller initiation gap (0.76 mm or 0.030" for the 727; 0.89 mm or 0.035" for the 705) and radiusing of the muzzle ends of the center and coaxial rails on the 727. The follow-on circuit was similar to that shown in Figure 4 except that no intentional inductance was used in the follow-on circuit. One to four 50 µF capacitors were used to provide the follow-on energy. The delivered energy was measured using the same system as used for the electrode erosion tests discussed earlier with one exception. Because of the uncertainty in measuring the voltage during follow-on (as discussed in the paper), because of the strong effect of delivered energy on durability, and because the voltage during follow-on is essentially constant, we integrated the measured current profile but assumed a constant follow-on voltage (85 V, the maximum follow-on voltage we had measured during our many previous measurements). Use of the maximum voltage expected yields an upper bound on the energy delivered. Because the voltage drop should be constant for constant rail separation distance, pressure, and gas composition, then all of the present comparisons at a constant delivered energy, as well as comparisons between different delivered energies, should be valid for these comparative purposes.

To allow comparison with our previous durability tests, the engine speed was set to yield a railplug firing rate of 18.33 Hz. Due to this engine's waste spark system, this is an engine speed of 1100 rpm. This engine speed is of further interest because it is relatively close to the 1300 rpm used in our previous engine tests (discussed in Section 5.2).

It was hoped that one advantage to measuring railplug durability in an engine would be that the definition of firings-to-failure would be straightforward - i.e., the number of firings until the engine stopped. However, in most cases when railplugs stop acting as miniaturized railguns, they continue to perform like spark plugs. That is, the follow-on event becomes erratic, but the breakdown event still occurs. This means that the engine continues to run even if there is no follow-on. In principle this problem could be overcome by operating the engine sufficiently lean that it can only run with railplugs. However, at the operating condition used for this study, the carburetor is operating via the idle circuit, and there was insufficient adjustment available to force the carburetor to deliver a mixture sufficiently lean ($A/F > \sim 21$). Thus, we developed instrumentation to examine the fraction of cycles for which we failed to get follow-on. A circuit was designed that converted the pulses from the stock magnetic pickup to light pulses that were routed via optical fibers to a MacIntosh II computer with National Instruments LabView data acquisition hardware and software. Each of these pulses represent a firing event. A second circuit was designed to convert the capacitor discharge events to a string of light pulses that were also routed to this data acquisition system. The system then logged the total number of successful firings accumulated and the total number of ignition events that should have occurred. This measurement did not allow determination of whether lack of follow-on was due to lack of breakdown (essential to provide a path for the follow-on current) or due to some difficulty with the follow-on circuit or the railplug itself. However, because the engine almost never

died during these tests, it is believed that consistent breakdown was achieved. We believe that the explanation for the process by which breakdown can occur - providing the required path for follow-on - but without the follow-on process that should occur automatically is that the voltage required to sustain the arc is dependent upon the separation distance between the rails. Because this distance increases as the rails erode, the follow-on process becomes more difficult as firings are accumulated.

The preceding paragraph is an introduction to the definition of "firings-to-failure" for the railplug durability tests in an engine. If railplugs are used in a very dilute charge application, then the number of firings until 1% of the ignition events do not yield follow-on would be a logical definition of railplug failure, since this would result in high cyclic variability. However, in practice this 1% criterion was often met during the first few thousand cycles after initial start-up, after which the system would settle into a stable state. Therefore, we defined firings-to-failure as the number of successful firings (firings with follow-on) at the time that the ratio of the cumulative number of ignition events without follow-on to the total number of ignition pulses reached 5%.

7.3.2 Engine Results

For comparison with the results of the previous bomb tests, the follow-on circuit was operated with delivered energy levels ranging from 0.5 J to 2.5 J. Additionally, the effects of the current pulse characteristics were studied. Of the various results obtained, only the most important are discussed below; the reader is referred to the paper (Chiu et al., 1994) for discussion of the additional results.

The effects of current pulse duration at 2.5 J delivered are illustrated in Figure 31. The pulse duration was varied via the capacitance of the follow-on circuit. In our previous CFR engine tests (discussed in Section 5.2), a capacitance of 100 μF was determined to yield the fastest combustion at 2.5 J delivered. In the present study, capacitances equal to and greater than this were examined, but limitations on our power supply would not allow examination of lower capacitances at 2.5 J delivered. It is expected that capacitances lower than that which yields best performance. To explore this possibility, a 50 μF test was done at 2.0 J delivered. As shown in Figure 31, increasing the capacitance above the value that yields fastest combustion results in a faster rate of increase of firings without follow-on. This trend is expected, because increasing the capacitance while holding the delivered energy constant requires decreasing the charging voltage. Thus, as the capacitance increases, the voltage available to sustain the arc decreases. As the center rail erodes with the accumulation of firings, the gap widens, more voltage is required to sustain the arc, but less voltage is available as the value of the capacitance is increased. However, Figure 31 also illustrates a second trend - as the capacitance is decreased, the number of cycles the engine could operate before it died and could not be restarted decreased. Here, it should be noted that before the engine died, few cycles without follow-on had been accumulated for the cases with the capacitance < 150 μF . Further, the number of cycles before the engine died is inversely related to the voltage available to sustain the arc. Thus, the problem was not that the arc could not be sustained. Rather, the inability to restart the engine for these conditions is believed to be related to the failure mode for these high delivered energy tests. As discussed in more detail later in this section, these railplugs exhibited "blisters" due to overheating, and we believe that these blisters may have quenched the flame that was ignited by the breakdown spark. It is also of interest to note that the slopes of the curves in Figure 31 indicate that the current pulse characteristics may have a significant effect on durability for the lower energy cases that do not exhibit this failure mode. Further, it is believed that matching the capacitance to the railplug geometry should result in improved durability.

The results of these engine tests also indicated that railplug durability does not necessarily increase exponentially with decreasing delivered energy. That is, durability is a function not only of the delivered energy but also of the capacitance/voltage combination used to obtain the desired delivered energy (i.e., electronics "matching"). This appears to

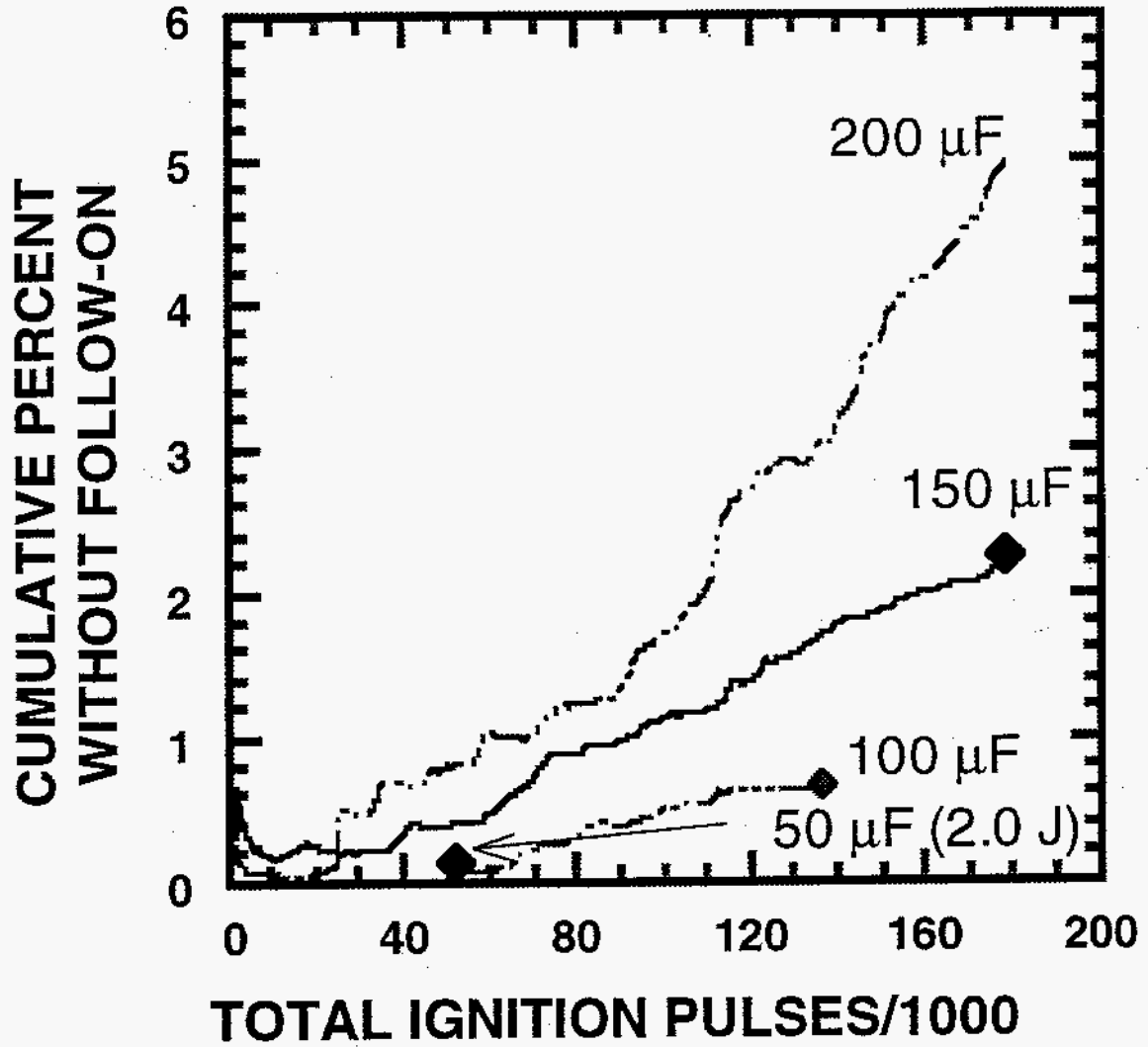


Figure 31. Effects of current pulse characteristics on railplug performance in an engine at a constant 2.5 J delivered (except for the 50 μF case, for which 2.0 J was delivered). The solid symbols indicate when the engine stopped and could not be restarted.

disagree with the erosion rate results discussed earlier and with our prior durability results since in those cases we found that durability increased exponentially with decreasing delivered energy. However, in all previous tests, including the erosion rate tests, the capacitance was decreased as the delivered energy was decreased in order to maintain the charging voltage at a convenient level. It is concluded that additional studies of the effects of capacitance should be performed at the lower energy levels of interest, since a different failure mode is encountered at these lower delivered energies, as discussed later in this section.

As illustrated in Figure 32, the railplug used for the 0.6 J test was run for 1,200,000 ignition pulses which resulted in almost 1,000,000 successful firings with follow-on and the tests could have been continued beyond this point. However, as illustrated in Figure 32, the follow-on process became less dependable as firings were accumulated. After this test, this railplug was disassembled for inspection. The failure mode observed is discussed later in this section.

The effects of materials were examined by comparing nickel center rails with copper-cored nickel. The copper core had an OD of 1.57 mm (0.062") and thus represented ~40% of the cross-sectional area available to conduct heat away from the center rail. This material was chosen because copper has a high thermal conductivity, which should aid the center rail cooling that we believe is important to durability, while the nickel outer layer was used because comparison of copper-cored nickel with pure nickel center rails provides additional information about the significance of conduction of heat away from the center rail. Surprisingly, the railplug with the copper-cored center rail exhibited only a 17% increase in durability in comparison to the railplug with a pure nickel center rail, rather than the ~70% that might be expected from the properties shown in Table 3. In both cases, the failure mode was wear near the initiation gap. The copper-cored railplug had lost only 0.18 mm off the center rail radius, so that the copper core had not been reached by the time this railplug reached our defined failure condition. Thus, the lack of a more significant effect of center rail material on the present results indicates that the poor erosion characteristics of the nickel dominated the failure of both the railplug with the nickel center rail and that of the railplug with the copper-cored nickel center rail. The failure modes are discussed additionally later in this section. As noted above, due to time constraints, we were not able to examine additional materials. However, although tungsten was determined to be a promising material in the electrode erosion tests, during prior CFR engine tests railplugs using tungsten center rails were not as durable as nickel railplugs due to what appeared to be an oxidation problem.

Table 3
Engine Tests of the Effects of Materials on Railplug Durability
(at 0.6 J delivered)

Coaxial Railplug	OD* (mm)	center rail material	k** (W/cm-K)	"effective" kA (W-cm/K)	No. Firings
Champion 727	2.54	Cu cored Ni	4.83	0.586	~360,000
Champion 727	2.54	95.5% Ni	1.7	0.344	~430,000

* - of center rail

** - of pure copper or nickel at 25 C and 101 kPa

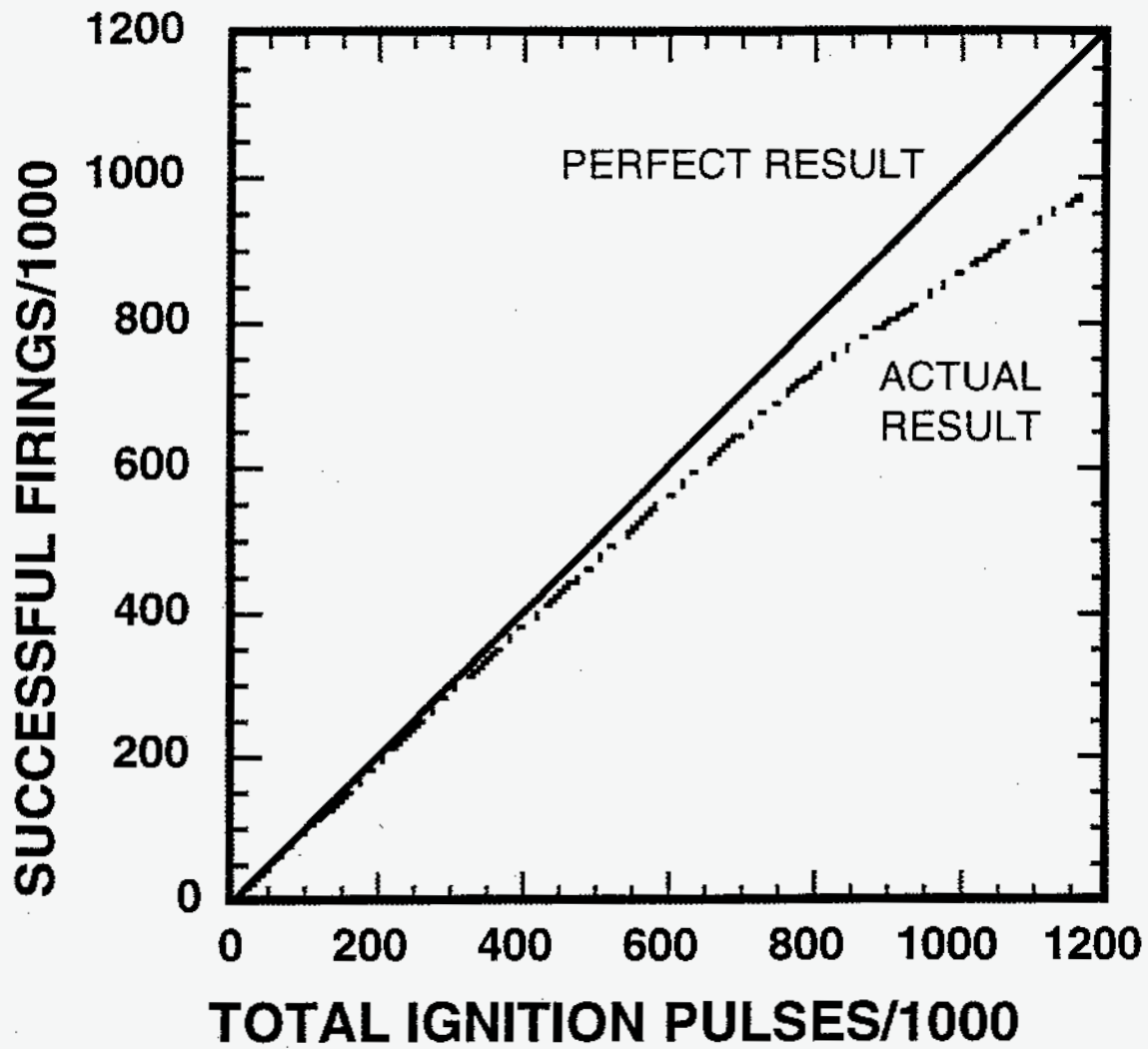


Figure 32. Behavior of the Champion 727 railplug with the nickel center rail at 0.6 J delivered with accumulation of ~1,000,000 firings with follow-on.

For the tests discussed above, two railplug failure modes were observed. Tests at 3.5 J delivered (not discussed above) using a variety of capacitances yielded very repetitive operation (very few cycles without follow-on) up to ~50,000 firings when the engine would die and restart was not possible. Inspection of these plugs revealed little wear near the initiation gap. However, further down the center rail, the nickel was gnarled with "blisters" about 0.25 mm high and wide, and thus appeared to have melted due to overheating. This failure mode was also observed for the 2.5 J cases, but was not observed for the 0.5 J cases). Additionally, since the railplugs tested at 2.5 J survived longer than those tested at 3.5 J, wear in the initiation gap was observed. For the 0.5 J tests discussed above, the railplugs failed due to erosion near the initiation gap, with the downstream portion of the center rail appearing almost pristine. Even for the nickel railplug run for ~1,000,000 successful firings at 0.5 J, the center rail appeared to be in good condition except for the vicinity near the initiation gap. For a distance of ~3.3 mm down the center rail beginning at the insulator nose, the center rail had worn with its diameter decreased from the original 2.5 mm to ~1.6 mm at its narrowest point. For the copper-cored railplug at 0.5 J, which was successfully fired only ~430,000 times before disassembly compared to the ~1,000,000 successful firings before disassembly of the nickel railplug, the downstream portion of the center rail appeared in almost new condition, but the portion near the insulator was worn over a distance of ~2.7 mm and had necked down to a diameter of ~2.3 mm at its narrowest point.

To gain further insight into these two failure modes, railplugs were run to a total of ~50,000 ignition pulses (virtually all of which resulted in follow-on) using a follow-on circuit capacitance of 50 μ F and variable charging voltage to yield variable delivered energy at constant current pulse duration. At 2.0 J and at 1.45 J delivered, the blistering of the center rail was isolated to the region just past the downstream end of the initiation gap, which, as expected, had been eroded less at 1.45 J than at 2.0 J. The distance down the center rail that exhibited this blistering also decreased with decreasing delivered energy, and tests at 1.0 J revealed no blistering of the center rail and, as expected, still less erosion in the vicinity of the initiation gap than was observed at 1.45 J. Because few firings had been attempted for these tests, it is concluded that rail blistering begins near the downstream end of the initiation gap and then propagates down the center rail toward the railplug muzzle. At 1.0 J and at 0.5 J, no blistering was observed. Thus, the division between the blistering mode of failure and failure due solely to erosion near the initiation gap appears to be in the range of 1.0-1.4 J.

Thus, at the energy levels of interest, the initial failure mode is erosion near the initiation gap. This high wear area is illustrated in Figure 33. Comparison of the high wear area of the center rail with the initiation gap geometry makes it apparent that the arc, or at least that portion of the arc that borders the center rail, is not traveling far from the initiation gap. This suggests that changes to the railplug geometry would be beneficial. When the bore widens from the initiation gap to the main body, the inductance gradient rapidly increases by a factor of two. This should promote movement of the arc past the initiation gap. However, it appears that the sudden discontinuity at the downstream edge of the initiation gap is holding the arc. Several changes in geometry are suggested by these observations:

- 1) Use a conical bore instead of a straight bore, to remove the sharp discontinuity at the end of the initiation gap, also yielding an inductance gradient that changes smoothly rather than abruptly.
- 2) Decrease the rail length (and make other modifications) to increase L/V .
- 3) Allow sufficient void space between the initiation gap and the insulator nose such that the ratio of the void volume to the total trapped volume equals the compression ratio.

This should ensure a combustible mixture in the initiation gap so that thermal expansion due to chemical energy release might help move the arc down the rails.

Designs that might promote aerodynamic cooling of the center rail should also be considered.

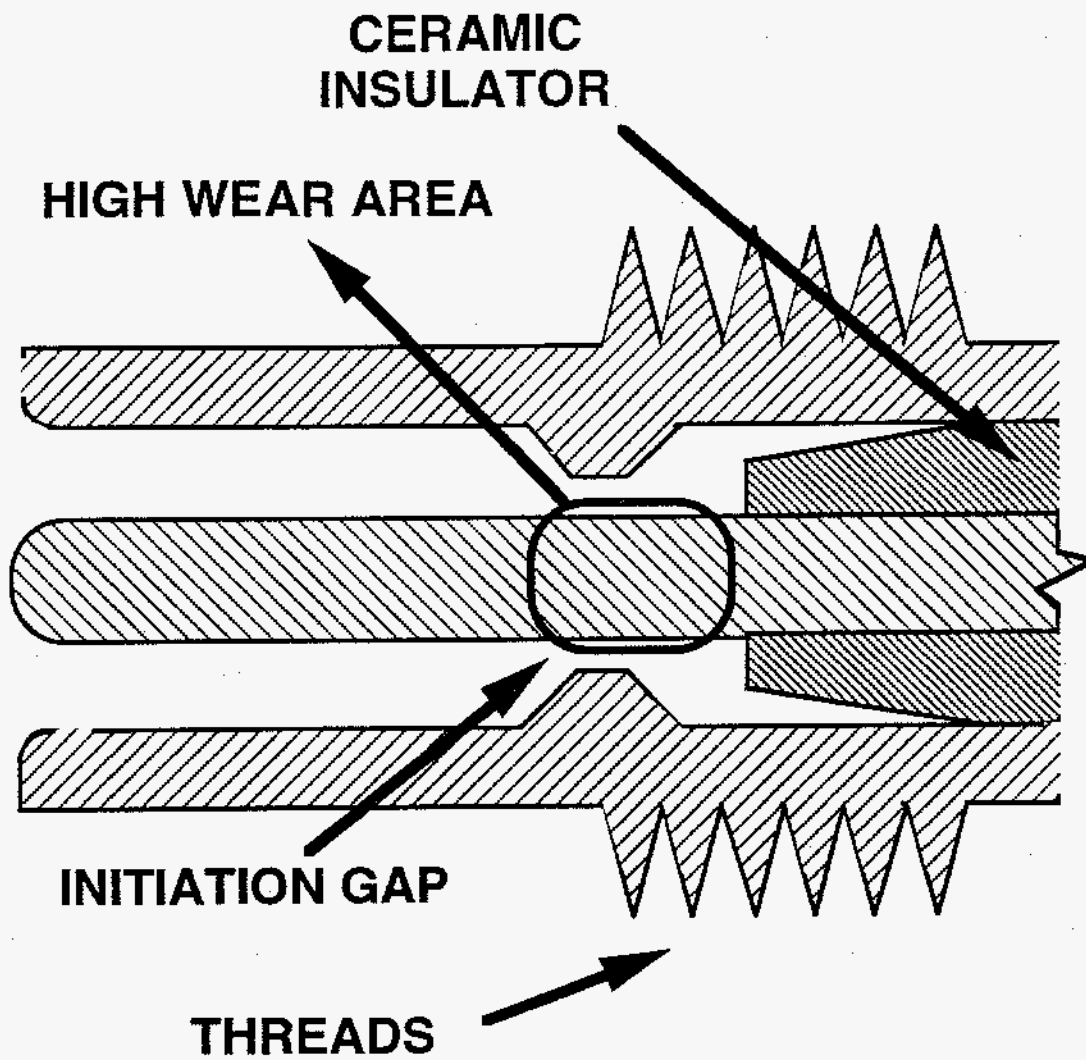


Figure 33. Schematic of the Champion 727 railplug, comparing the high wear area with the location of the initiation gap.

Further durability benefits are expected (from the results of our electrode erosion tests) to accrue via use of a high voltage firing circuit. Due to time constraints, we were not able to examine the potential benefits of the high voltage system, but such tests should be performed in the future. A railplug lifetime improvement of a factor of two or much more is expected from using a high voltage circuit rather than the low voltage circuit used in the present experiments. Also, additional benefits should be expected by using other materials, such as those discussed in Section 7.2. However, the main problem identified in these engine tests is that the geometry of our initiation gap appears to be holding the arc, thereby promoting poor durability.

7.4. Continuing Work

As discussed in the previous section, our durability studies in an engine revealed that the design of the railplug that we had been using for about the past 2 years had an inherent durability problem. Specifically, the abrupt change in cross-section at the end of the initiation gap appears to prevent the arc from moving further down the rails, so that the electrical energy is deposited over a shorter length of the center rail than would otherwise be possible. In turn, this results in difficulty regarding cooling of the center rail. Thus, after our last paper was completed, we began investigating other geometries.

One of the geometries investigated had a tapered outer rail. The minimum cross-section occurs at the breech end near the insulator and serves as an initiation section for breakdown. The outer coaxial rail then gradually increases in diameter, so that no abrupt change in cross-section is present to hold the arc. With 0.63 J delivered, we ran this railplug in the durability test engine for 670,000 firings with only 0.21% of the cycles lacking correct follow-on. Even though we could have operated this railplug much longer, we ended this test to disassemble the railplug to inspect it for wear. The results of this inspection are discussed below. To ensure that the new railplug design coupled to the much lower energy used for these durability tests in comparison to previous single cylinder engine tests of railplug performance (0.63 J compared to 2.5J) had not significantly affected railplug performance, we also conducted some performance evaluation in the same single cylinder research engine. These engine performance tests differed from those discussed previously only in that we did not set the ignition timing using Equation 16. Rather, the ignition timing was set to maintain the location of peak pressure at about 15 CA° ATDC. This LPP is often used as a "rule of thumb" for the LPP that yields minimum advance for best torque (MBT), but is actually slightly retarded from MBT for this engine under these operating conditions ($A/F \approx 20$ with all other conditions the same as those discussed in Section 5.2). This railplug, using only 0.8 J of delivered energy, decreased the COV of imep from 9.8% for the wide gap spark plug to 5.7%. These were first engine results with delivered energies this close to our goal and demonstrated that we can attain performance improvements with relatively little energy and, as importantly, that this railplug design - which appears to promise much improved durability - is still effective as far as performance is concerned.

Similar durability tests were performed with this railplug design using shorter current pulses and the durability was significantly decreased. Longer current pulses could not be studied because this requires charging voltages that are so low that the arc cannot be sustained using the consequent follow-on voltage.

Examination of the railplugs used for these studies revealed that the one that yielded high durability still exhibited wear near the initiation plane - although in this case not only the center rail but also the annular rail were worn - while the one with the very short current pulse had shorted due to overheating near the initiation plane. The result for the very short current pulse is not surprising while that for the high durability test was somewhat surprising. It indicates that even in this case the current pulse is too short (recall that we cannot use higher capacitances to yield a longer pulse at this energy level) or, equivalently, that the rails are too long. For this reason, we also examined the effect of rail length. In this case, we modified a Champion 727 railplug so that the initiation gap was closer to the

muzzle end. With 0.63 J delivered, this railplug also ran for 670,000 firings before the test was halted to allow examination of the rails. Similar to the tapered design, this also yielded very few cycles with poor follow-on - only 0.47% of the total cycles. In this case, the failure mode was high wear of the center rail again. In this case, wear of the center rail is promoted by the very large length of bare center rail between the initiation gap and the insulator, which impedes heat transfer away from this wear region.

The good results obtained for the tapered railplug and for the shorter railplug suggest that a short tapered railplug might offer significant durability benefits, especially if a longer insulator is used. We are working with Champion Spark Plug Company to generate railplugs of this new design.

8.0 SUMMARY AND CONCLUSIONS

A three year investigation of a new type of ignitor for internal combustion engines has been completed with funding from the Advanced Energy Projects Program of The Basic Energy Sciences Division of the U.S. Department of Energy and with matching funding from Research Applications, Inc. This research was supervised by three Principal Investigators (Profs. Ron Matthews, Bill Weldon, and Steve Nichols) and two Faculty Associates (Profs. Janet Ellzey and Matt Hall). The CES tasks were managed by James Chiu and those at CEM were managed by Richard Faidley. Additionally, several full-time researchers worked on this project (Mike Darden, Zheng Jie, and Harry Childs). This research contributed to two Master's theses (Mike Koenig and Gordon Weigand) and to three PhD dissertations (X.W. Zhao, K. Shen, and D.Y. Wu). A number of undergraduate students also worked on this project; of these, Chris Mitchell deserves special mention because he is performing all of the current studies of the effects of railplug geometry on performance and durability (discussed in Section 7.4).

The tasks performed during this project included:

- development of railplugs and driver electronics
- studies of the effects of railplug geometry and of the driver electronics on railplug performance
- use of models to improve understanding of railplug physics
- proof of principle for extension of the dilution tolerance of SI engines
- proof of principle for diesel cold start
- examination of the factors that influence the durability of railplugs

Durability studies were not originally included in the proposed work. However, after we began showing that railplugs showed significant promise, our External Advisory Board requested that we examine this issue. This additional task required that we decrease the level of effort on some of the tasks that were originally proposed.

Several generations of railplug designs were developed and evaluated. Also, several generations of driver electronics were also developed and evaluated. Our experimental tasks consisted of 1) fundamental studies of the effects of various parameters on railplug performance, 2) studies of the ability of railplugs to extend the dilution limit of spark ignition engines, 3) studies of the ability of railplugs to extend the cold start limit of a production diesel engine, and 4) railplug durability studies. In summary:

- 1) We learned much about the effects of railplug geometry on railplug performance (but believe that more can still be learned with respect to geometry effects).
- 2) We learned that the current pulse shape provided by the follow-on circuit must be matched to the specific geometry under study (thus adding another level of complexity to the experiments).
- 3) We learned that extremely high plasma jet velocities can be achieved and that this both creates turbulence at the flame front and induces flow in the unburned gases that, in turn, results in a preferred direction of flame propagation (along the jet axis).
- 4) We learned that parallel rail railplugs perform better than coaxial railplugs. However, parallel railplugs are extremely difficult to fabricate. Thus, we focused most of our

studies on the coaxial design. Most of the railplugs we used were made for us by Champion Spark Plug Company using standard spark plug production parts. This means that railplugs should cost little more than conventional spark plugs.

- 5) We believe that we convincingly proved that railplugs can extend the dilution limits of SI engines. This belief is supported by feedback from members of our External Advisory Board. Thus, the primary issue for commercialization is durability.
- 6) We proved that we can significantly improve the cold start limit of IDI diesels using railplugs with reasonable energies.
- 7) We successfully developed two different numerical models that proved useful in aiding our understanding of railplugs.
- 8) Over the course of the project, we improved the durability of railplugs from ~20,000 firings to ~1,000,000 firings. About 400,000,000 firings are required to be competitive with spark plugs. While we examined several materials (for the center rail, which is the site of failure due to inability to transfer heat away sufficiently fast) and several railplug geometries, we believe that much more can be accomplished in this area. Most importantly, we found that the design of our initiation gap was promoting failure so that additional geometries should be examined. We also know that use of a series power supply for the follow-on circuit aids durability, but never fabricated such a system that was adequate for engine testing. Further, we believe that further progress can be made with respect to center rail materials. Again, it should be noted that this task - durability - was added after the start of the project, so that it was not possible to devote as much manpower to this task as we would have preferred. We are continuing our work in this area, but with a low level of effort due to lack of funds.

That is, we believe that we have proven that railplugs can be effective both for extending the dilution limit of spark ignition engines and for extending the cold start limit of diesels. For the SI engine, the durability of railplugs remains as the major factor inhibiting applications to production engines. We have done much to improve the durability of railplugs in SI engines and believe that significant progress can still be made. We are continuing our work in this area - durability - but at a low level of effort due to the lack of funds.

Until adequate durability can be proven for the production SI engine application, one option is to explore applications that do not require as much durability. One example is diesel cold start. While we have not explicitly examined railplug durability in a diesel environment, only about 50,000 successful firings are required to be competitive with glow plugs and we have demonstrated at least 10 times more firings in a SI engine environment. Here, it is noteworthy that in our comparative cold start tests using glow plugs, we found that they did not survive very well. Thus, if durability is raised as an issue for this application, we will need to generate some type of standardized durability testing technique for the diesel application. However, the U.S. auto manufacturers appear to be abandoning the IDI diesel in favor of DI diesels for light duty vehicles. While we believe that our IDI experiments also serve as a proof of principle for DI diesels, others would like to see direct proof and no funds are available for these additional experiments.

Another example of a potential railplug application with lower durability requirements is cold start of neat alcohol engines. In this case, the railplug would function as a railplug to achieve cold start and then would function as a spark plug during normal operation, thereby minimizing the number of high energy firings required (we have shown that railplugs operate very satisfactorily as spark plugs if we only provide the breakdown pulse without the high energy follow-on pulse). We submitted a Letter of Intent for exactly this type of project to NREL, but were not requested to submit a formal proposal. We are now exploring possibilities in this area with researchers at Southwest Research Institute.

Another example is drag racing of highly turbocharged engines. Achieving ignition in these engines is very difficult, so that they use very high energies, but find that the spark plugs have vaporized before the end of the 1/4 mile race. We have shown - but have not

reported - that railplugs are much more durable than spark plugs when the same high energy is supplied to both. The difficulty with this application is finding a source of funding. One attribute of this application is that it would generate a lot of positive attention, thereby possibly making it easier to attract the funding needed for additional durability research.

A different option is to explore SI engine applications for which the achievement of lean-burn may be more important than is the required plug replacement interval. The large bore stationary natural gas engine is one example. These engines use lean burn to control NOx emissions, but suffer high hydrocarbon and formaldehyde emissions as a result of operating so lean that the partial burn limit is encountered. As noted above, we have shown that railplugs can extend the partial burn limit to leaner mixtures, at least for small bore gasoline engines. We are exploring the possibilities of funding for this application with investigators at Southwest Research Institute.

Thus, we are continuing our efforts at a low level and are seeking additional funding. Our continuing efforts are in the durability area and in additional performance testing as applied to high EGR spark ignition engines.

ACKNOWLEDGEMENTS

We wish to thank Dr. Walt Polansky and Dr. Duane Barney of the Advanced Energy Projects Program, Basic Energy Sciences Division, U.S. Department of Energy for their support. We also wish to thank Frank McBee, Dale Mosier, and Jack Locy of Research Applications, Inc. We especially wish to thank Dr. Dan Tribble and Tim Timco of Champion Spark Plug Company for their guidance, advice, and efforts in the areas of railplug design and fabrication. Appreciation is also expressed to the members of the Railplug External Advisory Board for their guidance, time, and efforts on our behalf. Brian Harden deserves special recognition for initially conceiving the railplug.

BIBLIOGRAPHY

- Abdel-Gayed, A.G., D. Bradley, and A.K.C. Lau (1989), "The straining of premixed turbulent flames", *22nd Symposium (International) on Combustion*, the Combustion Institute, Pittsburgh, pp. 731-738.
- Arkless, S. (1992), "The design, manufacture and application of spark plugs for race engines", *Racecar Engineering* 2(5):70-71.
- Asik, J.R., P. Piatkowski, M.J. Foucher, and W.G. Rado (1977), "Design of a plasma jet ignition system for automotive application", SAE Paper 770355.
- Bradley, D., and I.L. Crichley (1974), "Electromagnetically induced motion of spark ignition kernels", *Combustion and Flame* 22:143-15.
- Chiu, J.P., M.H. Darden, R.D. Matthews, H.E. Childs, R.W. Faidley, J. Zheng, G. Weigand, W.F. Weldon, and S.P. Nichols (1994), "Examination of the factors that influence the durability of railplugs", SAE Paper 940201, also in *Advanced Power Plant Concepts*, SAE Special Publication SP-1038.
- Clements, R.M., P.R. Smy, and J.D. Dale (1981), "An experimental study of the ejection mechanism for typical plasma jet ignitors," *Combustion and Flame* 42: 287-295.

- Dale, J.D., P.R. Smy, and R.M. Clements (1978), "The effects of a coaxial spark igniter on the performance of and the emissions from an internal combustion engine", *Combustion and Flame* 31:173-185.
- Dale, J.D., and A.K. Oppenheim (1981), "Enhanced ignition for IC engines with premixed gases", SAE Paper 810146.
- Edwards, C.F., A.K. Oppenheim, and J.D. Dale (1983), "A comparative study of plasma ignition systems," SAE Paper 830479.
- Edwards, C.F., H.E. Horton, and A.K. Oppenheim (1985), "A photographic study of plasma ignition systems," SAE Paper 850077.
- Faidley, R.W., M.H. Darden, and W.F. Weldon (1992), "The railplug: a new ignitor for internal combustion engines", *Proceedings of the 6th Symposium on Electromagnetic Launch Technology*, Institute for Advanced Technologies, the University of Texas at Austin.
- Fitzgerald, D.J. (1976), "Pulsed plasma igniter for automotive use," SAE Paper 760764.
- Fitzgerald, D.J. , U.S. Patent 4,122,816, 1978.
- Gmurczyk, G.W., T. Lezanski, T., M. Kesler, T. Chomiak, T. Rychter, and P. Wolanski (1992), "Single compression machine study of pulsed jet combustion (PJC)", *Twenty-Fourth Symposium (International) on Combustion*, The Combustion Institute, Pittsburgh, pp.1411-1448.
- Gomez, A.J. and P.E. Reinke (1988), "Lean burn: a review of incentives, methods, and tradeoffs," SAE Paper 880291.
- Hall , M.J., H. Tajima, R.D. Matthews, M.M. Koeroghlian, W.F. Weldon, and S.P. Nichols (1991), "Initial studies of a new type of ignitor: the railplug", SAE Paper 912319, also in *Journal of Engines* 100:1730-1746 (1992).
- Hall, M.J., J.L. Ellzey, H. Tajima, and X.W. Zhao (1993), "Plasma plume generation by a railplug ignitor and simulation by multidimensional modeling", *Experiments in Fluids* 14:416-422.
- Harrison, A.J., and F.J. Weinberg (1974), "A note on electromagnetically induced motion of spark ignition kernels", *Combustion and Flame* 22:263-265.
- Heywood, J.B. (1988), *Internal Combustion Engine Fundamentals*, McGraw-Hill, New York.
- Koenig, M.H. (1991), "An experimental investigation of the railplug ignition system in a lean burn engine", Master's Thesis, Dept. of Mech. Eng., the University of Texas, Dec.
- Kupe, J., H. Wilhelm, and W. Adams (1987), "Operational characteristics of a lean-burn SI engine: comparison between plasma-jet and conventional ignition systems", SAE Paper 870608.

- Lezanski, T., M. Kesler, T. Rychter, A. Teodorczyk, and P. Wolanski (1993), "Performance of pulsed jet combustion (PJC) system in a research engine", SAE Paper 932709.
- Matthews, R.D., M.J. Hall, R.W. Faidley, J.P. Chiu, X.W. Zhao, I. Annezer, M.H. Koenig, J.F. Harber, M.H. Darden, W.F. Weldon, and S.P. Nichols (1992), "Further analysis of railplugs as a new type of ignitor", SAE Paper 922167, also accepted for publication in the *Journal of Engines*, 1993.
- Maxon, J.A., and A.K. Oppenheim (1990), "Pulsed jet combustion - key to refinement of the stratified charge concept", *Twenty-Third Symposium (International) on Combustion*, The Combustion Institute, Pittsburgh, pp. 1041-1046.
- Modien, R.M., and J.D. Dale (1991), "The effect of enhanced ignition systems on early flame development in quiescent and turbulent conditions", SAE Paper 910564.
- Murase, E., S. Ono, K. Hanada, and S. Nakahara (1989), "Plasma jet ignition in turbulent lean mixtures," SAE Paper 890155.
- Namekawa, S., H. Ryu, and T. Asanuma (1988), "LDA measurement of turbulent flow in a motored and firing spark-ignition engine with a horizontal prechamber", SAE Paper 881636.
- Oppenheim, A.K., K. Teichman, K. Hom, and H.E. Stewart (1978), "Jet ignition of an ultra lean mixture" SAE Paper 780637.
- Oppenheim, A.K., J. Beltramo, D.W. Farris, J.A. Maxon, K. Hom, and H.E. Stewart (1989), "Combustion by pulsed jet plumes: Key to controlled combustion engines," SAE Paper 890153.
- Orrin, J.E., I.M. Vince, and F.J. Weinberg (1981), "A study of plasma jet ignition mechanisms", *Eighteenth Symposium (International) on Combustion*, The Combustion Institute, Pittsburgh.
- Shen, K., J.P. Chiu, R.W. Faidley, M.H. Darden, R.D. Matthews, W.F. Weldon, and S.P. Nichols (1994), "Initial studies of railplugs as an aid for cold starting of diesels", SAE Paper 940108; also in *1994 Subzero Engineering Conditions Conference Proceedings*, SAE Special Publication P-273, 157-164.
- Smy, P.R., R.M. Clements, and D.R. Topham (1985), "Efficiency and erosion of plasma jet ignitors", *Comb. Sci. and Tech.* 42: 317-324.
- Tamai, R., J.A. Maxon, I. Shepard, R.K. Cheng, and A.K. Oppenheim (1992), "Rayleigh scattering density measurements of combustion in an enclosure", *Twenty-Fourth Symposium (International) on Combustion*, The Combustion Institute, Pittsburgh,
- Tozzi, L., and E.K. Dabora (1982), "Plasma jet ignition in a lean-burn CFR engine", *Nineteenth Symposium (International) on Combustion*, The Combustion Institute, Pittsburgh, pp. 1467-1474.
- Weinberg, F.J., K. Hom, A.K. Oppenheim, and K. Teichman (1978), "Ignition by plasma jet", *Nature* 272:341-343.

- Wiegand, G. (1993), "An investigation of electrode erosion due to plasma armatures in a repetitively fired railplug: A new miniature railgun used as a spark ignition source", Masters Thesis, Univ. of Texas at Austin.
- Wyczalek, F.A., "Plasma jet ignition of lean mixtures (1975)", SAE Paper, 750349.
- Zhao, X.W., J.L. Ellzey, and R.D. Matthews (1993), "Three-dimensional numerical simulation of flame propagation in spark ignition engines", SAE Paper 932713.
- Zhao, X.W., J.L. Ellzey, and R.D. Matthews (1994), "Numerical simulations of combustion in SI engines - comparison of the Fractal Flame Model to the Coherent Flame Model", *Proceedings of the Third International Symposium on Diagnostics and Modeling of Combustion in Internal Combustion Engines*, JSME/JSAA, pp. 157-162.
- Zheng, J., S. Capiiaux, J.P. Chiu, R.D. Matthews, R.W. Faidley, M.H. Darden, W.F. Weldon, and S.P. Nichols (1993), "Effects of railplugs on the dilution tolerance of a spark ignition engine", SAE Paper 931800.

Appendix A.
**List of Theses and Dissertations Supported in Whole or in Part by the
Railplug Project**

- Koenig, M.H. "An experimental investigation of the railplug ignition system in a lean burn engine", Master's Thesis, Dept. of Mech. Eng., The University of Texas, Dec. 1991.
- Shen, K. "Investigation of railplugs as an aid for cold starting of diesels", PhD Dissertation, Department of Mechanical Engineering, The University of Texas, expected to be completed May, 1995.
- Wiegand, G. "An investigation of electrode erosion due to plasma armatures in a repetitively fired railplug: A new miniature railgun used as a spark ignition source", Masters Thesis, The University of Texas, Dec. 1993.
- Wu, D.-Y. "Effects of railplugs in high EGR rate spark ignition engines", PhD Dissertation, Department of Mechanical Engineering, The University of Texas, in progress.
- Zhao, X.W. "Numerical simulations of combustion in SI engines - comparison of the Fractal Flame Model to the Coherent Flame Model", PhD Dissertation, Department of Mechanical Engineering, The University of Texas, May, 1994.

Appendix B.
Copies of Publications Resulting from the Railplug Project

The papers below are enclosed in this appendix in chronological order:

Hall, M.J., H. Tajima, R.D. Matthews, M.M. Koeroghlian, W.F. Weldon, and S.P. Nichols (1991), "Initial studies of a new type of ignitor: the railplug", SAE Paper 912319, also in *Journal of Engines* 100:1730-1746 (1992).

Faidley, R.W., M.H. Darden, and W.F. Weldon (1992), "The railplug: a new ignitor for internal combustion engines", *Proceedings of the 6th Symposium on Electromagnetic Launch Technology*, Institute for Advanced Technologies, the University of Texas at Austin.

Hall, M.J., J.L. Ellzey, H. Tajima, and X.W. Zhao (1993), "Plasma plume generation by a railplug ignitor and simulation by multidimensional modeling", *Experiments in Fluids* 14:416-422.

Matthews, R.D., M.J. Hall, R.W. Faidley, J.P. Chiu, X.W. Zhao, I. Annezer, M.H. Koenig, J.F. Harber, M.H. Darden, W.F. Weldon, and S.P. Nichols (1992), "Further analysis of railplugs as a new type of ignitor", SAE Paper 922167, also accepted for publication in the *Journal of Engines*, 1993.

Zheng, J., S. Capiiaux, J.P. Chiu, R.D. Matthews, R.W. Faidley, M.H. Darden, W.F. Weldon, and S.P. Nichols (1993), "Effects of railplugs on the dilution tolerance of a spark ignition engine", SAE Paper 931800.

Shen, K., J.P. Chiu, R.W. Faidley, M.H. Darden, R.D. Matthews, W.F. Weldon, and S.P. Nichols (1994), "Initial studies of railplugs as an aid for cold starting of diesels", SAE Paper 940108; also in *1994 Subzero Engineering Conditions Conference Proceedings*, SAE Special Publication P-273, 157-164.

Chiu, J.P., M.H. Darden, R.D. Matthews, H.E. Childs, R.W. Faidley, J. Zheng, G. Weigand, W.F. Weldon, and S.P. Nichols (1994), "Examination of the factors that influence the durability of railplugs", SAE Paper 940201, also in *Advanced Power Plant Concepts*, SAE Special Publication SP-1038.

Reprints removed
dyed separately